Characterizing the Pregnane X Receptor's Interactions and Biophysical Properties

Virginia Elaine Carnahan

A thesis submitted to the faculty of the University of North Carolina at Chapel Hill in partial fulfillment of the requirements for the degree of Master of Science in the Department of Biochemistry and Biophysics.

Chapel Hill
2007

Approved by:

Matthew R. Redinbo

Donald P. McDonnell

Charles W. Carter, Jr.

Abstract

VIRGINIA ELAINE CARNAHAN: Characterizing the Pregnane X Receptor's Interactions and Biophysical Properties
(Under the direction of Dr. Matthew R. Redinbo.)

Pregnane X Receptor is a ligand-activated transcription factor critical in protecting tissues from xenobiotics and endobiotics. PXR is shown to interact with GRIP-1 and PGC-1α on DR-4 and XREM-CYP3A4 promoters. Experiments with full-length PXR have been limited by the inability to produce it. This study reports production of full-length PXR from *Spodoptera frugiperda* and use in peptide phage display experiments. PXR LBD was also mapped using peptide phage display. Sequencing results demonstrate a conserved motif consistent with class II nuclear receptor boxes but adding an additional residue, a polar residue in the -3 position. There is a novel intermolecular β-sheet mediating homodimerization in all PXR LBD structures. Mammalian two-hybrid studies demonstrated that a mutant of PXR that disrupts the homodimerization interface and eliminates basal transcriptional activity is unable to recruit SRC-1. Thermal denaturation studies of other PXR LBD mutants that affect basal transcriptional activity show changes in overall protein stability.

Dedicated to my family

and in loving memory of

Cynthia Ann Turpen.

Acknowledgements

It is difficult to think of everyone that should be acknowledged in this accomplishment. So many people have supported, encouraged, and enabled me to reach this goal. I'd like to offer many thanks to the National Science Foundation for the honor and funding of the Graduate Research Fellowship, as well as to the department of Biochemistry and Biophysics and the Biophysics training program.

I'd like to thank you, Matt, for the opportunity to work in your lab. I'd like to thank you for your training and investment in me, as well as your flexibility and understanding when things turned out differently than anticipated. Your willingness to work with me and your support of my leave of absence while making a very difficult decision was exceedingly helpful.

I'd like to thank all of the members of the Redinbo lab, past and present for camaraderie, helpful discussions, and bearing with my lab meetings even thought they involved very little structure. Thanks to the first five students and Yu Xue for taking me in. Schroeder Noble, thanks for all the late-night/early-morning companionship and demonstrating that it is indeed possible to enjoy prepping for two or three days straight when you have good company (or at least entertaining music). I also owe a good deal of thanks to Schroeder and Thu Lesher for basic lab training; thanks for letting me use many of your basic protocols so that (coming from an orgo background) I at least had a starting point. Thu, I really value the friendship that we started in the Redinbo lab and then continued when you followed me over to the LSRC for a little while. Thanks for your

friendship and for sharing the secretary duties. (Oh, and for the fried rice recipe. That was a pretty funny night.) Thanks to Scott Lujan for sharing my soda vice and putting up with me as a TA. Eric Ortlund, thanks for answering random questions, always being accessible for helpful discussions, and for taking all the undergrads once they are well-trained. (Kidding! I'm glad that once I headed over to Duke Janet had the chance to work with you and get published.) And, of course, I'd like to thank Ryan Watkins who solved the first structure of PXR LBD in our lab and Paula Davis-Searles for initiating the thermal denaturation studies.

Donald, thank you for making a home away from home for me in your lab at Duke. I almost feel like I had the opportunity to go to graduate school twice, once in biochemistry/structural biology and once in pharmacology/biology. I am very appreciative of all that I learned in your lab, both from you and from the members of your lab. Though I thank each of the members of Donald's lab for welcoming me and taking part in my training, special thanks go to Ching-Yi Chang, Tanya Hartney, Julie Hall, Martin Tochacek, Daju Fan, Rebecca Stein, Andrea Sherk, Neeru Mettu, Suzanne Wardell, and (of course) Trena Martelon. The friendships that I made have enriched my life in so many ways.

Dr. Laura Wright, thank you for the inspiration you have been to me. It must be almost eight years ago now since I sat down in your Chem11 class and wondered at the strange anomaly I experienced for the first time: a woman with a PhD in chemistry. Truly I have found that there are many strong, intelligent women in the hard sciences; but I never even dreamed of the possibility of graduate school until I sat down in your Chem11 class. And I have you to thank for any good lab and safety practices that I retained from

my time spent in your lab. Thank you for taking a chance and letting a freshman participate in research.

Dr. Clinton Stewart and the team at St. Jude Children's Research Hospital, thank you for the opportunity to work with you all. As I look back on the time in your lab, I find that it shaped me in so many ways that I did not even realize at the time. With you I learned what it looks like to work as a team of interdisciplinary scientists and doctors, as well as how to maximize the benefits and negotiate the challenges of such environments. It was during my stint in your lab that I fell in love with studying topo I for the first time, resulting in my excitement when I eventually met Matt at the UNC poster session. Small world!

Dr. Moses Lee, thank you for my time as a Lee's Flea. Your teaching, advice, and guidance are appreciated. I cannot thank you and the entire Furman University Chemistry faculty enough for focusing on teaching us how to think. Beyond doubt that is the ability that opens all doors and disciplines.

Janet Hager and Ariadne Sanders, thank you for the chance to mentor you and for all the things that you taught me in that process. I hope that you've forgiven me for not always giving you an easy answer, but making you talk through it until you discover the answer yourself.

I would not have made it through graduate school without the support of Loretta Shaia. I have grown so much professionally and personally during this period of time. I think I expected the professional growth, but much of the growth in my personal life was, in some ways, a bit of a surprise.

Thank you most importantly to the Lord. His faithfulness, presence, and strength never cease to restore and enable me when I think it is impossible. Thank you to my communities at Chapel Hill Bible Church, especially College Encounter, MEOW, Frances Hardy, Tina Goss, and Amanda Kepler. Nikki DeSanctis, thank you for your unwavering friendship and support. I feel blessed to have you in my life. Mary Newton Robbins, thank you for the inspiration and encouragement you have been to me through this entire process, both at UNC and after graduating. Heather Madsen and Cara Bostrom, thank you also for your dear friendship and for helping me maintain perspective.

Finally, I'd like to thank my entire family. I've dedicated this work in memory of my mom, who always berated her own ability to understand science, but encouraged me that I could do whatever I desired. I'd like to thank my dad for his interest and encouragement in math and the sciences, including his involvement in many science fair projects over the years. Michael, my loving husband, you have been such an encouragement to me. I feel grateful to be going through life with you by my side. Thank you for your faith in me and your sense of fun. Makayla, becoming a mother has changed me even more than I thought possible…I find that it has made me stronger, more confident, and more patient in the very least. Thank you for the joy that you have been, I treasure the time we have had and look forward to the precious years to come.

Table of Contents

List of Tables

List of Figures

List of Abbreviations and Symbols

α#	specific alpha helix, e.g. α2 = alpha helix 2
αAF	activation function alpha helix
μM	micromolar, 1 x 10^{-6} moles/liter
μL	microliter, 1 x 10^{-6} liters
Å	Angstroms, 1 x 10^{-10} m
$Å^2$	square Angstroms
$Å^3$	cubic Angstroms
A, ala	alanine
AF-1	activation function-1
AF-2	activation function-2
C, cys	cysteine
CAR	constitutive androstane receptor
clogP	calculated partition coefficient
C-terminus	carboxy-terminus
CYP3A4	cytochrome P450, family 3, subfamily A, polypeptide 4
D, asp	aspartic acid
Da	Daltons
DBD	DNA-binding domain
DNA	deoxyribonucleic acid
DR-3	direct repeat separated by three nucleotides
DR-4	direct repeat separated by four nucleotides
DR-5	direct repeat separated by five nucleotides

DRIP205	Vitamin D receptor-interacting protein complex 205kDa component
E, glu	glutamic acid
EC_{50}	half maximal effective concentration
ER-6	everted repeat separated by six nucleotides
ER-8	everted repeat separated by eight nucleotides
ET-743	ecteinascidin 743
F, phe	phenylalanine
G, gly	glycine
GRIP-1	glutamate receptor interacting protein 1
H, his	histidine
HNF-4	hepatocyte nuclear factor 4
I, ile	isoleucine
K, lys	lysine
L, leu	leucine
LBD	ligand-binding domain
M, met	methionine
MDR1	multidrug resistance 1
mL	milliliter, 1×10^{-3} liters
N, asn	asparagine
NCoR	nuclear corepressor
nM	nanomolar, 1×10^{-9} moles/liter
NR	nuclear receptor
N-terminus	amino-terminus

P, pro	proline
PBP	peroxisome proliferator-activated receptor-binding protein
PCN	pregnenolone 16a-carbonitrile
PGC-1α	PPAR gamma coactivator-1 alpha
PXR	pregnane X receptor
Q, gln	glutamine
R, arg	arginine
RIP-140	receptor-interacting protein-140
RXRα	retinoid X receptor alpha
S, ser	serine
SMRT	silencing mediator of retinoic acid and thyroid hormone receptor
SNP	single nucleotide polymorphism
SPRM	selective PXR modulator
SRC-1	steroid receptor coactivator-1
SUG1	suppressor for gal-1
SXR	steroid and xenobiotic receptor
T, thr	threonine
TRAP220	thyroid hormone receptor-associated protein complex 220 kDa component
UGT1A1	UDP-glucuronosyltransferase 1 family, polypeptide A1
V, val	valine
W, trp	tryptophan
X	any amino acid

XRE	xenobiotic response element
XREM-CYP3A4	xenobiotic response element from the cytochrome P450 3A4
Y, tyr	tyrosine

Chapter 1

Structure and Function of the Human Nuclear Xenobiotic Receptor PXR

Reproduced with permission from *Current Drug Metabolism* (2005) **6**: 357-67.

Virginia E. Carnahan[1] and Matthew R. Redinbo[1,2,*]

[1]Department of Biochemistry and Biophysics,
[2]Department of Chemistry, and the Lineberger Comprehensive Cancer Center,
University of North Carolina at Chapel Hill, Chapel Hill, NC 27599

*Corresponding Author: Matthew R. Redinbo, PhD.
Department of Chemistry
Campus Box #3290
University of North Carolina at Chapel Hill
Chapel Hill, NC 27599-3290
redinbo@unc.edu

Supported by an NSF graduate research fellowship to V.E.C. and by NIH grant DK62229 to M.R.R.

Abstract

The Pregnane X Receptor (PXR; NR1I2; also termed PAR, SXR) is a member of the nuclear receptor family of ligand-regulated transcription factors. Like many former orphan nuclear receptors, it contains both DNA and ligand binding domains, and binds to response elements in the regulatory regions of target genes as a heterodimer with RXRα. Unlike the vast majority of nuclear receptors, however, PXR responds to a wide variety of chemically-distinct xenobiotics and endobiotics, regulating the expression of genes central to both drug and bile acid metabolism. We review the structural basis of PXR's promiscuity in ligand binding, its recruitment of transcriptional coregulators, its potential formation of higher-order nuclear receptor complexes, and its control of target gene expression. Structural flexibility appears to be central to the receptor's ability to conform to ligands that differ in both size and shape. We also discuss the clinical implications of PXR's role in the drug-drug interactions, cancer, and cholestatic liver disease.

Introduction

The pregnane X receptor (PXR; NR1I2; also PAR, SXR) is a member of the nuclear receptor superfamily that plays a central role in protecting tissues from potentially toxic exogenous and endogenous compounds (xenobiotics and endobiotics, respectively). Originally an orphan receptor, PXR was cloned based on sequence homology to other nuclear receptors (NRs) and prior to assignment of its cognate ligand or its biological function. It was found first to respond to endogenous pregnanes, which gave rise to its name, but was subsequently shown to detect a wide variety of endobiotics and xenobiotics including many clinical drugs, with typical EC_{50}'s in the high nanomolar or low micromolar range (Bertilsson, G., et al. 1998; Blumberg, B., et al. 1998; Kliewer, S.A., et al. 1998; Lehmann, J.M., et al. 1998). PXR has since been firmly adopted as a xenobiotic receptor that regulates the expression of numerous drug metabolism genes, an endobiotic sensor involved in regulating cholesterol homeostasis and bile acid metabolism genes, and as an important player in the development of specific forms of cancer.

In this review, we examine numerous aspects of the structure and function of PXR. We first cover the regulation of PXR, in terms of its activation by ligands, its interaction with transcriptional coregulators, the retinoid X Receptor (RXRα) and DNA, as well as documented single nucleotide polymorphisms (SNPs), subcellular trafficking and degradation. Second, we examine what biological pathways are regulated by PXR, focusing on its well established roles in drug and cholesterol metabolism. Third, we discuss the clinical implications of PXR's action, including its role in drug interactions, in

variations in drug action in individuals, in drug resistant cancers, and as a putative target for the treatment of liver cholestasis. Finally, we end by presenting future directions for the examination of PXR, in particular the search for potential selective PXR modulators (SPRMs) for a variety of clinical applications.

Regulation of PXR

Genetic and Functional Features

PXR contains the conserved domain structure characteristic of nuclear receptors (**Figure 1.1**). At its far N-terminus is a short activation function 1 (AF-1) region that allows the regulation of receptor action in a ligand-independent fashion. The DNA binding domain (DBD) of human PXR (amino acids 41-107) contains two zinc fingers and binds to specific DNA response elements as a heterodimer with the retinoid X receptor-α (RXRα). The sequence and structure of NR DBDs are highly conserved across the receptor superfamily, although monomeric variations have also been described. The PXR DBD also contains a reported bipartite nuclear localization sequence (Kawana, K., et al. 2003). The DBD and ligand binding domain (LBD) in PXR are separated by a hinge region (amino acids 107-141) that is considerably shorter than for other nuclear receptors. The PXR LBD (amino acids 141-434) contains both the ligand binding pocket and the ligand-dependent activation function 2 region (AF-2). The LBD of PXR is expected to heterodimerize with the LBD of RXRα using an extensive set of polar and nonpolar interactions, similar to those seen in structures of other NR LBDs with the

RXRα LBD (Gampe, R.T., Jr., et al. 2000a). Conformational changes in AF-2 upon ligand binding are responsible for recruitment of coregulator proteins (*e.g.,* members of the p160/SRC family), leading to changes in transcription of target genes (Nolte, R.T., et al. 1998; Renaud, J.P., et al. 1995; Xu, H.E., et al. 2002).

Several non-synonymous SNPs in human PXR have been reported (Hustert, E., et al. 2001; Koyano, S., et al. 2002; Zhang, J., et al. 2001) and are labeled in **Figure 1.1**. Three coding changes within or adjacent to the PXR LBD, Val-140-Met, Asp-163-Gly and Ala-370-Thr, were found to alter the action of variant receptors in vitro. One coding alteration detected in this analysis leads to the replacement of Arg-122 in a DNA-binding helix in the PXR DBD with a glutamine, which was shown to reduce DNA binding. This alteration has only been found in heterozygotes with one normal PXR allele, however, which leads to no detectable change in response to activating ligands. Taken together, these results suggest that loss of PXR action may be a clinically-relevant state for certain patients and pose a risk for drug toxicities and/or liver disease.

The phosphorylation of NRs impacts many aspects of receptor activity, including DNA, ligand and coregulator binding, as well as the formation of receptor homo- and heterodimers (reviewed in (Rochette-Egly, C. 2003)). This is not surprising given the well documented role of kinase/phosphatase cascades in controlling numerous transcription factors. NetPhos 2.0 (Blom, N., et al. 1999) was used to predict phosphorylation sites in PXR, and only residues with scores ≥ 0.8 are depicted in **Figure 1.1**. It was recently shown that the protein kinase C pathway appears to down-regulate the expression of xenobiotic metabolism enzymes, particularly cytochrome P450 3A isoforms, by promoting the interaction of human PXR with the transcriptional coregulator

NCoR while repressing the receptor's interaction with the coactivator SRC-1 (Ding, X.S., et al. 2005). Protein kinase A was shown to phosphorylate directly both the DBD and LBD of human PXR and, in contrast to protein kinase C, to enhance the interaction of PXR with corepressors in mammalian two-hybrid experiments (Ding, X.S., et al. 2005). Unraveling the detailed roles that specific phosphorylation sites on PXR and coregulator proteins play in transcriptional control and receptor trafficking remains an important area for future study.

Crystal structures of the human PXR LBD have been determined alone, in complexes with several xenobiotics, and with a peptide fragment of the transcriptional coactivator SRC-1 (Chrencik, J.E., et al. 2005; Watkins, R.E., et al. 2001; Watkins, R.E., et al. 2003a; Watkins, R.E., et al. 2003b). Like other nuclear receptor LBDs, the PXR LBD contains three layers of α-helices arranged in a so-called "α-helical sandwich" that surrounds the receptor's ligand binding cavity (**Figures 1.2A, B**) (Watkins, R.E., et al. 2001). While most nuclear receptor LBDs contain a short, two- to three-stranded β-sheet, PXR extends that beta structure to a five-stranded antiparallel sheet (Chrencik, J.E., et al. 2005; Watkins, R.E., et al. 2001; Watkins, R.E., et al. 2003a; Watkins, R.E., et al. 2003b). The PXRs contain an insert of approximately 60 amino acids (residues 175-235) that is novel in the nuclear receptor superfamily, but is largely conserved in the PXRs of known sequence. Exceptions to this rule are certain PXR splice variants that lack this insert and are considerably less promiscuous in their response to ligands (Kliewer, S.A., et al. 1998).

The novel sequence insert in the PXR LBD is partially disordered in the structures determined to date; amino acids between residues 178 to 191 have consistently been too

mobile to be visualized in numerous crystal structures. The remaining residues in this insert, however, are ordered and fold into a distinct α–β-turn-β motif adjacent to the receptor's ligand binding pocket (**Figures 1.2A, B**). The novel α2 extends along the "bottom" of the ligand binding pocket, and is a particularly mobile region that is key to the receptor's broad response to activating ligands (as discussed below). The two additional β-strands, β1 and β1', generate the longer β-sheet in PXR. These β-strands also interact between LBD monomers to create a novel homodimeric complex that has been observed in all PXR structures to date (**Figure 1.2A**) (Chrencik, J.E., et al. 2005; Watkins, R.E., et al. 2001; Watkins, R.E., et al. 2003a; Watkins, R.E., et al. 2003b). The homodimer formed by the PXR LBD does not interfere with the heterodimer it is expected to form with the RXRα LBD. The amino acids involved in this homodimer interface are conserved in the PXRs of known sequence and are also unique to the PXRs within the NR superfamily. Studies are currently ongoing to determine the biological relevance of this homodimer, although initial results indicate that the formation of this higher-order structure in PXR is central to its transcriptional activity (Noble and Redinbo, unpublished).

The ligand-binding pocket is large, flexible, and capable of varying in volume between 1,280 and >1,600 $Å^3$ in the crystal structures of apo and ligand-bound complexes reported to date. Thus, PXR is on par with the largest known NR ligand binding cavity, which is 1,619 $Å^3$ for the fatty acid-binding receptor PPARγ (Nolte, R.T., et al. 1998). The receptor's cavity is predominantly hydrophobic but contains eight polar residues distributed throughout the surface of the pocket (Watkins, R.E., et al. 2001). In this way, PXR's pocket reflects the general character of the xenobiotic ligands to which it

binds, which are typically lipophilic compounds with a limited number of polar groups (Lipinski, C.A., et al. 2001). A more detailed discussion of the recognition of ligands by PXR is provided below. The PXR LBD ends with a final short α–helix termed αAF, as it generates a key part of PXR's AF-2 motif. As in other nuclear receptors, the interacting region of the transcriptional coactivator SRC-1 (yellow in **Figure 1.2B**) binds in a groove formed with residues from αAF, α3, and α4 (Watkins, R.E., et al. 2003a). The invariant leucines in this coactivator LxxLL motif (where x is any residue) fit into hydrophobic pockets in the receptors AF-2 region, and the short helix formed by the LxxLL sequence is capped by a glutamic acid and lysine residue from PXR around the N- and C-terminus, respectively, of the helix (**Figure 1.2C**).

Ligand Binding

PXR is distinct in the nuclear receptor superfamily because it responds promiscuously to a wide variety of chemically-distinct ligands ranging in mass from 232 Da (phenobarbital) to >800 Da (taxol, rifampicin) (Bertilsson, G., et al. 1998; Jones, S.A., et al. 2000; Kliewer, S.A., et al. 1998; Lehmann, J.M., et al. 1998; Synold, T.W., et al. 2001) (**Figure 1.3A**). While most compounds act as agonists, a small number of chemicals with potential antagonist activity have been reported, including ecteinascidin 743 (ET-743) (Synold, T.W., et al. 2001) and ketoconazole (Takeshita, A., et al. 2002). Although each PXR isoform examined to date is promiscuous, a clear pattern of inter-species differences in specificity has been observed. For example, mouse PXR is not activated efficiently by SR12813 (a cholesterol-lowering compound), but human and rabbit PXR are; mouse PXR, in contrast, is activated by PCN (pregnenolone 16α-

carbonitrile), while human and rabbit PXR are not (Blumberg, B., et al. 1998; Jones, S.A., et al. 2000; Lehmann, J.M., et al. 1998). The LBDs of the PXRs vary considerably in sequence between related mammalian isoforms (e.g., by as much as 76% between human and rat (Jones, S.A., et al. 2000)), which is uncommon in the NR superfamily. It is clear that a small number of amino acid changes are responsible for this "directed promiscuity" observed between the PXRs of mammalian species. For example, the human residue (Leu308) or group of three residues (Gln317, Leu324, and Tyr328) confers rifampicin sensitivity to rat PXR (Tirona, R.G., et al. 2004). These residues are located at the end of β4, in α7, and in the unstructured loop between these two secondary structure elements.

It has been speculated that a common ancestral ligand exists that regulated the action of the first PXR. Krasowski and colleagues recently suggested that endogenous bile acids may have been the original ligands that drove PXR's evolution and species-specific variability (Krasowski, M.D., et al. 2005) Indeed, several groups have shown that PXR plays a crucial role in detecting the build-up of potentially toxic bile acids and up-regulating the expression of bile acid metabolizing enzymes to protect the liver and other tissues. These data support PXR's adopted role as a molecular sentinel that detects the presence of potentially harmful endobiotic and xenobiotic compounds.

The clogP characteristics of PXR ligands were examined to determine if the receptor functions simply as a "hydrophobic sink", where interactions between the receptor and ligand are driven by non-specific hydrophobic binding to the PXR pocket, or whether the receptor has more selective characteristics in ligand binding. The hydrophobicity of known PXR ligands (as represented by clogP) was plotted as a

function of ligand molecular weight, and compared to a set of 10,000 compounds with drug-like qualities (**Figure 1.3B**). PXR ligands did not cluster in a particular region of this plot, but instead appear to sample many regions of this drug-like space. PXR is not the transcription factor equivalent of a serum albumin, which binds non-specifically to an extremely diverse set of chemicals in circulating plasma. Indeed, functional and structural studies have shown that the PXRs from distinct species exhibit promiscuity directed toward distinct regions of endobiotic and xenobiotic chemical space.

Several crystal structures show ligand binding to PXR induces significant conformation changes in the pocket of the receptor (**Figure 1.4A**). While most of the amino acid side chains that line the ligand binding pocket of PXR remain in a consistent position in the apo (unliganded) and numerous ligand-bound structures, a small number of residues undergo significant rotamer changes or shifts in position in both main chain and side-chain atoms (**Figure 1.4B**). For example, the side chain of His-407 undergoes rotamer shifts of up to 7 Å between different PXR LBD structures, while both the side chain and main chain atoms of Leu-209 have also been observed to shift translationally in position by up to 7 Å. Both residues have been found by mutagenesis to be critical to the receptor's response to distinct ligands (Chrencik, J.E., et al. 2005; Watkins, R.E., et al. 2003a; Watkins, R.E., et al. 2003b). An examination of **Figure 1.4B** reveals that most of the mobile residues in PXR (in particular residues 206-211) reside in the sequence insert novel to the PXRs.

Flexibility is critical to PXR's promiscuity by enabling the receptor to change shape to accommodate structurally-distinct chemicals. For example, the small agonist SR12813 was initially shown through detailed crystallographic studies to bind to PXR in

numerous distinct orientations at once (**Figure 1.4B**) (Watkins, R.E., et al. 2001). When the LxxLL motif of the transcriptional coactivator SRC-1 binds to the surface of PXR, however, this same agonist shifts to a single, unique binding orientation. These results suggest that the receptor's inherent flexibility (or "breathing") can occur even with a small ligand bound, but that interactions with a coactivator partially lock the receptor to restrict such flexibility. Numerous other ligands have been examined in complex with PXR, including the St. John's wort compound hyperforin, the antibiotic rifampicin, as well as additional small agonists and endogenous steroids. In the structure of each complex, the ligand binding pocket changes shape to accommodate the distinct features of the ligand. The most dramatic example of the "induced fit" nature of PXR is its interaction with the macrolide rifampicin. Initial PXR structures suggested that the receptor's pocket would have to change shape and size significantly to accommodate this 823 Da ligand. Rifampicin binding causes the bottom, flexible portion of the binding cavity, in particular the regions on the 60 amino acid insert novel to PXR, to become disordered and not to be observed in the electron density maps of this structure. These results suggest that the receptor is capable of activating transcription even if portions of its ligand binding domain are relatively unstructured. This appears to be a key feature of this xenobiotic receptor's ability to respond promiscuously to small and large compounds that vary in chemical nature and structure.

Subcellular Localization

Previous reports based on GFP-tagged human PXR (hPXR) localization experiments and immunocytochemistry of hPXR in cells indicated that PXR always

localized to the nucleus regardless of the presence or absence of ligand (Koyano, S., et al. 2004; Sueyoshi, T., et al. 2001). Other groups, however, have detected ligand-dependent translocation of PXR from the cytoplasm to the nucleus in the liver of mice treated with PCN (Kawana, K., et al. 2003; Squires, E.J., et al. 2004). Squires and colleagues further showed that PXR binds in the cytoplasm to heat shock protein 90 (Hsp90) and the constitutive active/androstane receptor retention protein (CCRP) in HepG2 cells, and that these proteins assist with (but do not follow) the receptor in its translocation to the nucleus upon ligand binding (Squires, E.J., et al. 2004). Determining whether and to what degree these interactions with known NR binding proteins in the cytoplasm impact PXR's promiscuity in response to ligands is an important area for future study.

DNA Binding

PXR forms a heterodimer with RXRα upon binding to specific repeats of AG(G/T)TCA in the promoter regions of genes (Blumberg, B., et al. 1998; Lehmann, J.M., et al. 1998; Mangelsdorf, D.J., et al. 1995). The DBDs of both receptors are expected to be highly similar in structure to the RXRα DBD, which is a double zinc-finger motif that contacts DNA in a sequence-specific manner. The response elements are arranged as direct repeats (both sequences in the same 5'-3' direction) with 3 to 5 bases separating DBD binding sites (DR-3, DR-4, and DR-5 elements), as well as everted repeats (with the beginning of each sequence in proximity) separated by six or eight bases (ER-6 and ER-8, respectively) (Blumberg, B., et al. 1998; Kast, H.R., et al. 2002; Lehmann, J.M., et al. 1998). Because PXR response elements vary between direct and everted repeats, the DBDs of the two receptors within the physiologically relevant

heterodimer must be able to reorient themselves to contact efficiently these distinctly arranged response elements. Since the LDBs of PXR and RXRα are expected to form only a single type of heterodimeric complex, the regions that connect the DBDs and LBDs must allow significant flexibility to allow relative variations in DBD positions. There is evidence that the PXR-RXRα heterodimer recruits distinct transcriptional coregulators depending on the nature of the ligand and response element bound (see below). The control of gene expression by PXR appears to involve subtleties beyond the well established canonical steps in NR function – DNA, ligand and coregulator binding.

Coregulator Binding

In contrast to well-characterized receptors like the estrogen receptor isoforms, the complexes PXR forms with partner proteins to control the expression of target genes is poorly understood. A simplified prototypical model of regulation would suggest that PXR is retained in the cytoplasm until some signal causes a translocation to the nucleus and the formation of a heterodimer with RXRα on target XREs. In the absence of agonist or the presence of antagonist, corepressors (*e.g.,* NCoR and SMRT) are thought to bind to the receptor and deacetylate histones, preventing transcription of the target genes. In the presence of an activating ligand, the receptor-agonist complex can associate with coactivators (*e.g.* SRC-1) and allow large transcription complexes to form on target gene promoters. Either the coactivators or the proteins they recruit have histone acetylase activity, leading to chromatin decondensation and gene transcription. Such a simplified model is complicated by the fact that receptor activity is also influenced by promoter

location, the nature of the agonist, and the expression levels of coregulators in particular tissues or cell lines.

Early studies determined via co-immunoprecipitation that PXR bound SRC-1 (Kliewer, S.A., et al. 1998). Subsequent data on coactivator interactions were derived largely from directed yeast and mammalian two-hybrid studies. In a yeast two-hybrid experiment, Masuyama et al. confirmed that, in the presence of nonylphenol or phthalic acid, full length mouse PXR interacts with steroid receptor coactivator-1 (SRC-1) and receptor interacting protein 140 (RIP-140), but not suppressor for gal-1 (SUG1). (Masuyama, H., et al. 2000) In the presence of progesterone, dexamethasone or pregnenolone, mPXR interacted with SRC-1, RIP140, and SUG1. (Masuyama, H., et al. 2001) As discussed above, the cross-species specificity of PXR emphasizes the importance of performing experiments to confirm these interactions for human PXR. Most studies to date of coregulator interactions with human PXR employ only the receptor's LBD (fused to Gal4 or VP16), and several have confirmed PXR's interaction with SRC-1 (Synold, T.W., et al. 2001; Takeshita, A., et al. 2001; Takeshita, A., et al. 2002; Wentworth, J.M., et al. 2000). One of these studies also demonstrated interactions between hPXR LBD and glucocorticoid receptor interacting protein 1 (GRIP1), human activator for thyroid hormone and retinoid receptors (ACTR), and human vitamin D receptor-interacting protein complex component (DRIP205, also called PBP and TRAP220) in the presence of paclitaxel or docetaxel (Synold, T.W., et al. 2001). A recent study demonstrated that full length human PXR interacts with PGC-1α, and subsequently interferes with HNF-4 signaling (Bhalla, S., et al. 2004). Building up these more intricate

complexes, and elucidating the effects they have on signaling by other transcriptional systems, remains an exciting area for future study.

PXR and the related constitutive androstane receptor (CAR) both possess substantial basal activity. CAR plays an overlapping but distinct role in regulating the expression of genes involved in xenobiotic metabolism, as well as cholesterol and endobiotic homeostasis. While the structural basis of CAR's constitutive activity has recently been examined in detail (Moore, D.D. 2005; Shan, L., et al. 2004; Suino, K., et al. 2004; Xu, R.X., et al. 2004), it is not so clear for PXR. Indeed, site-directed mutations located far away from the AF-2 region in PXR have been shown to enhance (and in some cases to repress) the basal activity of the receptor. A structural explanation for these effects has remained elusive. Recent work by Ueda et al., however, showed that a conserved threonine (Thr-248) interacts with a threonine in the αAF of the AF-2 region to confer constitutive activity (Ueda, A., et al. 2004). This is an important step forward in understanding the basal activity of PXR, and the next challenge will be to extend the analysis to regions of the receptor seemingly removed from the αAF and AF-2 area.

The interaction of PXR with corepressors is more poorly understood than its interaction with coactivators. SMRT and NCoR, known corepressors of nuclear receptor transcription, have been tested *in vitro* for their ability to form complexes with PXR. Synold et al. observed that PXR interacted with both SMRT and (to a lesser extent) NCoR in the absence of ligand, and different ligands had differing abilities to prevent these interactions (Synold, T.W., et al. 2001). Subsequently, two other groups examined corepressor effects on the CYP3A4 promoter in specific cell lines (Takeshita, A., et al. 2002; Zhou, C.C., et al. 2004). In HepG2 cells (but not CV-1 cells), PXR showed

increased interactions with SMRT in the presence of the agonist rifampicin, and these interactions lead to decreased basal and ligand-induced activity on the CYP3A4 promoter (Takeshita, A., et al. 2002). In contrast, NCoR was responsible for repression of tocotrienol-induced CYP3A4 gene expression in LS180 cells (Zhou, C.C., et al. 2004), but a separate mechanism appeared to be required for the repression of UGT1A1 and MDR1 expression in the same cell line (Zhou, C.C., et al. 2004). These findings support the emerging conclusion for many members of the NR family that regulation is a highly complex ligand- and tissue-specific process.

Degradation pathways

Degradation pathways play important roles in nuclear receptor function via modulating protein levels and mediating receptor turnover. Degradation of PXR has not been studied in-depth; however, preliminary data indicate that PXR is degraded by the proteasome. PXR was found to interact with SUG-1, a component of the 26S proteasome complex, in the presence of progesterone but not in the presence of endocrine disrupting chemicals (Masuyama, H., et al. 2000). Further investigation confirmed that the proteasome is responsible for PXR degradation, and that ligands that do not enhance PXR's interaction with SUG1 (*e.g.,* non-natural endocrine disrupting chemicals) strongly block degradation of PXR (Masuyama, H., et al. 2002). Similar to the recruitment of coregulators, PXR's interactions with SUG1 and the receptor's degradation by the proteasome appear to be complex processes that warrant continued investigation.

Regulation by PXR

Tissue Expression Patterns of PXR

The function of the PXR receptor is linked to its expression pattern in different tissues. Originally, Northern blots detected human PXR expression in liver, colon, and small intestine (Lehmann, J.M., et al. 1998), sites associated with detecting and combating xenobiotics and potentially toxic endobiotics related to bile acid and cholesterol homeostasis. RT-PCR studies have confirmed presence of PXR mRNA in these three tissues, in addition to finding expression in stomach, fetal liver, thalamus, spinal cord, and low levels in heart, bone marrow, adrenal gland, pons and medulla (Lamba, V., et al. 2004). Dotzlaw and colleagues demonstrated that PXR is expressed in breast tumors and surrounding normal breast tissue (Dotzlaw, H., et al. 1999), and Masuyama and colleagues have shown that PXR is up-regulated in endometrial cancer cell lines (Masuyama, H., et al. 2003). These emerging results begin to link PXR to the progression and drug resistance of neoplastic tissues, a potentially important area of continued study (see "Clinical Implications" below) (Masuyama, H., et al. 2003; Masuyama, H., et al. 2005).

Genes Regulated by PXR

The list of genes regulated by PXR continues to grow, and now includes not only systems related to drug and xenobiotic metabolism but also those central to cholesterol and bile acid metabolism and excretion. The first list of gene products shown to be

regulated by PXR were CYP3A1 and CYP3A2 (Kliewer, S.A., et al. 1998), for mouse PXR, and subsequently CYP3A4 for human PXR (Lehmann, J.M., et al. 1998). More comprehensive systematic studies followed these initial reports and showed that human PXR regulates the expression of numerous gene products involved in all phases of xenobiotic metabolism and excretion (Maglich, J.M., et al. 2002; Rosenfeld, J.M., et al. 2003; Watkins, R.E., et al. 2003b). Phase 1 (oxidation) drug metabolism gene products regulated by PXR include numerous cytochromes P450, aldehyde and alcohol dehydrogenases, carboxylesterases, and several enzymes related to heme production and support of the P450 reaction cycle, such as aminolevulonic acid synthase and P450 oxidoreductase (Maglich, J.M., et al. 2002; Rosenfeld, J.M., et al. 2003; Watkins, R.E., et al. 2003b). In particular, the promiscuous and highly expressed human cytochrome P450 3A4 isoform (CYP3A4) is efficiently up-regulated by PXR, so much so that PXR has been termed a master regulator of CYP3A4 expression in human tissues. This CYP metabolizes over 50% of human therapeutic compounds (Maurel, P. 1996). Phase 2 drug metabolism gene products, which are involved in conjugating xenobiotics, are also regulated by PXR, including the abundant and highly active UDP-glucuronosyltransferases, as well as sulfotransferases and glutathione S-transferases (Dunn, R.T., et al. 1999; Falkner, K.C., et al. 2001; Rosenfeld, J.M., et al. 2003; Runge-Morris, M., et al. 1999; Watkins, R.E., et al. 2003b). Drug efflux pumps, central to Phase 3 “elimination” stage of drug metabolism, are also up-regulated by PXR, including numerous ATP-binding cassette integral membrane pumps of the multidrug resistant (MDR) family (Dussault, I., et al. 2001; Geick, A., et al. 2001; Kast, H.R., et al. 2002; Rosenfeld, J.M., et al. 2003; Staudinger, J.L., et al. 2001; Synold, T.W., et al. 2001;

Watkins, R.E., et al. 2003b). Taken together, these results support the central role PXR plays in coordinating the up-regulation of the complete process of drug metabolism in response to activating xenobiotic agonists.

PXR's original adoption as a receptor that responds to endogenous pregnanes has also lead to detailed studies of its role in endobiotic detection and metabolism. Initial experiments had identified Cyp7A and Oatp2 (Staudinger, J.L., et al. 2001; Xie, W., et al. 2001b) as target genes regulated by PXR, results that were supported and expanded by more comprehensive subsequent studies. PXR clearly plays several important roles in detecting oxysterols and bile acids, and is central to the proper maintenance of cholesterol homeostasis and fatty acid metabolism. Related gene products known to be regulated by PXR include fatty acid and HMG CoA synthases, organic anion transporters, and cytochromes P450 involved in cholesterol and bile acid metabolism (Dussault, I., et al. 2003; Goodwin, B., et al. 2003; Rosenfeld, J.M., et al. 2003; Xie, W., et al. 2003). In particular, it was shown that PXR's ability to down-regulate the expression of CYP7A in response to rifampicin involved the displacement of the transcriptional coactivator PGC-1α from the related HNF4 nuclear receptor, and direct binding of HFN4 by PXR (Bhalla, S., et al. 2004; Li, T.G., et al. 2005). These data further indicate that PXR's role in controlling gene expression involves mechanisms beyond the fundamental "ligand binding and coregulator recruitment" paradigm.

It is interesting to note that PXR regulates the expression of the related CAR receptor in response to agonists (Maglich, J.M., et al. 2002; Rosenfeld, J.M., et al. 2003). CAR plays overlapping but distinct roles in regulating key xenobiotic and endobiotic metabolism pathways. In addition to the well established drug and endobiotic metabolism

systems regulated by PXR, other intriguing genes linked to PXR regulation include the insulin-regulated gene pathways, the Huntington protein, and the oncogene A-raf serine/threonine kinase (Rosenfeld, J.M., et al. 2003). These results indicate that PXR likely plays important, but relatively unexamined, roles in numerous human disease states.

Clinical Implications of PXR Action

Drug-Drug Interactions

Activation of PXR by clinical drugs, herbal remedies, and vitamin supplements has been linked to potentially dangerous drug-drug interactions. Perhaps the best characterized example of this involves the activation of PXR by hyperforin, the active agent of the unregulated herbal antidepressant remedy St. John's wort. The use of St. John's wort had been shown to reduce the serum levels of several clinical therapeutics, including antivirals used to treat HIV and immunosuppressant agents prescribed to organ transplant patients (Piscitelli, S.C., et al. 2000; Ruschitzka, F., et al. 2000). Hyperforin was found to be a potent PXR agonist (with an EC_{50} of 32 nM) and to up-regulate the expression of a variety of drug metabolism and excretion genes in primary human hepatocytes, including significant inductions of CYP3A4 expression (Moore, L.B., et al. 2000; Watkins, R.E., et al. 2003b; Wentworth, J.M., et al. 2000). This provided a clear molecular link between St. John's wort, the activation of drug metabolism pathways, and the unwanted elimination of therapeutic agents. In addition to rifampicin, which is a well

established “inducer” of drug metabolism systems, the list of ligands that activate PXR now includes the chemotherapeutic agents paclitaxel (Synold, T.W., et al. 2001) and cisplatin (Masuyama, H., et al. 2005). The scope has widened to include vitamins with the demonstration that both vitamin E (tocopherol) and vitamin K2 are activators of PXR-mediated expression of target genes (Landes, N., et al. 2003; Tabb, M.M., et al. 2003). Taken together, these observations signal that patients and caregivers should continue to be aware of potentially life-threatening drug-drug and unregulated supplement-drug interactions involving the activation of PXR.

Individual Responses to Therapeutics

The identification of non-synonymous polymorphisms in the PXR gene in human populations has validated the role this receptor plays in individual sensitivities to clinical drugs. It is conceivable that as personalized approaches to medical treatments evolve (ones in which the genetic background of the patients is considered), characterizing potential variations in PXR sequence would become an important test to identify patients at risk for adverse reactions to drugs or drug combinations. As a first pass, simple modifications to the erythromycin breath test procedure, which assesses CYP3A4 activity, can provide a non-invasive measure of PXR’s action in patients (Hariparsad, N., et al. 2004). In situations where altered PXR function is suspected, a more careful examination of the PXR gene could be performed to identify SNPs or other variations in DNA sequence. In addition, tissue-specific splice variants of PXR could impact therapeutic efficacy and tolerance (Gardner-Stephen, D., et al. 2004), so the continued

study of such variations may also improve our ability to avoid unwanted reactions to clinical treatments.

Cholestasis

PXR has been known since its adoption as a pregnane sensor to respond to endogenous compounds based on the cholesterol and/or steroid scaffold, including oxysterols and bile acids. Now numerous lines of evidence support PXR's role in detecting endogenous bile acids and cholesterol precursors *in vivo*. For example, increased PXR activity has been shown to protect the liver and other tissues from exposure to excess dietary bile acids and to the build-up of cholesterol precursors caused by the elimination of key enzymes in the cholesterol homeostasis pathways (Goodwin, B., et al. 2003). The impact of a high cholesterol and cholic acid diet of PXR knockout mice was recently shown to cause lethal damage to the liver in 100% of these animals, but not to exert a similar effect on wild-type mice (Sonoda, J., et al. 2005). These data highlight PXR's importance in responding to the presence of toxic levels of bile acids and other potentially harmful endobiotics. Indeed, the PXR agonist rifampicin and the herbal remedy St. John's wort (containing the potent PXR agonist hyperforin) have been used to treat cholestatic liver disease, which is associated with the build up of bile acids and other endogenous compounds (Bachs, L., et al. 1992; Ozturk, Y., et al. 1992). Identifying additional or improved PXR activators may provide a novel set of tools to treat cholestasis.

Cancer

PXR plays an obvious role in cancer treatment because it is activated by chemotherapeutic compounds like paclitaxel (Synold, T.W., et al. 2001) and cisplatin (Masuyama, H., et al. 2005). Indeed, the up-regulation of drug metabolism and excretion genes by the receptor is one of the reasons that high doses of such antineoplastic agents are required for clinical efficacy. It would be advantageous to identify lead compounds or codrugs that limit PXR's activation of xenobiotic metabolism pathways to avoid the toxicities and potential drug-drug interactions associated with anticancer drugs.

Beyond this connection to cancer treatment, and more basic link between PXR and cancer development is emerging. In PXR's role as a bile acid sensor, the receptor protects tissues from the potentially toxic effects of these compounds, which are known to promote colon cancer (Uppal, H., et al. 2005). PXR also appears to be manipulated by cancerous cells to promote tumor growth. Dotzlaw et al. showed in 1999 that both the normal and shorter splice variant of PXR (PXR.2, which lacks a portion of the sequence insert in the receptor that is linked to its promiscuity) are expressed in human breast cancer cells (Dotzlaw, H., et al. 1999). Indeed, these authors found that PXRs isoforms were more abundantly expressed in breast cancer cell lines that lacked expression of the estrogen receptor (ER). These data suggest that local concentrations of endogenous compounds, as well as therapeutic agents, may be significantly altered in tumor cells by the overexpression of PXR.

A related pattern of PXR up-regulation combined with ER down-regulation was identified in endometrial cancer cells but not in normal cells from the same tissue (Masuyama, H., et al. 2003), suggesting again that PXR provides a growth advantage to

neoplastic cells by processing steroid-like compounds and/or xenobiotics. Indeed, in a follow-up paper, the same group has recently examined the effect of steroids, endocrine disrupting chemicals (EDCs), and anticancer agents on PXR-mediated expression from response elements derived from two different promoters, MDR1 and CYP3A4 (Masuyama, H., et al. 2005). Remarkably, they found that the steroid/EDC compounds like estradiol and phthalate utilized the CYP3A4 promoter more efficiently than MDR1, and conversely that the anticancer agents paclitaxel and cisplatin preferred the MDR1 over the CYP3A4 promoter. The molecular basis of this effect was traced to preferential recruitment of specific coactivators in a promoter- and ligand-specific fashion. Estradiol and phthalate exhibited a clear preference for the coactivator SRC-1 on the CYP3A4 promoter, while the anticancer drugs strongly recruited AIB-1 to the MDR1 promoter. These results and related data show that different ligands recruit different coregulators to the surface of PXR, and that these differential associations are promoter-specific (Song, X.L., et al. 2004). These results also indicate that opportunities exist for the identification of selective PXR agonists that may be useful in the direct treatment of cancer, or in tuning the efficacy of other chemotherapeutic compounds.

Future Directions

While our understanding of the regulation and action of PXR grows, both on the structural and functional level, several important areas of future study have emerged. The structure of the full-length PXR receptor in a ternary complex with RXRα and DNA remains a critical target for crystallographic studies. Such a structure would greatly

advance our understanding of nuclear receptor function in general, including how the flexible hinges between the receptors' DNA binding and ligand binding domains allow the heterodimer to contact both direct and everted regulatory elements. Initial strides have been made in examining the role that phosphorylation plays in PXR function, but clearly more work needs to be done on PXR and other members of the NR superfamily to elucidate how phosphorylation cascades impact receptor stability and function. In addition, while enticing recent work indicates that the activation of PXR by different ligands on different promoter elements leads to the recruitment of distinct transcriptional coactivators, it will be of tremendous interest to elucidate the role that such fine levels of ligand control play in PXR's function in numerous distinct tissues. Finally, the differential up-regulation of PXR in certain human cancers, as well as our growing understanding of the manner in which the receptor is activated by ligands, suggests that selective PXR modulators (SPRMs) might be of considerable use in treating neoplastic as well as metabolic diseases. PXR has moved quickly from an orphan receptor to an established transcriptional regulator and putative drug target. It seems clear, however, that we are only beginning to unravel the function and therapeutic potential of this unusual member of the nuclear receptor superfamily.

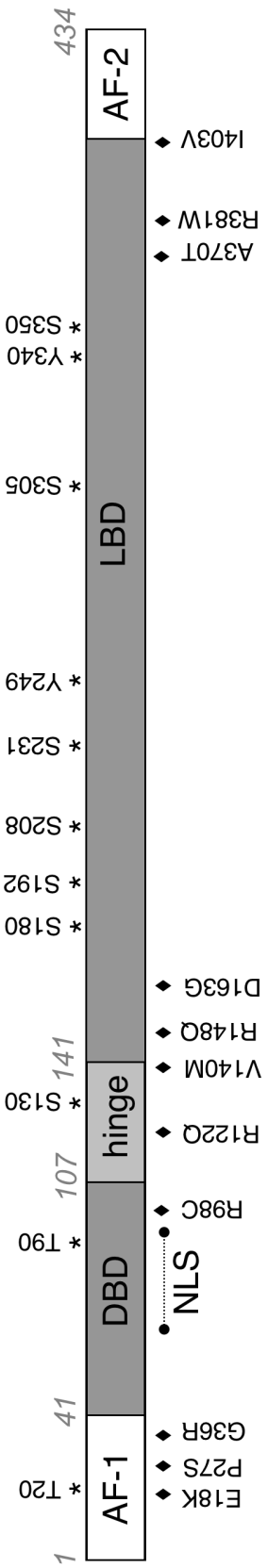

Figure 1.1. Cartoon depiction of human PXR domain structure and important features. The domain structure of human PXR is presented, including the N-terminal ligand-independent activation function 1 (AF-1), the DNA binding domain (DBD), the relatively short hinge region, and the ligand binding domain (LBD), which contains the ligand-dependent activation function 2 (AF-2). Reported spice variants and putative phosphorylation sites are depicted with diamonds and asterisks, respectively.

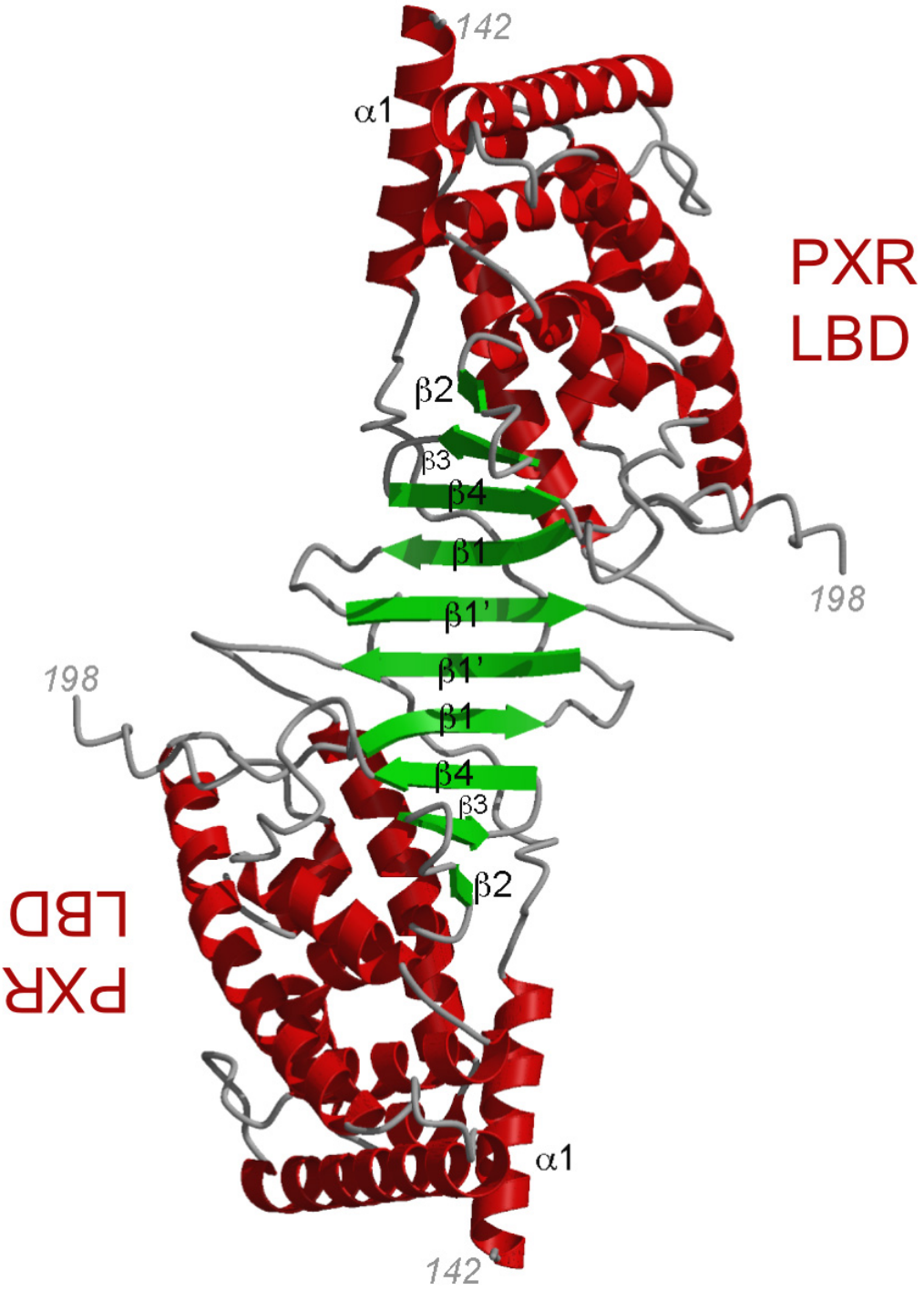

Figure 1.2A. PXR LBD homodimer. The homodimer of the human PXR ligand binding domain (LBD) as observed in the crystal structures reported to date.

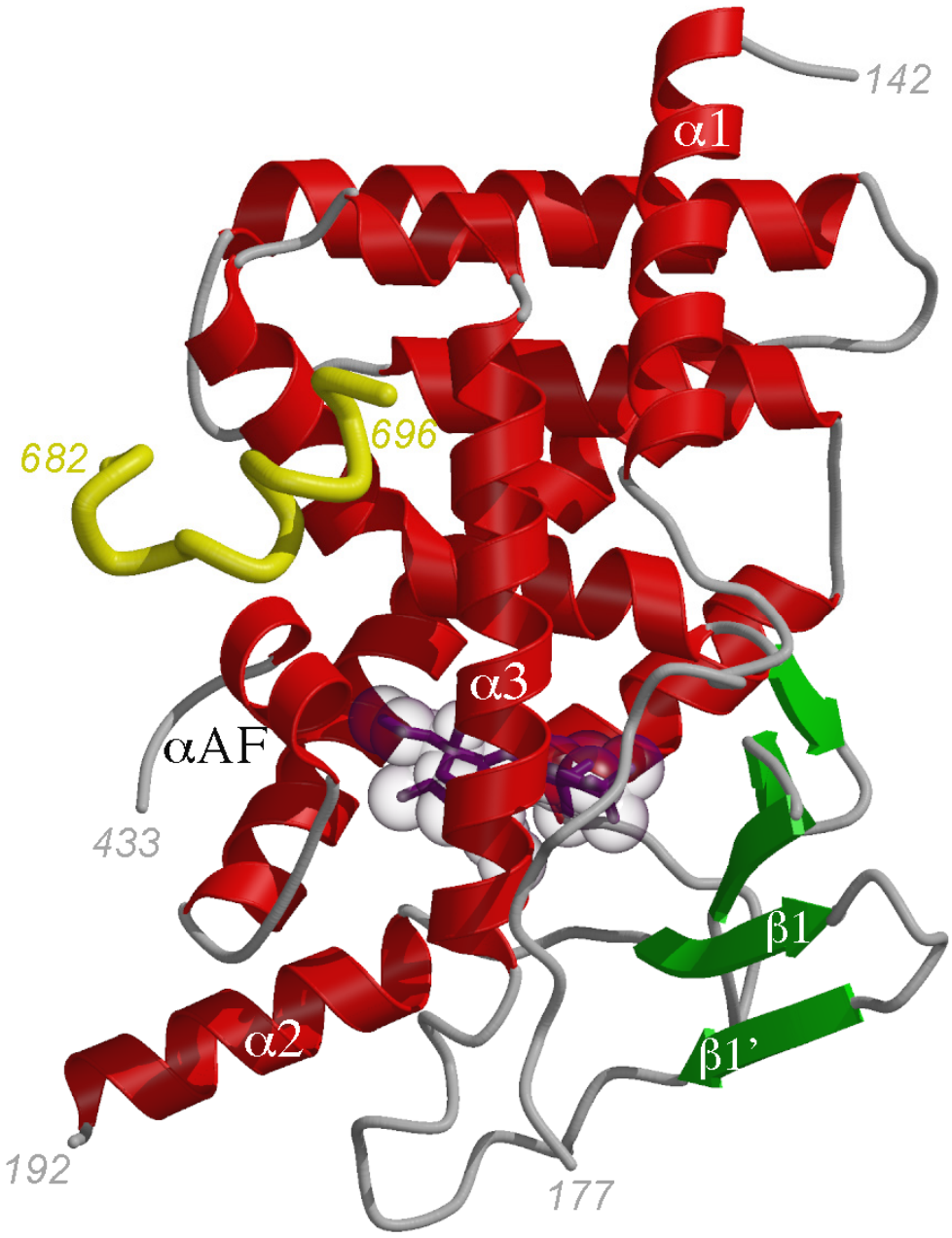

Figure 1.2B. Structure of PXR LBD bound to SR12813 and SRC-1 peptide. A monomer of the human PXR LBD in complex with the small cholesterol-lowering agonist SR12813 (purple) and a fragment of the human transcriptional coactivator SRC-1 (yellow). Amino acids 178-191 of the LBD are disordered in this structure.

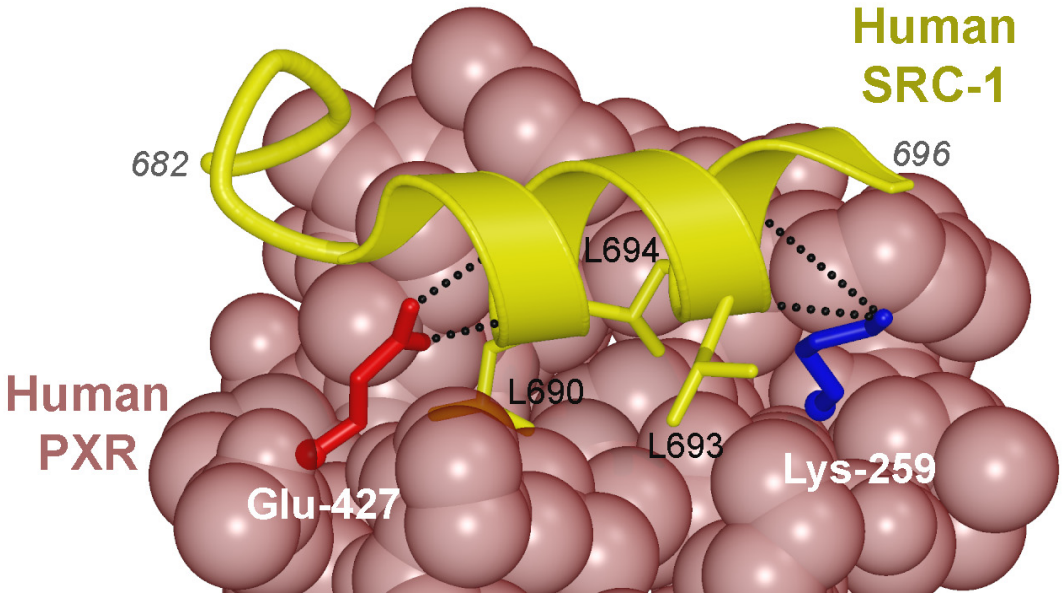

Figure 1.2C. Interaction of SRC-1 peptide with PXR LBD charge-clamp. A fragment of human SRC-1, containing three leucines of an LxxLL motif, stabilized on the surface of the human PXR LBD by the charge clamp formed by Lys-259 and Glu-427, which hydrogen bond to the main-chain of the coactivator helix.

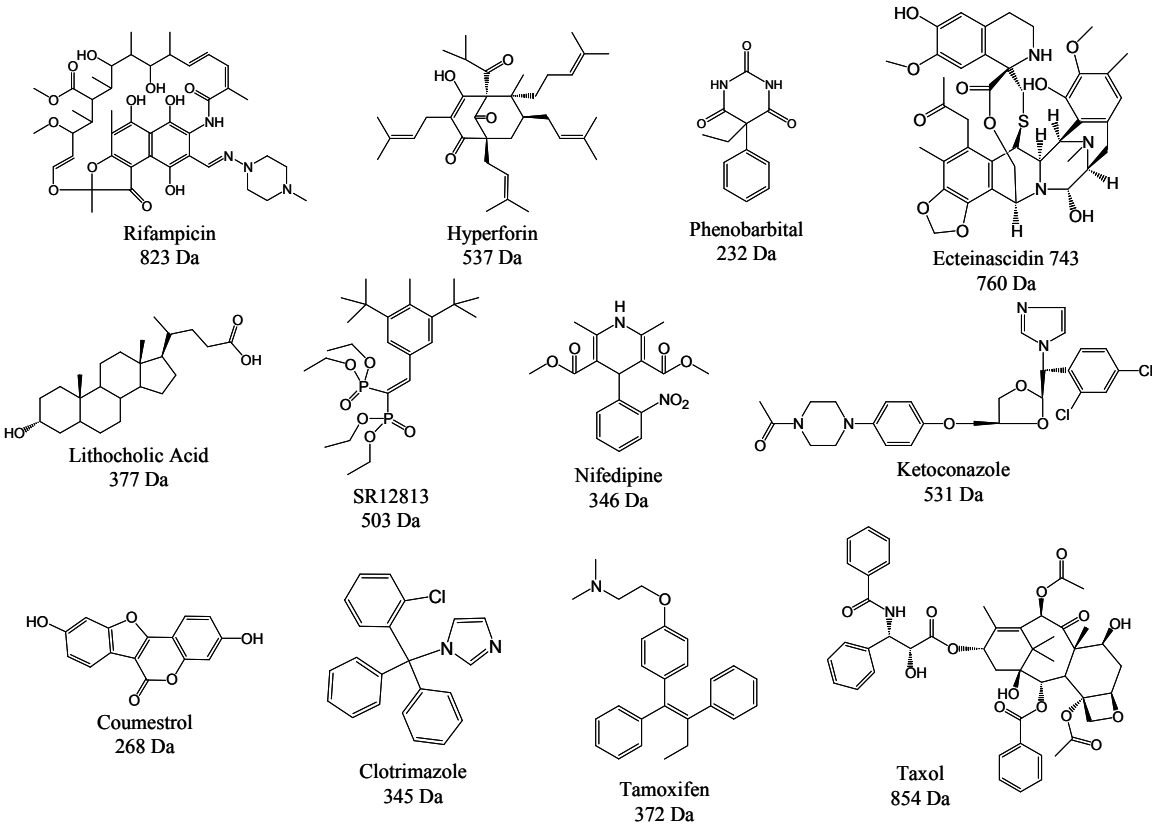

Figure 1.3A. PXR ligands. Endogenous and xenobiotic compounds of various sizes and shapes are ligands for PXR.

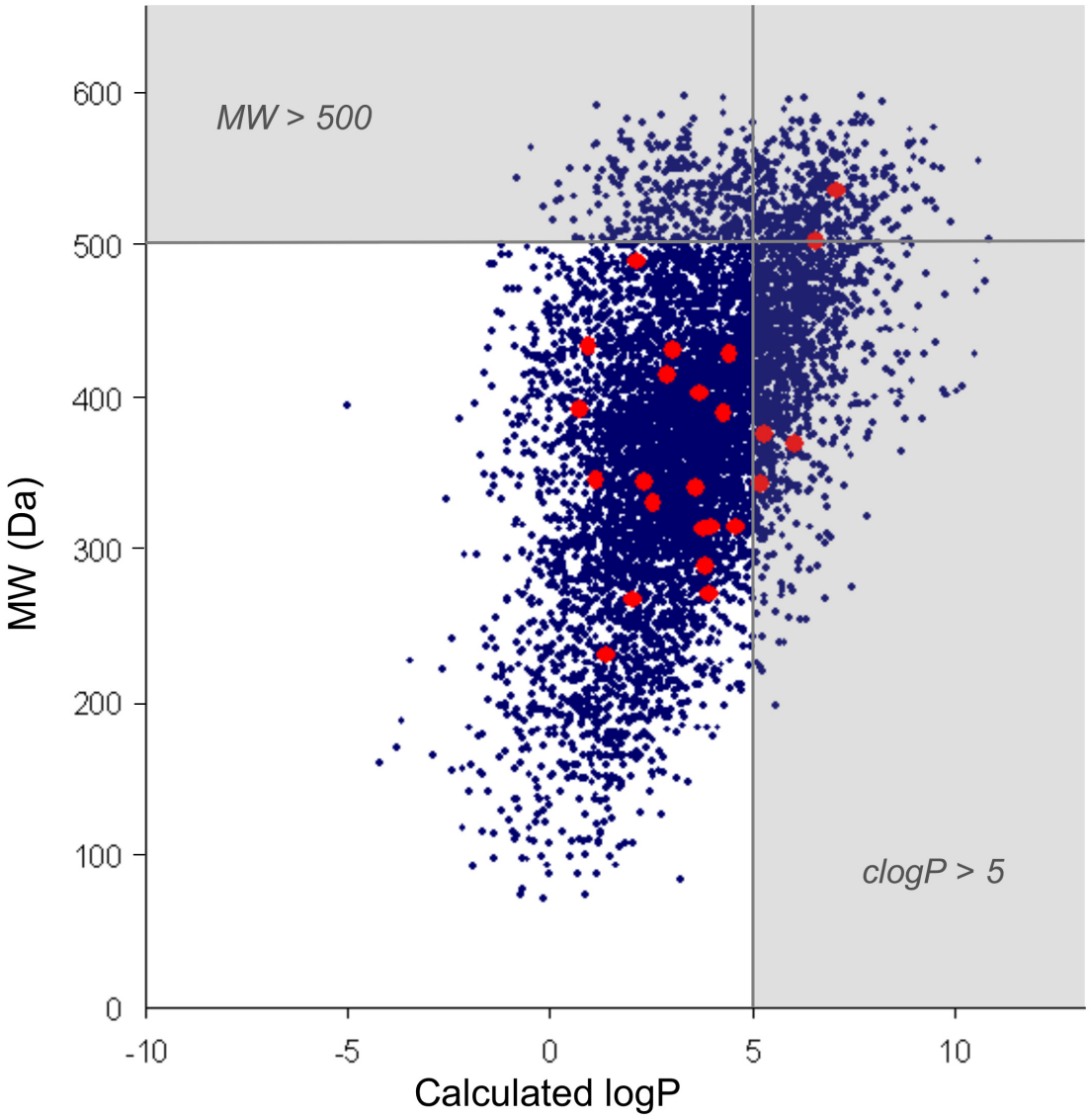

Figure 1.3B. The hydrophobicity versus molecular weight of PXR ligands compared to a database of drug-like molecules. The hydrophobicity (clogP) versus molecular weight of PXR ligands (red circles) compared to a database of 10,000 drug-like molecules (blue circles). The common limits in size and logP characteristics associated with successful drugs are shown.

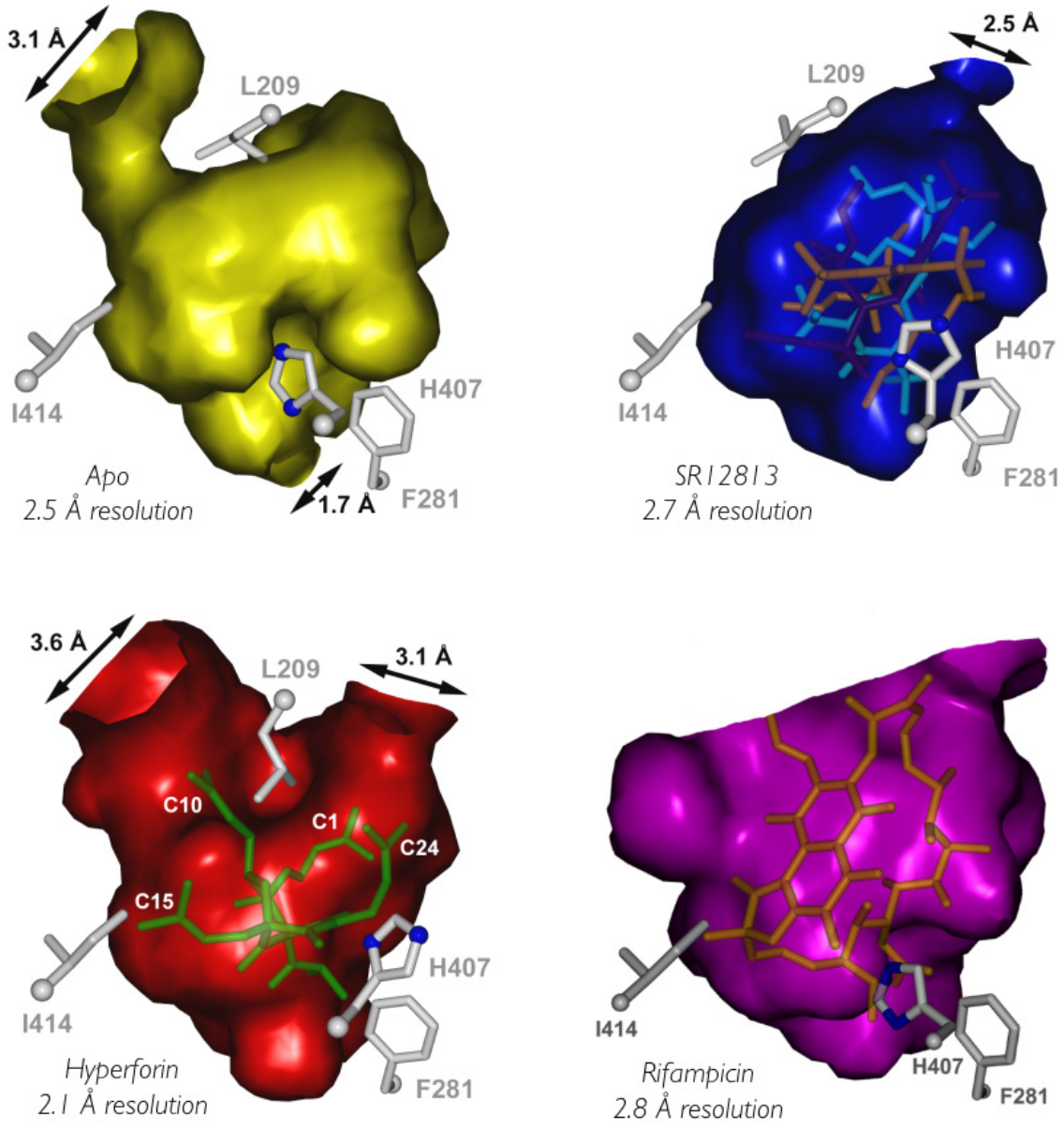

Figure 1.4A. PXR accommodates different ligands by changing the shape of the ligand binding pocket. The molecular surface of the PXR ligand binding pocket has been observed in several crystal structures to change in shape to accommodate distinct ligands.

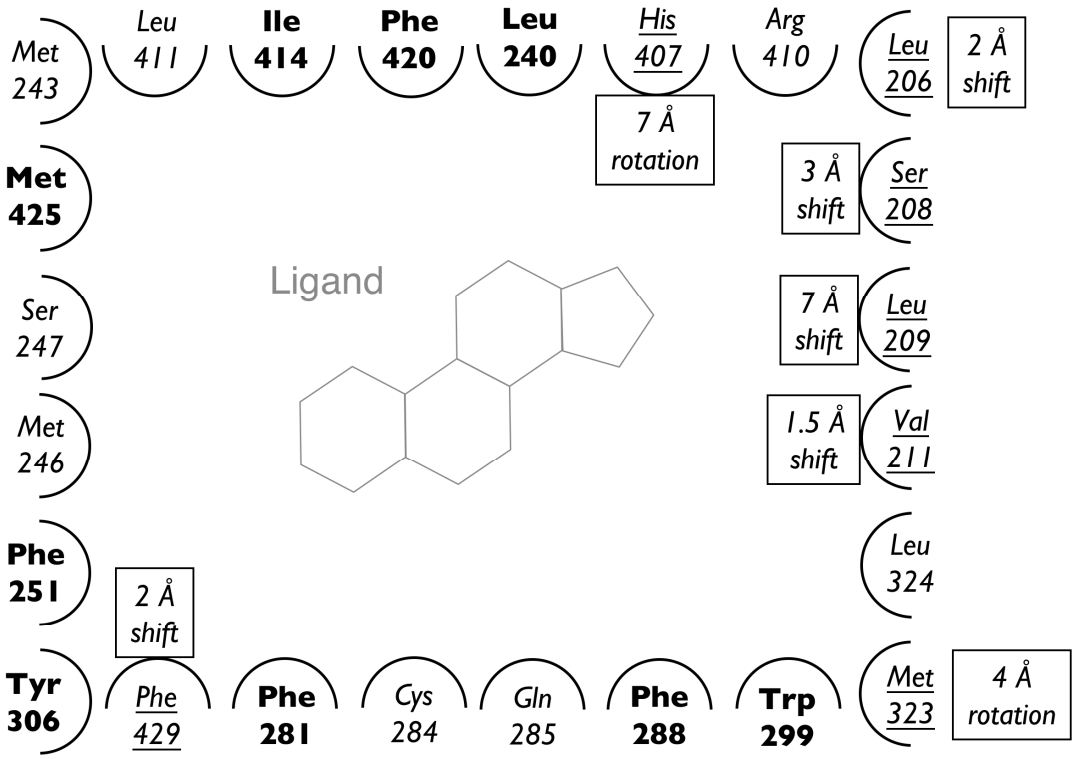

Figure 1.4B. PXR pocket side chains that shift. Amino acids side chains that line the PXR pocket have been observed to be rigid (bold), to exhibit small rotamer changes (italics), or to undergo relatively large rotamer changes or shifts in position (italics and underlined with magnitudes indicated).

Chapter 2

Discovery of a Consensus Motif in PXR LBD-Interacting Peptides and Production of Full-Length PXR for Future Studies

Abstract

The nuclear pregnane X receptor (PXR) regulates expression of many genes essential in mammalian drug metabolism including cytochrome P450-3A4 (CYP3A4), which degrades more than 50% of all prescription drugs. PXR is, like most nuclear receptors, a ligand-activated transcription factor, but it is unique in that it responds to a wide variety of structurally distinct compounds. Though sometimes PXR is represented as a binary switch, either on or off, variable modulation of PXR may lead to a wider range of responses via differential recruitment of transcriptional coregulators. In work presented here, GRIP-1 and PGC-1α were shown to coactivate PXR transcriptional activity on a DR-4 promoter and XREM-CYP3A4-luciferase promoter in both HepG2 and HeLa cells. This study then investigated whether PXR LBD in complex with different ligands recruits distinct peptide sequences by mapping the surfaces that PXR LBD presents in the presence of different ligands using phage-display and verifying these interactions in mammalian two-hybrid screens. Because portions of the N-terminal domain as well as the DNA it binds to are known to influence LBD conformation and coactivator binding preference, it is necessary to study this pathway in the context of the full-length receptor; therefore, full-length PXR was also expressed and purified for use in determining whether full-length PXR exposes novel surfaces (not present in the LBD alone) involved in tissue-specific protein-protein interactions. Additionally, a small intestine library was generated in a T7 bacteriophage system for use in determining full-length PXR-protein interactions and analyzing whether they differ between libraries generated from specific tissues. Attempts can be made to link these key surfaces of PXR

to function(s) by using peptides identified in this study to block PXR interaction with any proteins identified in the future from the T7 libraries. The preliminary results of these experiments as well as continued experiments with reagents generated in this study are necessary to understand clearly the regulatory mechanisms of PXR and how they influence drug efficacy or drug-drug interactions.

Introduction

PXR as a target for evaluating therapeutics

The pregnane X receptor (PXR) is a nuclear receptor that regulates expression of many genes essential in mammalian drug metabolism, including members of the 2B and 3A subfamilies of cytochrome P450s (CYP2B and CYP3A) and the xenobiotic efflux pump MDR1 (human multidrug resistance 1 protein). (Goodwin, B., et al. 2002) The 3A4 isoform is the predominant CYP expressed in the human adult liver and small intestine; this isoform is known to metabolize more than 50% of prescription drugs and is thought to be the key player in drug-drug interactions. (Guengerich, F.P. 1999; Li, A.P., et al. 1995; Maurel, P. 1996; Michalets, E.L. 1998) For instance, it is clear that activation of PXR by hyperforin (the psychoactive constituent of St. John's Wort) is responsible for decreased serum levels of vital drugs such as cyclosporin and indinavir. (Moore, L.B., et al. 2000) Additionally, in patients taking the antibiotic rifampicin, PXR has been implicated in increased clearance of cyclosporin A, oral contraceptives, glucocorticoid derivatives, and calcium channel blockers. (Takeshita, A., et al. 2002) Regulation of important xenobiotic metabolism genes by PXR has been well-documented; however, the mechanisms regulating PXR are poorly understood. With an increasing number of diseases necessitating combination therapies (AIDS, cancers, etc.) and rampant self-medication with over-the-counter remedies, it is critical to characterize the PXR signaling pathway.

Overview of PXR

Originally an orphan receptor, PXR was cloned prior to assignment of its cognate ligand or biological function, but was soon found to respond to the endogenous pregnanes and exogenous drugs. Like other nuclear receptors, PXR contains a highly conserved DNA binding domain (DBD) with two zinc finger domains and a ligand binding domain (LBD) in the C-terminal region. PXR is known for its ability to bind a wide variety of structurally distinct compounds (with ligands ranging in size from 200-850 Da). Though PXR is highly promiscuous, it does show inter-species differences in specificity: for example, mouse PXR is not activated efficiently by SR12813 (a cholesterol drug), but human and rabbit PXR are; and mouse PXR is activated by PCN (pregnenolone 16α-carbonitrile), while human and rabbit PXR are not. (Watkins, R.E., et al. 2001)

The structure of the human PXR LBD has been determined in the absence of ligand and in the presence of hyperforin (Watkins, R.E., et al. 2003b) or SR12813 and a peptide fragment of coactivator SRC-1 (Watkins, R.E., et al. 2001; Watkins, R.E., et al. 2003a). The structure is shown in **Figure 1.2B**; it contains ten alpha helices and a five-stranded beta sheet (in contrast to the typical nuclear receptor's three-stranded beta sheet). (Watkins, R.E., et al. 2001; Watkins, R.E., et al. 2003a; Watkins, R.E., et al. 2003b) The ligand-binding pocket is very large (1100-1500$Å^3$) and predominantly hydrophobic with the eight polar residues evenly distributed throughout the twenty hydrophobic residues that line the pocket. (Watkins, R.E., et al. 2001) The coactivator fragment (cyan in **Figure 1.2B**) binds in a groove formed with residues from the AF-2 helix (αAF; activation function), α3, and α4; the coactivator binds adjacent to the AF-2 helix that is responsible for ligand-dependent transcriptional activation (labeled αAF in

Figure 1.2B). The additional beta strands and the novel α2 are part of a 60 residue insert not found in sequences of other nuclear receptors. (Watkins, R.E., et al. 2003a) Indeed, at least thirteen residues of this sixty amino acid insert are disordered in the structure (Figure 1), providing tantalizing clues for an additional or novel surface on PXR (beyond the coactivator cleft) for protein-protein interactions, underscoring the relevance of mapping and characterizing these surfaces of full-length PXR that mediate protein interactions contributing to transactivation.

Coregulators of PXR

While PXR shares many characteristics with other members of the nuclear receptor superfamily, it also exhibits traits that are significantly unique. For example, though PXR is a ligand-activated transcription factor, it is distinctive from other nuclear receptors in that it responds to a large number of structurally diverse ligands. While some receptors are well-characterized (such as the estrogen receptor), PXR is less well understood, especially regarding the binding partners that help PXR stimulate or repress transcriptional activation of a target gene. Like other nuclear receptors, PXR binds to XREs (xenobiotic response elements) as a heterodimer with RXRα in the nucleus on the DNA of target genes. PXR has been shown to interact with the corepressor SMRT in the absence of agonist. (Johnson, D.R., et al. 2006) The corepressor prevents transcription of the target genes by deacetylating histones within their promoter regions. In the presence of agonist, the receptor-agonist complex can associate with coactivators (*e.g.* SRC-1) (Itoh, M., et al. 2006; Li, T., et al. 2007; Masuyama, H., et al. 2005) and allow large transcription complexes to form on target gene promoters. Either the coactivators or the

proteins they recruit have histone acetyl transferase activity, leading to chromatin decondensation and gene transcription. However, transcriptional activity is also influenced by promoter, nature of the agonist, and expression levels of coregulators in particular cell lines.

The discovery of selective estrogen receptor modulators (SERMs), compounds with the ability to act as agonist or antagonist depending on the tissue context, has altered the view of nuclear receptor ligands. (McDonnell, D.P. 1999) More specifically, a compound may behave as an agonist in one tissue and an antagonist in another. Clearly a binary switch is insufficient to represent such intricacies as these tissue-specific interactions or the influence of differential cofactor expression levels. The diversity in ligand structure alone may add a level of complexity not shared by prototypical nuclear receptors.

Recent data analyzing PXR protein interactions include directed yeast and mammalian two hybrid studies, as well as GST pull-down and coimmunoprecipitation assays (Bhalla, S., et al. 2004; Sugatani, J., et al. 2005; Synold, T.W., et al. 2001; Takeshita, A., et al. 2002). In a yeast two-hybrid experiment, Masuyama et al. confirmed that full length mouse PXR (mPXR) in the presence of some endocrine disrupting chemicals (nonylphenol or phthalic acid) interacts with steroid receptor coactivator-1 (SRC-1) and receptor interacting protein 140 (RIP-140), but not suppressor for gal-1 (SUG1). (Masuyama, H., et al. 2000) However, in the presence of progesterone, dexamethasone, or pregnenolone mPXR interacted with SRC-1 and RIP140, as well as SUG1. (Masuyama, H., et al. 2001) As discussed above, the cross-species specificity of PXR emphasizes the importance of performing these experiments with *human* PXR.

Studies of coregulator interactions with human PXR to date use an LBD-only construct and are summarized below. (Synold, T.W., et al. 2001; Takeshita, A., et al. 2002) In 2001, directed mammalian two-hybrid experiments were performed in CV-1 cells using human PXR LBD (hPXR LBD) in the presence of paclitaxel or docetaxel, demonstrating that hPXR LBD interacts with human SRC-1, mouse glucocorticoid receptor interacting protein 1 (GRIP1), human activator for thyroid hormone and retinoid receptors (ACTR), and human vitamin D receptor-interacting protein complex component (DRIP205, also called PBP and TRAP220). (Synold, T.W., et al. 2001) In this same study, hPXR LBD alone and in the presence of docetaxel interacted with the corepressor silencing mediator of retinoid and thyroid hormone action (SMRT), and to a lesser extent nuclear receptor corepressor (NCoR). (Synold, T.W., et al. 2001) However, because the N-terminal domain and DBD of nuclear receptors has been shown to modulate conformation of and interactions with the adjacent LBD (Hall, J.M., et al. 2002), it is critical to determine these interactions in the context of the full-length receptor, which this study enables. Additionally, a subsequent study has suggested that the effects of a xenobiotic on the PXR LBD-SMRT interaction are cell-type specific because the PXR LBD-SMRT interaction was increased by rifampicin or corticosterone treatment in HepG2 cells, while this effect did not occur in CV-1 cells. (Takeshita, A., et al. 2002) These findings suggest that regulation of PXR is indeed a complex, cell type-specific process.

In order to better characterize PXR, M13 phage display system was used to identify peptides that PXR LBD binds in the presence and absence of two very different ligands (small SR12813, and large rifampicin). Additionally, full-length PXR was

generated and panned with M13 phage display. Three surfaces are present in the ligand binding domain (LBD) of PXR: i. the coactivator binding cleft, ii. the interface for heterodimerization with RXR, and iii. a novel PXR homodimerization interface. It is possible that full-length PXR exposes novel surfaces involved in tissue-specific protein-protein interactions; this study identified a consensus sequence for peptides that bound to PXR LBD and created tools to help advance understanding of PXR's interaction profile.

Materials and Methods

PXR LBD expression and purification

PXR LBD was expressed and purified as previously determined in our laboratory. (Watkins, R.E., et al. 2001) Briefly, human PXR LBD (residues 130-434) was N-terminally His-tagged and coexpressed with a fragment of SRC-1 (residues 623-710) in *Escherichia coli* BL-21 Gold cells (Stratagene). Cells were lysed by sonication, and the clarified cell lysate was purified using ProBond nickel-chelating resin (Invitrogen). The Ni-column fractions were analyzed using a Bradford assay only, and all fractions containing protein were loaded to an SP sepharose column as they eluted from the Ni-column. Protein eluting from the SP column was diluted to prevent precipitation caused by high salt concentrations. The fractions containing PXR were concentrated to 5 mg/mL.

Full length PXR and RXR expression and purification

Full-length PXR was subcloned from the pSG5 vector (generaous gift from G. Bruce Wisely at GlaxoSmithKline) into the pDW464, a BioBac baculovirus transfer vector (Duffy, S., et al. 1998) The BioBac technology fuses a 23 amino acid biotin acceptor peptide (BAP) to the preferred terminus of a protein (in this case the N-terminus), and allows co-expression of the protein of interest and *E.coli* biotin holoenzyme synthetase (BirA) in *Spodoptera frugiperda* (Sf9) cells. BirA attaches a biotin moiety to a single lysine residue in the BAP sequence. The pDW464 transfer vector encoding full length human PXR and *E.coli* biotin holoenzyme synthetase (BirA) was recombined with baculovirus DNA in vivo using the Bac-to-Bac baculovirus expression system (Invitrogen). Cellfectin Reagent (Invitrogen) was used according to manufacturer's instructions to transfect 9 x 10^5 Sf9 cells (in one well of 6-well plate) with the generated bacmid (1 μg). After transfection, the cells were incubated at 27°C for 3 days. The virus-containing media was collected and 0.4 mL (estimated MOI = 0.25 pfu/cell) was used to infect 8 x 10^6 cells in a 10 cm plate for 2 days. Sequential amplifications were performed in 10 cm plates with 8 x 10^6 cells. Virus-containing media was saved, and cells were scraped, lysed, and analyzed by sequential Western blot as described below to verify production of biotinylated PXR. The RXR recombinant baculovirus used was a gift from Julie Hall (Duke University).

Sf9 cells were grown in suspension culture in Sf-900II Serum-free medium (SFM) at 27°C. 100 mL of cells at a density of 2.5 x 10^6 cells/mL were infected with either 1 mL of PXR baculovirus or 0.75 mL of RXR baculovirus then allowed to grow for 48 hours. Centrifugation was used to harvest the cells, and cell pellets were snap-frozen

in a dry-ice/ethanol bath then stored at -20°C. Cells pellets were thawed on ice, resuspended in lysis buffer (50 mM Tris-HCl pH 8.0, 10 mM β-mercaptoethanol, 100 mM KCl, 1% NP-40, 1:200 protease inhibitor cocktail set III, 50 mM NaF, 50 mM β-glycerophosphate) and rocked at 4°C for 1 hour to allow lysis. Lysate was then cleared by centrifugation at 48,000 x g for 30 min at 4°C. Affinity purification was done according to the commercial protocol using streptavidin mutein matrix (Roche); however, a different elution buffer was used (50 mM Tris-HCl pH 8.0, 200 mM NaCl, 2 mM EDTA, 4 mM DTT, 10% glycerol, 1 mM CHAPS, 5 mM biotin).

Western Blot analysis

Cell lysates, purification washes, and fractions from above expression and purification were separated on a 10% SDS-PAGE gel, then transferred to nitrocellulose (Amersham Biosciences, Inc.). PXR protein was detected using the PXR N-16 antibody and horseradish peroxidase-conjugated donkey anti-goat IgG (Santa Cruz Biotechnology). Biotinylated proteins were detected using the streptavidin-horseradish peroxidase conjugate (Amersham Biosciences, Inc.). Chemiluminescence was used for visualization (Amersham Biosciences, Inc.).

Phage Display

Phage display has been successfully used for many different nuclear receptors (Chang, C., et al. 1999); and when determining the adaptability of PXR to this protocol, ERβ (estrogen receptor beta) was used simultaneously as a positive control. For panning,

10 pmol of pure PXR (LBD or full length) per well was diluted in 100μL of $NaHCO_3$ (pH 8.5) containing the appropriate ligand (1 μM of either SR12813, rifampicin, or 17-β estradiol) and incubated in a 96-well tissue culture plate (Corning) at 4ºC overnight. The wells were then blocked with MPBS [2% milk in PBS, 137mM NaCl, 2.7 mM KCl, 4.3 mM Na_2HPO_4, 1.4 mM KH_2PO_4 (pH 7.4)] containing appropriate ligand at room temperature for one hour, and the phage library was pre-cleared by mixing 5 x 10^9 phage per well with 100 μL MPBS (with ligand, if appropriate) on ice for one hour. The blocking/pre-clearing step ensures that the peptides that non-specifically bind protein were removed from the library. Subsequently, the wells coated with target protein were washed five times with 300 μL PBST (PBS plus 0.1% Tween 20); then the pre-cleared phage libraries were added to the wells. Phage were incubated with the target protein for 2 hours at room temperature, then wells were washed ten times with 300 μL PBST to remove phage that had not bound to the immobilized protein. The phage that bound were eluted from the wells with 100 μL of 0.1 M HCl for 10 minutes, excess acid was neutralized at the end of elution with 50 μL of 1 M Tris-HCl (pH 7.4). The eluted phage (minus 15 μL reserved to determine elution titer) were inoculated into 5 mL of log-phase DH5αF' for 20 minutes without shaking at 37°C, then amplified for 5 hours in a shaking incubator at 37°C. The supernatant of the DH5αF' culture containing the amplified phage was harvested and stored at 4ºC. To determine titers, serial 10x dilutions were made of eluted phage and amplified phage in PBST; the dilutions (10^{-3}, 10^{-4}, 10^{-5} for elution titer and 10^{-7}, 10^{-8}, 10^{-9} for amplification titer) were plated with X-gal, IPTG, and fresh DH5αF'. After overnight incubation, the blue colonies were counted and used to determine the pfu (plaque forming units) for each elution and amplification. Increases in

elution titer are indicative of selection for phage expressing peptides that specifically bind to the target protein. In the next pan, 5×10^9 amplified phage from the previous pan was used in place of the library, and the steps were repeated three more times. Enzyme-linked immunosorbent assay (ELISA) detecting the M13 coat protein (described below) was used to confirm enrichment of phage that bound to PXR LBD. Peptide inserts were amplified with PCR and subcloned into the pM3.1 vector for mammalian two-hybrid testing. Twenty-four constructs were randomly selected from each library-ligand combination and sequenced. The sequencing results were individually verified and translated.

Enzym-linked immunosorbent assay

For the ELISA, protein was immobilized onto a 96-well tissue culture plate (Corning) using the same procedure used for panning. Unlike panning, however, for each protein well a corresponding well was coated overnight with only milk to be used for the milk control. Just as described above for panning procedure, all wells were blocked with MPBS. A volume of supernatant corresponding to 5 x 10^9 phage was blocked with MPBST (PBS plus 2% milk and 0.1% Tween 20) for 1 hour on ice. The wells were then rinsed five times with 300 μL PBST, and the phage/MPBST solution was incubated with the target protein (or milk for the control) in the wells for 1 hour at room temperature. Wells were washed five times with 300 μL PBST to remove non-binding phage; but, instead of eluting, an ELISA was performed. Horseradish peroxidase-conjugated anti-M13 antibody (Pharmacia) was diluted 1:5000 in PBST, then 100 μL of the diluted conjugate was added to each well and incubated at room temperature for 1 hour. The

wells were washed ten times with 300 μL PBST, then 100 μL of ABTS solution (2'-2'-azino-bis-ethylbenzthiazoline-6-sulfonic acid solution with freshly added 0.05% H_2O_2) was added to each well. After 10 minutes, the absorbance at 405 nm was read using a microtiter plate reader. Comparison of each phage pool incubated with PXR LBD to the matching phage + milk control demonstrated the isolated phage specifically interacted with PXR LBD.

Cell culture and transient transfections

HepG2 and HeLa cells were cultured as previously described in the literature using minimum essential medium (GIBCO, Invitrogen) supplemented with 10% fetal bovine serum (FBS, HyClone), 0.1 mM nonessential amino acids, and 1 mM sodium pyruvate (GIBCO, Invitrogen) and were maintained in a humidified 37°C incubator 5% CO_2. (Chang, C., et al. 1999) 24 hours before transfection, the cells were seeded into 96-well or 24-well plates. For mammalian two-hybrid, a modification of the CloneTech protocols was used. (Chang, C., et al. 1999) First, the phage peptides were amplified by PCR using primers to the identical vector sequences flanking the diverse peptides. Then these sequences containing the diverse peptides were ligated into the mammalian two-hybrid pM GAL4-DNA binding domain cloning vector (CloneTech). Initially, five colonies were chosen at random for each of the eight samples (peptides from the LxxLL library that bound PXR alone, PXR and SR12813, PXR and rifampicin, or PXR and 17β-estradiol and peptides from the CoRNR library that bound each of these species); the DNA was amplified in and isolated from DH5α. HepG2 cells were transiently transfected using Lipofectin (Invitrogen) per the manufacturer's instructions in a 96-well plate with a

single pM (Gal4DBD) vector, the VP16 vector containing full length PXR, the 5×Gal4Luc3 plasmid, and the CMVβGal plasmid. The cells were incubated with the DNA-Lipofectin mix for 5 hours; then the solution was removed to stop the transfection and new medium was added. After 24 hours, media was exchanged for fresh media containing ligands (1 μM SR12813, 10 μM rifampicin, and 100 μM 17β-estradiol) were added. After 16 hours incubation at 37ºC, luciferase and β- galactosidase activities were measured. Normalization of luciferase induction with β-galactosidase activity expressed from a constitutive cotransfected control plasmid represented specific interaction between peptide and PXR.

For activation of transcription by SRC-1, GRIP-1 or PGC-1α, Lipofectin was used to transfect the following plasmid amounts per triplicate: 50 ng of either pcDNA3.1nvDEST or pcDNA3.1_PXR, 1500 ng of either pGL3_XREMluc+ or pDR-4, 100 ng CMVβGal, and increasing amounts of either pSG5-SRC-1, pSG5-HA-GRIP-1, or pcDNA-M-H-fl-PGC1a plasmid. The number of moles of promoter was held constant by using appropriate concentrations of empty pSG5 or pcDNA3.1 vectors; finally, total DNA input was balanced using the empty plasmid PBSII. The cells transfected, treated, and analyzed as above.

Generation of T7 libraries

Human small intestine poly(A) RNA was purchased from Ambion, Inc. T7 Select protocols and reagents, including Orient Express cDNA cloning system, (Novagen) were used according to the manufacturer's instructions to generate 10-3 and 1-1 T7 libraries from small intestine mRNA (Ambion).

Results and Discussion

Activation of PXR Transcription by GRIP-1 and PGC-1α

To determine whether PGC-1α and GRIP-1 were able to potentiate PXR activity on the DR-4 and XREM-CYP3A4-luciferase (Watkins, R.E., et al. 2001) promoter reporter constructs, HepG2 and HeLa cells were transiently transfected with fixed amounts of PXR and increasing amounts of coactivator plasmid in the presence and absence of rifampicin. Both GRIP-1 and PGC-1α activated PXR transcription on the DR-4 and XREM promoters in HepG2 and HeLa cells. Activation profiles on the XREM-CYP3A4-luciferase promoter from HepG2 cells are presented in **Figures 2.1, 2.2, and 2.3**. (HeLa and DR-4 data not presented for redundancy.) The same experiment was performed using SRC-1 for comparison. GRIP-1 and PGC-1α expression resulted in nearly 2-fold greater transactivation than did SRC-1. Additionally, **Figure 2.4** shows a dose-response of PXR transfected together with a constant (500 ng) amount of GRIP-1. Coexpression of PXR with GRIP-1 or SRC-1 resulted in a small amount of rifampicin-independent transcription that was substantially increased by addition of rifampicin. However, coexpression of PXR and PGC-1α primarily seemed to affect the activity of PXR in the absence of ligand, though addition of rifampicin did enhance the transcriptional activity. This data could be explained by PGC-1α interacting with the DBD of PXR, as has been observed for FXR (Zhang, Y., et al. 2004).

PXR has been shown to bind to PGC-1α and to compete with HNF-4 for interaction with PGC-1α, thereby interfering with HNF-4 activity on CYP7A1 and

CYP8B1 (Bhalla, S., et al. 2004). Additionally, PXR demonstrated an ability to interact with GRIP-1 in a GST pull-down assay (Sugatani, J., et al. 2005). The results presented here demonstrate that GRIP-1 and PGC-1α are quite effective at potentiating PXR transcription on the DR-4 promoter and the XREM-CYP3A4-luciferase promoter in HepG2 and HeLa cells.

Production of full length PXR and RXR

Much of the information currently available about PXR-coregulator interactions was determined using LBD constructs. Though some surfaces presented by full-length PXR may overlap with those presented by the LBD alone, it is critical to use full-length receptor for studying the PXR cellular signaling pathway. Until now, this effort has been hindered by the inability to prepare sufficient quantities of pure PXR. These difficulties were overcome by utilizing the BioBac baculovirus expression system in *Spodoptera frugiperda* (Sf9) cells. (Duffy, S., et al. 1998) The BioBac technology fuses a ~23 amino acid biotin acceptor peptide (BAP) to the preferred terminus of a protein (the N-terminus of PXR), allowing the co-expressed *E.coli* biotin holoenzyme synthetase (BirA) to attach a biotin moiety to a single lysine residue in the BAP sequence. The RXR baculovirus used was also generated using the BioBac technology. Full length PXR and RXR were purified separately using a single step of affinity chromatography with streptavidin mutein matrix (Roche Applied Science). Sequential Western blot analysis demonstrated that the band migrating at approximately 52 KDa was biotinylated PXR. Each 100 mL of Sf9 culture yielded approximately 300μg of pure RXR and 100 μg of pure PXR.

Panning PXR LBD and full length PXR.

To determine consensus peptide motifs that interact with PXR LBD, the LxxLL and CoRNR (CoRepressor of Nuclear Receptors) libraries have been screened against wild-type PXR LBD alone or in the presence of 1 μM agonist (SR12813, rifampicin, or 17β-estradiol). The peptide sequences from interacting phage were amplified using PCR, then subcloned into a mammalian two-hybrid vector for testing interaction with full length PXR. Additionally, full-length PXR has been used as a target for screening the LxxLL, C-S, and X_6LX_6 libraries. For full-length studies, three rounds of panning were completed; however, due to time constraints cloning and mammalian two-hybrid verification of interaction were not completed.

PXR LBD panning results

The LxxLL library is based on the known coactivator motif, but contains randomized flanking sequences of seven amino acids (x_7-L-x-x-L-L-x_7). (Chang, C., et al. 1999) Similarly constructed, the CoRNR library is based on the known corepressor motif L-x-x-H/I-I-x-x-x-I/L. (Huang, H.J., et al. 2002) **Figure 2.5** contains elution titer data for pans of PXR LBD in the presence of rifampicin with both libraries; these data are representative of data for all pans. As **Figure 2.5** indicates, sequential panning (using the phage from the previous pan) leads to an increase of elution titer indicating enrichment of phage displaying peptides that bind to the PXR LBD-rifampicin complex. (In these experiments, pans with ERβ were performed in parallel as a positive control; results not shown.) Elution titer is only a rough estimate of target phage interaction, so the more sensitive ELISA was used to verify that the panning enriched for those phage bearing

peptide sequences that bind to PXR LBD. The ELISA results indicate that the phage bound to PXR LBD with an increase in binding phage seen in the second pan for the CoRNR library (**Figure 2.6**). The signal for the LxxLL library was already high in the first pan, indicating a rapid enrichment for this library (**Figure 2.6**). The milk control did not show enrichment, confirming that this binding was specific for PXR LBD-ligand (data not shown). Decrease in interaction seen by ELISA in later pans with LxxLL could be explained by loss of weak binders in later pans or by some phage species amplifying much faster than the rest. For initial mammalian two-hybrid studies, phage from the second pan for both libraries in the presence of each PXR LBD/ligand combination were chosen to try to ensure the greatest diversity of peptide sequences.

To determine whether the peptides found to interact in the phage display assay also interact in a cell-based system, mammalian two-hybrid experiments were conducted. Each mammalian two-hybrid screen was performed at least twice with triplicate samples in each experiment. Interaction patterns were classified as one of five categories:

A) peptide construct was not recruited by full-length PXR in the absence or presence of agonist

B) peptide construct was not recruited by full-length PXR in the absence of agonist, but was recruited with the addition of agonist

C) peptide construct was recruited equally well in the absence and presence of agonist

D) peptide construct was recruited in the absence of agonist, but presence of agonist further enhanced the interaction

E) peptide construct was recruited in the absence of agonist, and addition of agonist diminished the interaction.

Results representative of each class of peptide are presented in **Figure 2.7**. All results are summarized and classified in **Tables 2.1-6**. Initially, 96-well plates were used for the mammalian two-hybrid assays; subsequently, 24-well plates were used because it was determined that the 24-well plate format provided less experimental variation.

Sequences that interacted with a class D pattern (the most abundant) were examined for conserved motifs and were compared to known NR box classes I-IV. **Figure 2.8.** A proline in the -2 position was highly conserved among peptides that interact with PXR LBD; and many of these sequences also contained a hydrophobic residue at the -1 position, making them members of class II NR boxes. Know coactivators with class II NR boxes include TRAP220 and RIP140 (Chang, C., et al. 1999). The motif discovered for PXR extends beyond the class II NR box: preferring a polar residue in the -3 position.

One unexpected result was that CoRNR peptides bound to PXR LBD in complex with agonist. Sequence analysis demonstrated that while these peptides had the conserved corepressor motif discussed, some also had LxxLL-like (LxxML, IxxLL, etc.) motifs. (**Figure 2.9**) All had at least one of the three preferred upstream residues, and most of the peptides had all three. One CoRNR construct demonstrated interaction pattern E (pM_R_C3). Two other constructs (pM_alone_L18 and pM_alone_L19) also demonstrated interaction pattern E, although pM_alone_L19 interaction was only consistent in the presence of rifampicin. The pM_alone_L18 construct (and pM_alone_L19 in the presence of SR12813) exhibited interaction profile C in other trials.

The sequences of the three peptides that interacted with pattern E are shown in **Figure 2.10**. The pM_R_C3 sequence only has the -3 polar residue. However this is also true of the pM_alone_C1 sequence (identical sequence to pM_S_C15 and pM_R_C1) which interacts with PXR in a different profile in the mammalian two-hybrid system.

Of the peptides that followed the class A profile of interaction, 40% did not sequence. Poor sample quality would explain the lack of interaction in the mammalian two-hybrid assay for these constructs. For the other 60%, however, other options must be considered. These constructs are listed with their sequences in **Figure 2.11**. Two of them were identical to sequences from other phage that did interact in the mammalian two-hybrid system. Because the sequences discussed in this section were selected using PXR LBD, it may be that some of the profile A sequences do not interact with full length PXR which was used in the mammalian two-hybrid assay, but will interact when tested with a PXR LBD construct. Two of the sequences do not contain any of the upstream three residues of the described interaction motif, but several of the sequences contain one or more of those characteristics. Clearly the next step in this process is to test all of the peptides in the mammalian two-hybrid system using a PXR LBD pVP16 construct.

Full-length PXR panning results

Full-length PXR alone and in the presence of 1μM SR12813 or rifampicin was used to pan the LxxLL, C-S, and X_6LX_6 libraries. Three rounds of panning were completed, and ELISA results are depicted in **Figure 2.12**. Full-length PXR behaved quite differently than did PXR LBD as evidenced by the LxxLL library not beginning to enrich until the third round of panning. At least one more pan of the X_6LX_6 library and

two more pans of the LxxLL library should be performed, followed by cloning and mammalian two-hybrid verification of interaction with full-length PXR and PXR LBD pVP16 constructs.

Generation of T7 libraries

With the example of SERMs variable regulation of the estrogen receptor and the discrepancy between PXR results in CV-1 and HepG2 cells, it is increasingly necessary to think of PXR regulation in a tissue-specific context. For this reason, a high-throughput screen of tissue-specific T7 libraries should be done on full-length PXR. The T7 cDNA expression system is novel because its libraries are tissue specific and, because the phage lyse, the protein fragment size is not as limited as it is in the M13 system; indeed the T7 system has up to a 1200 amino acid capacity. Libraries existing in the lab include those developed from liver and colon cell lines as well as brain (where PXR is suggested to play a role in mood). PXR is highly expressed in liver, colon, and small intestine; since no library for small intestine had been generated yet, 1-1 (0.1-1 copy target per phage) and 10-3 (5-15 copies target per phage) small intestine libraries were successfully generated from purchased human poly(A) RNA, although time did not permit screening.

Future Directions

The preliminary results presented here indicate that full length PXR can be produced and that PXR is amenable to the phage display and mammalian two-hybrid

protocols developed in the McDonnell lab. To complete the studies, the M13 peptides found by panning PXR LBD should be tested in mammalian two-hybrid with the VP16_PXR LBD constructs that have been generated. Additionally, the M13 phage that were found by panning full length PXR should be carried forward through amplification, sequencing, and mammalian two-hybrid (analyzing with ligand panned with, and other ligands) as well. It will be interesting to compare and contrast those sequences to the ones found with LBD. These data will sample the full spectrum of interacting peptide sequences for PXR in the full-length receptor context and determine whether different sequences show specificity for different classes of PXR ligands. Another necessary step is determining the specificity of these peptides by cross-testing them with other nuclear receptors to ask whether their interactions are unique to PXR. Based on sequence similarity, I expect that at the very least many of the peptides found in the M13 PXR LBD screens may also bind to PPARs (unpublished results from Niharika Mettu). If one or more peptides are determined to be specific for PXR only, however, these can be utilized to make vital tools for examining PXR biology as has previously been done for ERR. (Gaillard, S., et al. 2006; Gaillard, S., et al. 2007)

The peptides from this study could also provide the missing link to allow crystallization of full-length PXR by binding to and stabilizing uncharacterized surfaces of the receptor, much like SRC-1 and other coactivator fragments stabilize AF2 for crystallization of ligand binding domains. The completion of T7 studies, panning the PXR-RXR heterodimer with tissue-specific libraries could greatly illuminate the understanding of which proteins bind to and regulate PXR function.

In conclusion, the studies initiated here lay the foundation for answering several fundamental questions regarding the regulation of xenobiotic metabolism, including those regarding (a) the surfaces full-length PXR presents in the presence of different ligands, (b) which coregulators mediate the transcriptional activity of PXR in context of the full-length receptor, (c) whether or not ligands produce distinct protein-PXR interactions in different tissues, and (d) whether coregulators show specificity for different classes of PXR ligands. The completion of these and future experiments will delineate in detail the PXR signaling pathway for xenobiotic metabolism. This knowledge could provide valuable insights into controlling dangerous drug-drug interactions and tailoring dosing regimen to individuals.

Plasmid Name	Sequence	Class of Interaction with SR12813	Class of Interaction with Rifampicin
pM_alone_L1	MGSRGPSDFPILWNLLTTSVSGDSSS	A	*n.d.*
pM_alone_L2	MGSRLGESHPLLMQLLTENVGTHSSS	D	*n.d.*
pM_alone_L3	MGSRLSALYPELSRLLSVDVHALSSS	a	*n.d.*
pM_alone_L4	MGSSTVDTYPLLRALLADSPSIGSSS	b	*n.d.*
pM_alone_L5	MGSRTVLDGMSLERLLIVGGLSVSSS	*n.d.*	*n.d.*
pM_alone_L13	MGSRLESLYPELYQLLSPGKLSLSSS	D	D
pM_alone_L14	MGSRLLEAHPLLTGLLGASSLELSSS	C	C
pM_alone_L15	MGSRVVDSYPVLTELLRRDEAELSSS	D	D
pM_alone_L16	MGSRGDLKCTMLASLLTDCSVASSSS	A	A
pM_alone_L17	no seq	A	A
pM_alone_L18	MGSRLMLENPLLAQLLGAELPSQSSS	C, E, C	C, E
pM_alone_L19	MGSRPWFDNPLLFKLLSEESHESSSS	C, E, C	E, E
pM_alone_L20	MGSRLGESHPLLMQLLTENVGTHSSS	D	D
pM_alone_L21	MGSRGPDGYPTLRELLGYPSTRVSSS	d	d
pM_alone_L22	no seq	A	A
pM_alone_L23	MGSSLSDSHPVLTALLAECMGDCSSS	D	D
pM_alone_L24	MGSSISSDYPLLHALLQDDYSSTSSS	D	*C

Table 2.1. LxxLL peptide data from pan 2 of PXR LBD in the absence of ligand. The LxxLL motif is underlined. Interaction classes are described in the text. Lower case letters for class of interaction indicate instances where the interaction seen was statistically significant over level of pM_construct interaction with empty pVP16, however the actual luciferase activity levels were quite low, on the order of those pM constructs that did not interact. Multiple letters indicate peptides that had different responses between replicate trials. Asterisks indicate data where the error bars are quite large; *n.d.*, not determined; no seq indicates peptides for which the sequencing reaction did not produce quality data.

Plasmid Name	Sequence	Class of Interaction with SR12813	Class of Interaction with Rifampicin
pM_alone_C1	MGSSDRLLRYYLSENIKQLIPGIEYNGSSS	D	D
pM_alone_C2	MGSSVSYYGANLNPIIRGYLTGGMWSMSSS	A	A
pM_alone_C3	MGSSWSNQAVILHPHIAGLLMPQETFTSSS	D	D
pM_alone_C4	MGSSHPILRDMLTNNIDPQIRETEGPLSSS	d	*n.d.*
pM_alone_C5	MGSSPRPVIEELYPNIHALLMSTREGASSS	*n.d.*	*n.d.*
pM_alone_C13	MGSSHPILRDMLTNNIDPQIRETEGPLSSS	A	*n.d.*
pM_alone_C14	no seq	C	*n.d.*
pM_alone_C15	MGSSTEYDLCTLYPNIMQALQNEPCHQSSS	*C	D
pM_alone_C16	MGSSHPILRDMLTNNIDPQIRETEGPLSSS	D	D
pM_alone_C17	no seq	A	A
pM_alone_C18	MGSSTEYDLCTLYPNIMQALQNEPCHQSSS	D	*A
pM_alone_C19	no seq	A, D	C
pM_alone_C20	MGSSHPILRDMLTNNIDPQIRETEGPLSSS	C	C
pM_alone_C21	MGSSPPILRDMLTNNIDPQIRETEGPLSSS	D	D
pM_alone_C22	no seq	A, C	C
pM_alone_C23	no seq	D, A	A
pM_alone_C24	MGSSNTRDLSSLYPLIHGLLIQNTEGVSSS	D	D, *C

Table 2.2. CoRNR peptide data from pan 2 of PXR LBD in the absence of ligand. The CoRNR motif is underlined. Interaction classes are described in the text. Lower case letters for class of interaction indicate instances where the interaction seen was statistically significant over level of pM_construct interaction with empty pVP16, however the actual luciferase activity levels were quite low, on the order of those pM constructs that did not interact. Multiple letters indicate peptides that had different responses between replicate trials. Asterisks indicate data where the error bars are quite large; *n.d.*, not determined; no seq indicates peptides for which the sequencing reaction did not produce quality data.

Plasmid Name	Sequence	Class of Interaction with SR12813	Class of Interaction with Rifampicin
pM_SR_L1	MGSSNGSDYQILRQLLASEQLLLSSS	A	*n.d.*
pM_SR_L2	MGSSISYEHPLLTGLLLEQRHVDSSS	A	*n.d.*
pM_SR_L3	MGSSLESLYPELYQLLSPGKLSLSSS	A	*n.d.*
pM_SR_L4	MGSRGVDAYPLLSALLSAENGVESSS	c	*n.d.*
pM_SR_L5	MGSSMISLNPVLMGLLQERLDWSSSS	D	D
pM_SR_L13	no seq	D	*n.d.*
pM_SR_L14	MGSSTWMAYPTLSELLQAPVEGVSSS	C	*n.d.*
pM_SR_L15	no seq	A	*n.d.*
pM_SR_L16	MGSRVELAFPLLRELLSQPLWVDSSS	*C	*n.d.*
pM_SR_L17	MGSSTIDSHPMLFNLLSKSESFVSSS	D	*n.d.*
pM_SR_L18	MGSSNAVLTPILQSLLLGADVKQSSS	*C	*n.d.*
pM_SR_L19	MGSSVLSDYPLLYQLLDYGLDRGSSS	*C	*n.d.*
pM_SR_L20	MGSRIIRDNPELCVLLDCSSERISSS	A, d	d
pM_SR_L21	MGSSVFLENRLLYGLLTSQTEPSSSS	C, D	D
pM_SR_L22	MGSSSWVETPMLYSLLRDDKTIWSSS	*C	*n.d.*
pM_SR_L23	MGSSTQMENPILEALLLGKAIQMSSS	D	*n.d.*
pM_SR_L24	MGSSIADDAPLLRSLLESGLTVSSSS	D, e	*n.d.*

Table 2.3. LxxLL peptide data from pan 2 of PXR LBD in the presence of 1 μM SR12813. The LxxLL motif is underlined. Interaction classes are described in the text. Lower case letters for class of interaction indicate instances where the interaction seen was statistically significant over level of pM_construct interaction with empty pVP16, however the actual luciferase activity levels were quite low, on the order of those pM constructs that did not interact. Multiple letters indicate peptides that had different responses between replicate trials. Asterisks indicate data where the error bars are quite large; *n.d.*, not determined; no seq indicates peptides for which the sequencing reaction did not produce quality data.

Plasmid Name	Sequence	Class of Interaction with SR12813	Class of Interaction with Rifampicin
pM_SR_C1	MGSSHPILRDMLTNNIDPQIRETEGPLSSS	D	*n.d.*
pM_SR_C2	MGSSITHSHPVLTGLILGDLPVDRTLLSSS	c	*n.d.*
pM_SR_C3	MGSSHPILRDMLTNNIDPQIRETEGPLSSS	D	*n.d.*
pM_SR_C4	MGSSPISHQYPLMLNILGHIDTHTTPTSSS	b	*n.d.*
pM_SR_C5	MGSSNENSAVQLHPIIRHMLLGSPETGSSS	*n.d.*	*n.d.*
pM_SR_C13	no seq	D	*n.d.*
pM_SR_C14	MGSSHPILRDMLTNNIDPQIRETEGPLSSS	*C	*n.d.*
pM_SR_C15	MGSSDRLLRYYLSENIKQLIPGIEYNGSSS	*C	*n.d.*
pM_SR_C16	no seq	D	*n.d.*
pM_SR_C17	MGSSHPILRDMLTNNIDPQIRETEGPLSSS	*C	*n.d.*
pM_SR_C18	MGSSITHSHPVLTGLILGDLPVDRTLLSSS	*C	*n.d.*
pM_SR_C19	MGSSYKQWNHQLSTHIKNPIQPTVTKHSSS	A	*n.d.*
pM_SR_C20	MGSSHPILRDMLTNNIDPQIRETEGPLSSS	D	*n.d.*
pM_SR_C21	MGSSPRPVIEELYPNIHALLMSTREGASSS	B	*n.d.*
pM_SR_C22	MGSSYSDTAHTLTPIIRSMLLPSFPNTSSS	A	*n.d.*
pM_SR_C23	MGSSHPILRDMLTNNIDPQIRETEGPLSSS	*C	*n.d.*
pM_SR_C24	MGSSHPILRDMLTNNIDPQIRETEGPLSSS	D	*n.d.*

Table 2.4. CoRNR peptide data from pan 2 of PXR LBD in the presence of 1 μM SR12813. The CoRNR motif is underlined. Interaction classes are described in the text. Lower case letters for class of interaction indicate instances where the interaction seen was statistically significant over level of pM_construct interaction with empty pVP16, however the actual luciferase activity levels were quite low, on the order of those pM constructs that did not interact. Multiple letters indicate peptides that had different responses between replicate trials. Asterisks indicate data where the error bars are quite large; *n.d.*, not determined; no seq indicates peptides for which the sequencing reaction did not produce quality data.

Plasmid Name	Sequence	Class of Interaction with SR12813	Class of Interaction with Rifampicin
pM_R_L1	MGSSSLHETPL<u>LLRLL</u>SSEPASVSSS	*n.d.*	B
pM_R_L2	MGSSTSLDFPV<u>LSSLL</u>NWNSEEVSSS	*n.d.*	b
pM_R_L3	MGSRGAEGYPL<u>LRQLL</u>AHTQPRLSSS	*n.d.*	b
pM_R_L4	MGSRLESLYPE<u>LYQLL</u>SPGKLSLSSS	*n.d.*	b
pM_R_L5	MGSSNFGPYPI<u>LTELL</u>SSGGSLVSSS	*n.d.*	*n.d.*
pM_R_L13	MGSRMVTEYPI<u>LSELL</u>QGPPTFVSSS	*n.d.*	D
pM_R_L14	MGSRTLDTTPL<u>LLQLL</u>QHPGSAESSS	*n.d.*	D
pM_R_L15	no seq	A	A
pM_R_L16	MGSSSWVETPM<u>LYSLL</u>RDDKTIWSSS	D	D
pM_R_L17	no seq	A	A
pM_R_L18	MGSRAFPDSPI<u>LRALL</u>SQSYGSPSSS	D	D
pM_R_L19	MGSRLESLYPE<u>LYQLL</u>SPGKLSLSSS	D	D
pM_R_L20	no seq	A, A	D, A
pM_R_L21	MGSSVTSPTPI<u>LLHLL</u>GDVSEHVSSS	D	D
pM_R_L22	MGSSQALDYPI<u>LRELL</u>GAPGLSLSSS	D	D
pM_R_L23	MGSSDLTRYPV<u>LWELL</u>TQGSGAESSS	D	D
pM_R_L24	MGSSIADDAPL<u>LRSLL</u>ESGLTVSSSS	B	B, A

Table 2.5. LxxLL peptide data from pan 2 of PXR LBD in the presence of 1 μM rifampicin. The LxxLL motif is underlined. Interaction classes are described in the text. Lower case letters for class of interaction indicate instances where the interaction seen was statistically significant over level of pM_construct interaction with empty pVP16, however the actual luciferase activity levels were quite low, on the order of those pM constructs that did not interact. Multiple letters indicate peptides that had different responses between replicate trials. Asterisks indicate data where the error bars are quite large; *n.d.*, not determined; no seq indicates peptides for which the sequencing reaction did not produce quality data.

Plasmid Name	Sequence	Class of Interaction with SR12813	Class of Interaction with Rifampicin
pM_R_C1	MGSSDRLLRYYLSENIKQLIPGIEYNGSSS	*n.d.*	b
pM_R_C2	MGSSHPILRDMLTNNIDPQIRETEGPLSSS	*n.d.*	D
pM_R_C3	MGSSVWVVNTDLDALIRSELLKGRGEKSSS	E	E
pM_R_C4	MGSSHPILRDMLTNNIDPQIRETEGPLSSS	*n.d.*	D
pM_R_C5	MGSSVLPGPLALYPNIMEWLRPVPNEESSS	*n.d.*	*n.d.*
pM_R_C13	MGSSHPILRDMLTNNIDPQIRETEGPLSSS	*n.d.*	D
pM_R_C14	MGSSPRPVIEELYPNIHALLMSTREGASSS	*n.d.*	B
pM_R_C15	MGSSTDVWSTYLSNLIRAQLNANPSQTSSS	A	A
pM_R_C16	MGSSHPILRDMLTNNIDPQIRETEGPLS	A	A
pM_R_C17	no seq	c	c
pM_R_C18	MGSSHPILRDMLTNNIDPQIRETEGPLSSS	D	D
pM_R_C19	no seq	D	D
pM_R_C20	MGSSHPILRDMLTNNIDPQIRETEGPLSSS	D	D
pM_R_C21	MGSSHPILRDMLTNNIDPQIRETEGPLSSS	D	D
pM_R_C22	no seq	A	A
pM_R_C23	MGSSNQTARLDLHPLIRSLLGASEGPQSSS	D	D
pM_R_C24	MGSSSSMSQQQLYPIIWSLISDSAMPTSSS	B	B

Table 2.6. CoRNR peptide data from pan 2 of PXR LBD in the presence of 1 μM rifampicin. The CoRNR motif is underlined. Interaction classes are described in the text. Lower case letters for class of interaction indicate instances where the interaction seen was statistically significant over level of pM_construct interaction with empty pVP16, however the actual luciferase activity levels were quite low, on the order of those pM constructs that did not interact. Multiple letters indicate peptides that had different responses between replicate trials. Asterisks indicate data where the error bars are quite large; *n.d.*, not determined; no seq indicates peptides for which the sequencing reaction did not produce quality data.

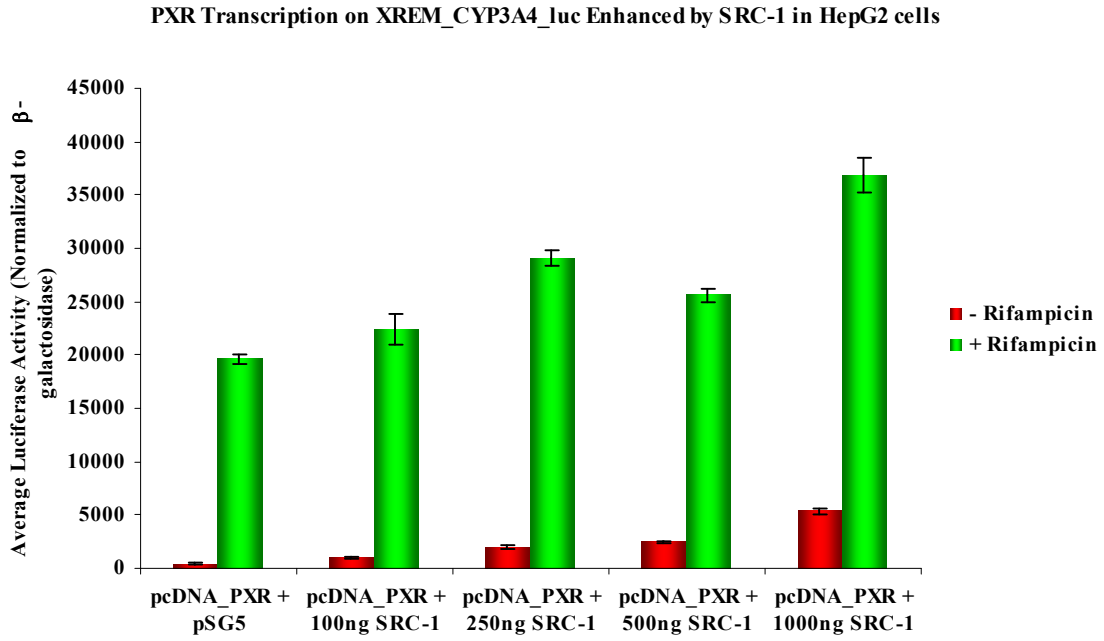

Figure 2.1. Transcriptional activation of PXR in the presence of SRC-1. SRC-1 enhances PXR transcription of a reporter construct containing the XREM of the CYP3A4 gene in HepG2 cells. HepG2 cells were transfected with PXR, the XREM_CYP3A4 reporter construct, and either empty pSG5 or increasing concentrations of pSG5_SRC-1 construct as indicated. Transfected cells were treated with DMSO or 10 μM rifampicin for 16 hours prior to lysis and analysis of luciferase expression.

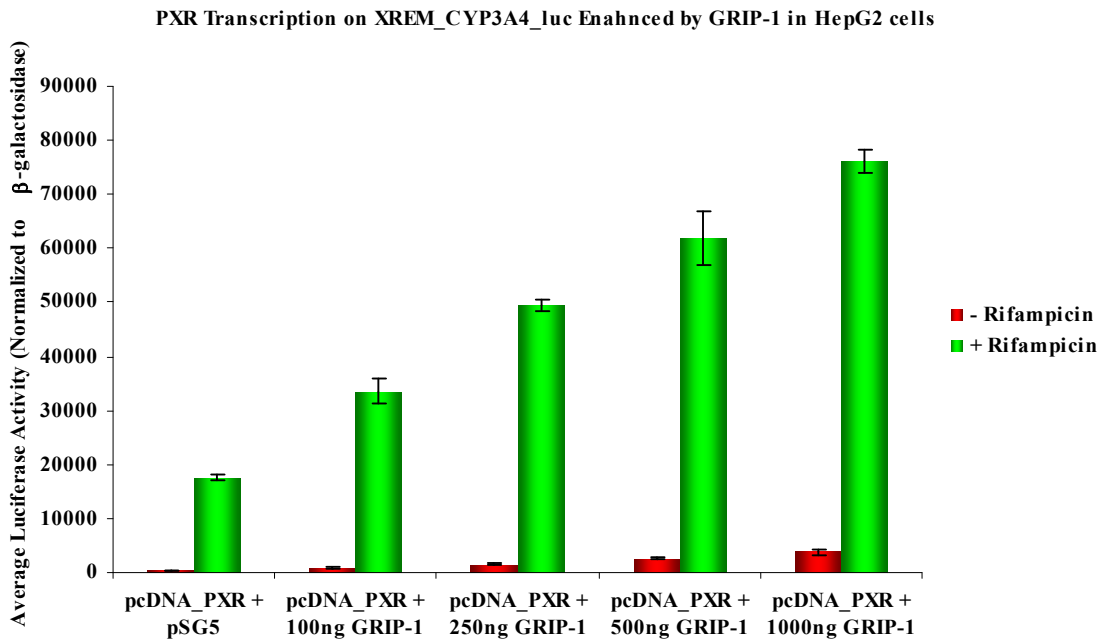

Figure 2.2. Transcriptional activation of PXR in the presence of GRIP-1. GRIP-1 enhances PXR transcription of a reporter construct containing the XREM of the CYP3A4 gene in HepG2 cells. HepG2 cells were transfected with PXR, the XREM_CYP3A4 reporter construct, and either empty pSG5 or increasing concentrations of pSG5_GRIP-1 construct as indicated. Transfected cells were treated with DMSO or 10 μM rifampicin for 16 hours prior to lysis and analysis of luciferase expression.

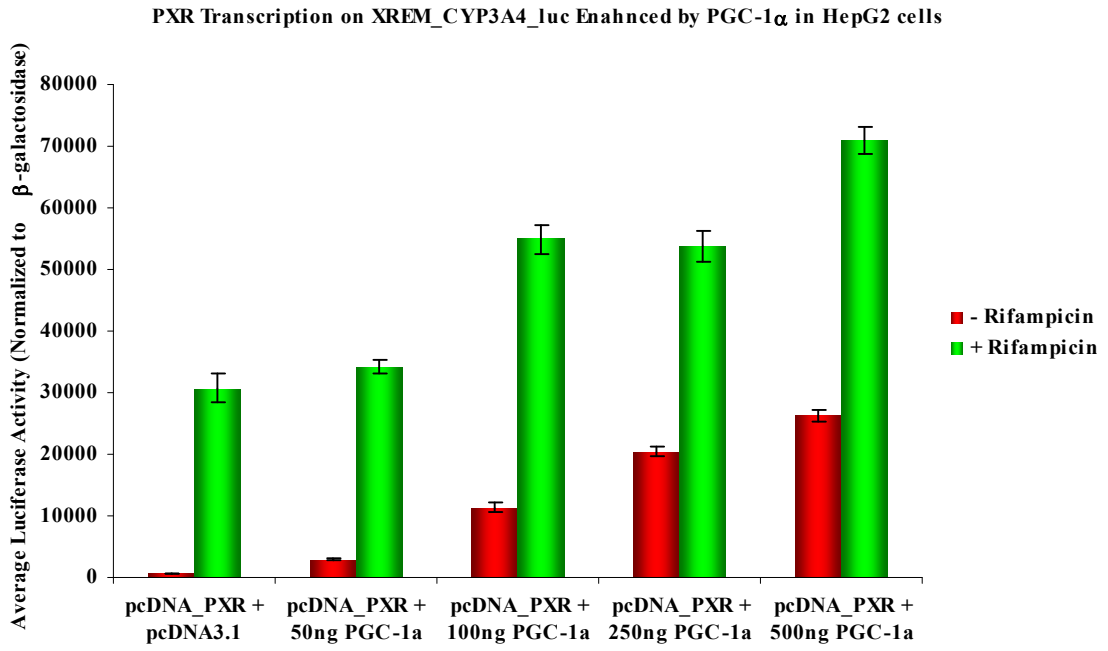

Figure 2.3. Transcriptional activation of PXR in the presence of PGC-1α. PGC-1α also enhances PXR transcription of a reporter construct containing the XREM of the CYP3A4 gene in HepG2 cells. HepG2 cells were transfected with PXR, the XREM_CYP3A4 reporter construct, and either empty pcDNA3.1 or increasing concentrations of pcDNA3.1_PGC-1α construct as indicated. Transfected cells were treated with DMSO or 10 μM rifampicin for 16 hours prior to lysis and analysis of luciferase expression.

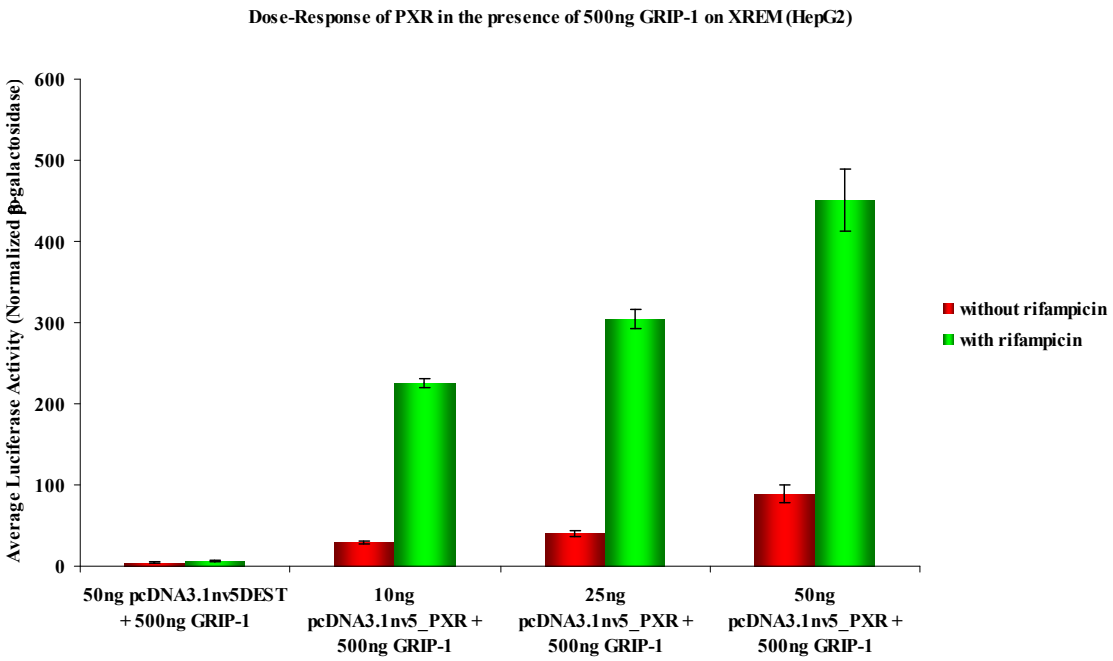

Figure 2.4. Dose-response of PXR in the presence of 500 ng GRIP-1. HepG2 cells were transfected with the XREM_CYP3A4 reporter construct, 500 ng of pSG5_GRIP-1, and increasing concentrations of pcDNA3.1_PXR construct as indicated. Transfected cells were treated with DMSO or 10 μM rifampicin for 16 hours prior to lysis and analysis of luciferase expression.

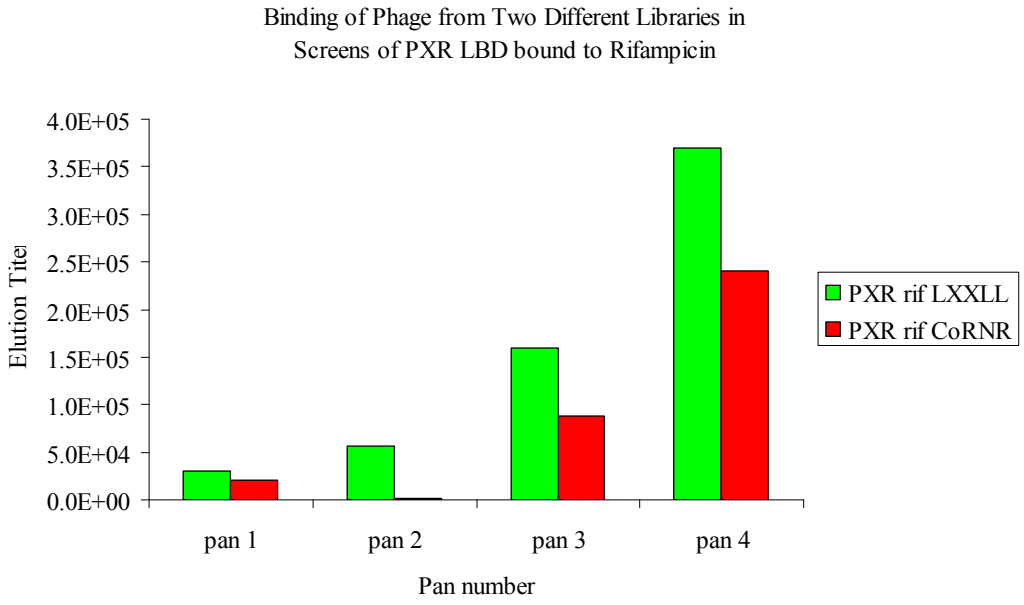

Figure 2.5. Elution titers for M13 pans of PXR LBD. Elution titers for phage bound to PXR LBD in the presence of 1 μM rifampicin increased over the course of panning both the LxxLL and CoRNR libraries.

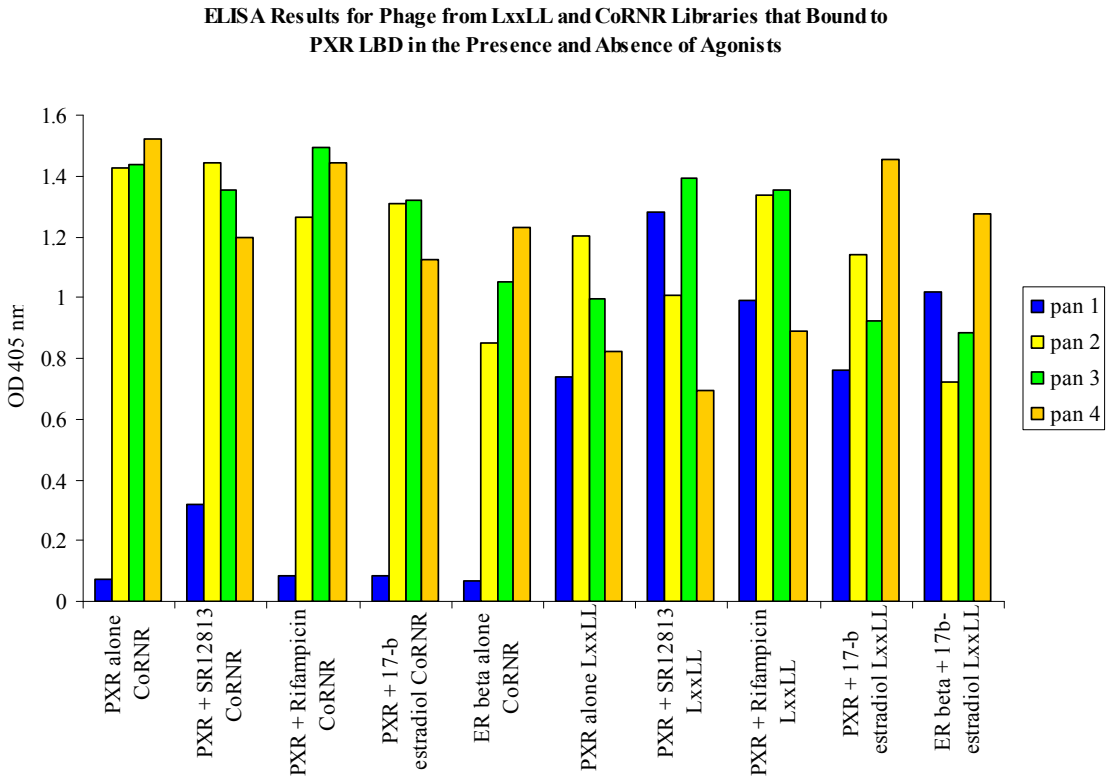

Figure 2.6. ELISA assay results from M13 pans of PXR LBD in the presence and absence of ligand. PXR LBD was immobilized on a 96 well plate and incubated with phage isolated from sequential panning prior to washing and immunodetection. ELISA assay results for phage from each pan of the CoRNR and LxxLL libraries confirmed that the libraries enriched for PXR LBD binders over the course of panning.

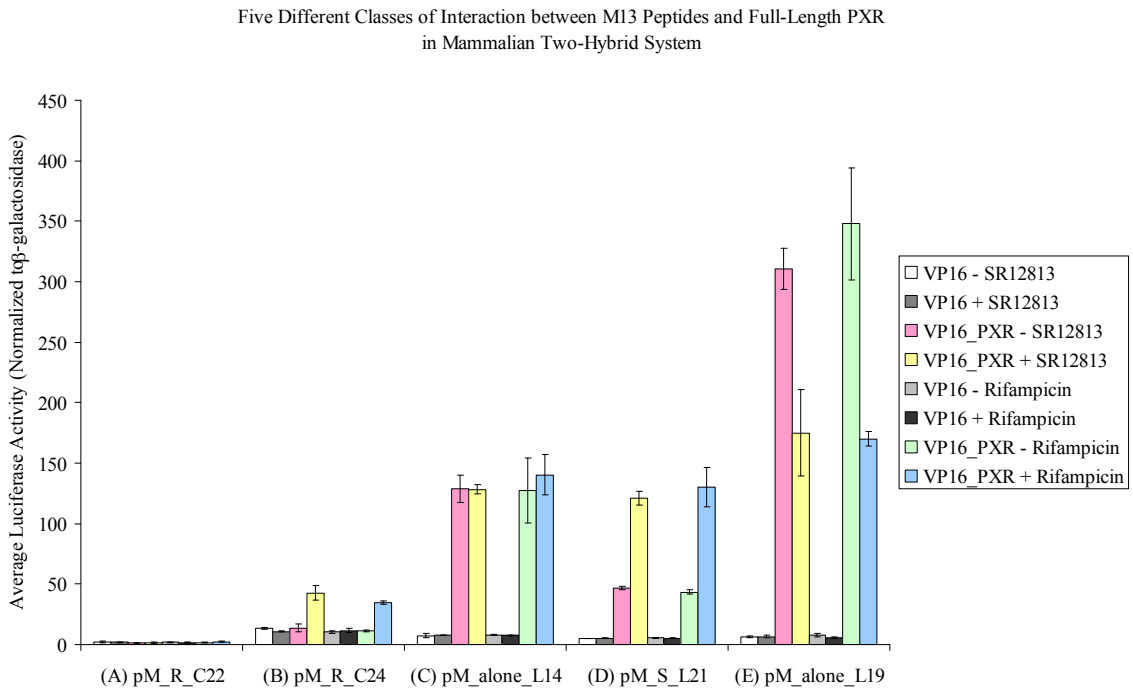

Figure 2.7. Data representative of each interaction profile. HepG2 cells were transfected with pM_peptide constructs, empty VP16 or pVP16_PXR (full length), the 5xGal4Luc3 reporter construct, and the CMVβGal plasmid. Transfected cells were treated with DMSO or 10 μM rifampicin for 16 hours prior to lysis and analysis of luciferase expression. The interaction profiles of peptide constructs and the full-length PXR VP16 construct were categorized as follows: A) peptide construct was not recruited by full-length PXR in the absence or presence of agonist; B) peptide construct was not recruited by full-length PXR in the absence of agonist, but was recruited with the addition of agonist; C) peptide construct was recruited equally well in the absence and presence of agonist; D) peptide construct was recruited in the absence of agonist, but presence of agonist further enhanced the interaction; E) peptide construct was recruited in the absence of agonist, and addition of agonist diminished the interaction. Data representative of each class are presented.

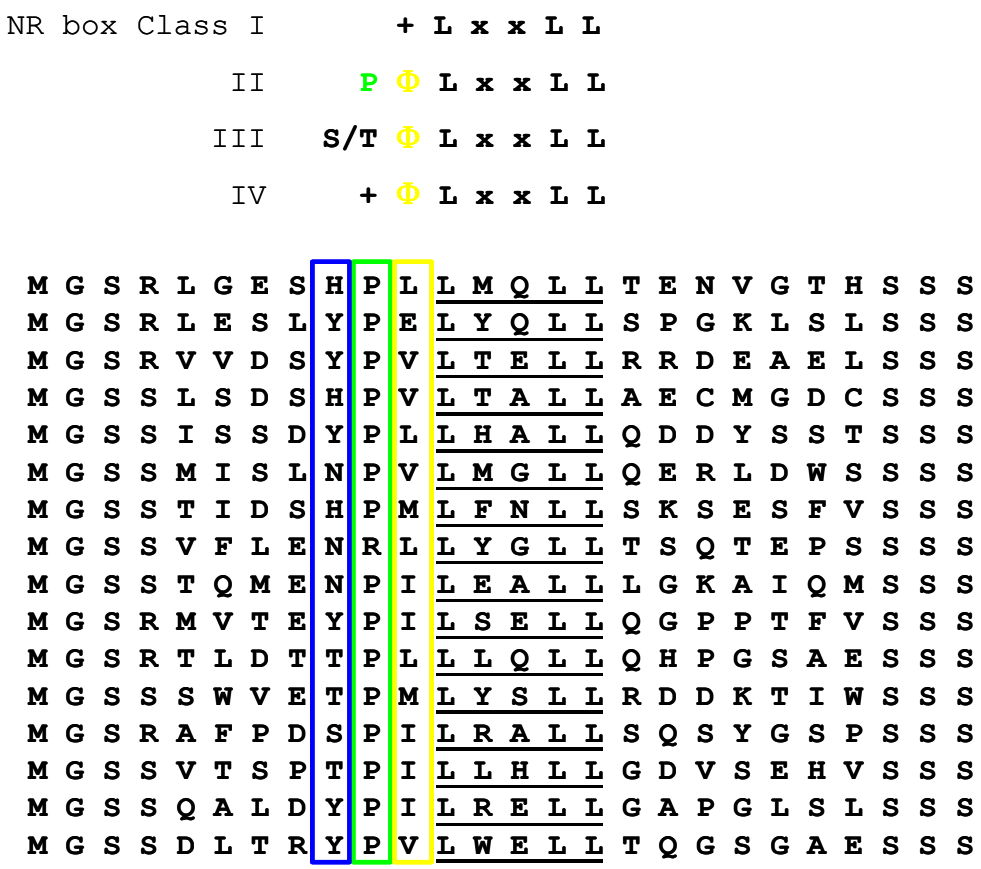

Figure 2.8. LxxLL peptides sequences that interacted with PXR. Conserved motifs were found in LxxLL sequences that interacted with PXR and that interaction was further enhanced by ligand. (Two sequences are omitted because they are identical to others in the figure.) All but one has a proline in the -2 position, and all but one has a hydrophobic residue in the -1 position. The known NR boxes (class I-IV) are depicted for comparison. The predominant profile found in these sequences follows class II pattern. In addition, PXR LBD seems to select a polar residue in the -3 position.

MGSSDRLLRYYLSENIKQLIPGIEYNGSSS

MGSSWSNQAVILHPHIAGLLMPQETFTSSS

MGSSHPILRDMLTNNIDPQIRETEGPLSSS

MGSSNTRDLSSLYPLIHGLLIQNTEGVSSS

MGSSITHSHPVLTGLILGDLPVDRTLLSSS

MGSSPISHQYPLMLNILGHIDTHTTPTSSS

MGSSPRPVIEELYPNIHALLMSTREGASSS

MGSSNQTARLDLHPLIRSLLGASEGPQSSS

MGSSSSMSQQQLYPIIWSLISDSAMPTSSS

Figure 2.9. CoRNR peptide sequences that did interact with PXR. The CoRNR peptides that interacted with any PXR complex in profiles B, C, or D did contain the corepressor motif (underlined); however, many also contained internal LxxLL-like motifs (red). Many of these motifs were further supported by a -3 polar residue (blue), a -2 proline (green), and a -1 hydrophobic residue (yellow). (In this figure the identical peptide sequences were not listed multiple times.)

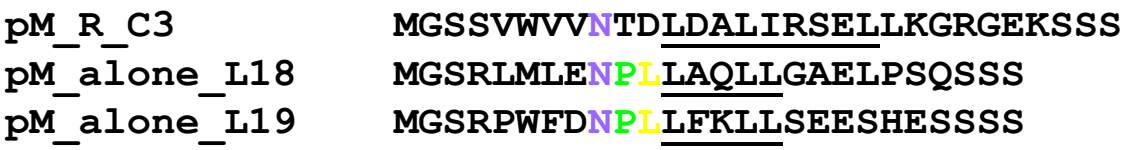

Figure 2.10. Three of the peptides demonstrated interaction profile E. The -3 polar residue was asparagines in each sequence. When present, the -2 proline is shown in green and the -1 hydrophobic residue is shown in yellow.

MGSSYSDTAHTLTPIIRSMLLPSFPNTSSS

MGSSVSYYGANLNPIIRGYLTGGMWSMSSS

MGSSYKQWNHQLSTHIKNPIQPTVTKHSSS

MGSSTDVWSTYLSNLIRAQLNANPSQTSSS

MGSSHPILRDMLTNNIDPQIRETEGPLS*

MGSRGPSDFPILWNLLTTSVSGDSSS

MGSRLSALYPELSRLLSVDVHALSSS

MGSRGDLKCTMLASLLTDCSVASSSS

MGSSNGSDYQILRQLLASEQLLLSSS

MGSSISYEHPLLTGLLLEQRHVDSSS

MGSSLESLYPELYQLLSPGKLSLSSS*

Figure 2.11. Peptide sequences that did not interact with full-length PXR in mammalian two-hybrid system. The above peptide sequences did not interact in the mammalian two-hybrid assay. Sequences marked with asterisks are identical to other constructs that did interact in the assay. LxxLL-like motifs are shown in red, -3 polar residues in blue, -2 proline in green, and -1 hydrophobic residues in yellow.

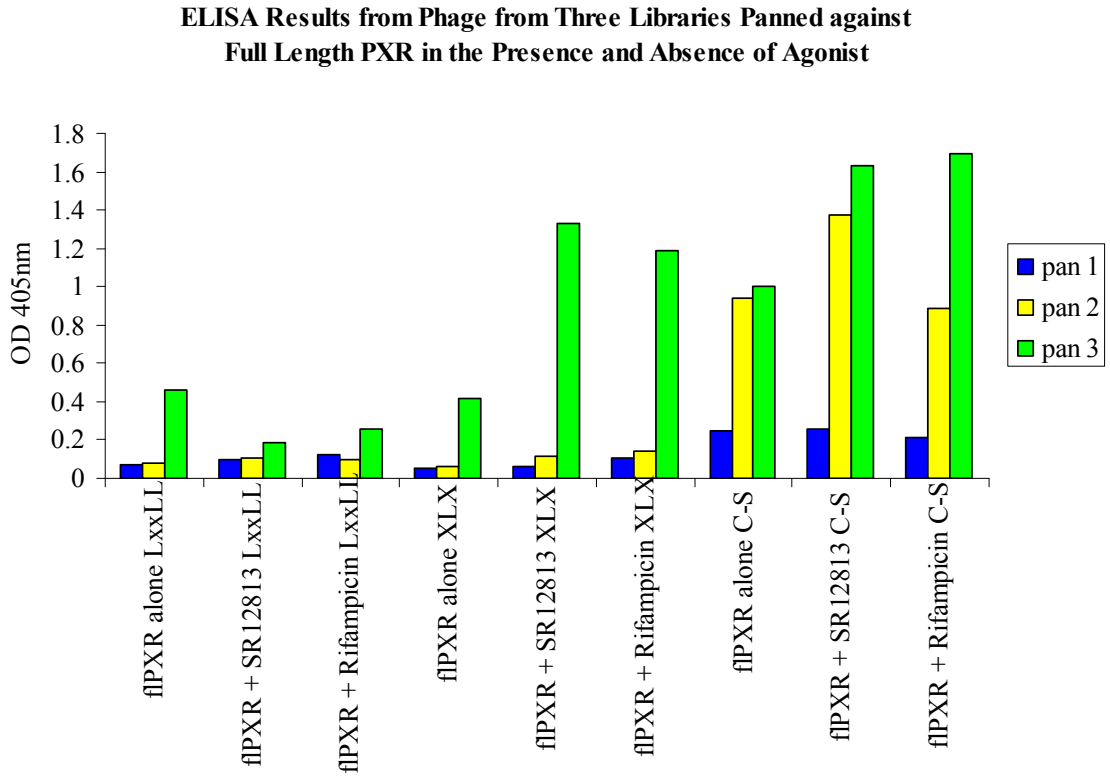

Figure 2.12. ELISA results for pans of LxxLL, XLX, and C-S libraries with full-length PXR in the presences and absence of agonist. Full-length PXR was immobilized on a 96 well plate and incubated with phage isolated from sequential panning prior to washing and immunodetection.

Chapter 3

Human PXR Forms a Tryptophan Zipper-Mediated Homodimer[†]

Schroeder M. Noble[‡], Virginia E. Carnahan[‡], Linda B. Moore[§], Tom Luntz[‖], Hongbing Wang[‖], Olivia R. Ittoop[§], Julie B. Stimmel[§], Paula R. Davis-Searles[+], Ryan E. Watkins[‡], G. Bruce Wisely[§], Ed LeCluyse[‖], Ashutosh Tripathy[‡], Donald P. McDonnell[⊥] and Matthew R. Redinbo[+, ‡, *]

[‡]Department of Biochemistry and Biophysics, University of North Carolina at Chapel Hill, Chapel Hill, NC 27599
[§]Nuclear Receptor Discovery Research, GlaxoSmithKline, Research Triangle Park, NC 27709
[‖]Division of Drug Discovery and Disposition, School of Pharmacy, University of North Carolina at Chapel Hill, Chapel Hill, NC 27599
[⊥]Department of Pharmacology and Cancer Biology, Duke University Medical Center, Durham, NC 27710
[+]Department of Chemistry, and the Lineberger Comprehensive Cancer Center, University of North Carolina at Chapel Hill, Chapel Hill, NC 27599

[†]This work was supported by NIH grant DK62229 (M.R.R.), NIH ATLAS grant DK62434 (D.P.M.), and a National Science Foundation Graduate Research Fellowship (V.E.C.).

[*]Corresponding Author: Department of Chemistry, Campus Box #3290, University of North Carolina at Chapel Hill, Chapel Hill, NC 27599-3290; redinbo@unc.edu

This manuscript was a collaborative effort. I performed the mammalian two-hybrid studies.

Abstract

The human nuclear receptor pregnane X receptor (PXR) responds to a wide variety of potentially harmful chemicals and coordinates the expression of genes central to xenobiotic and endobiotic metabolism. Structural studies reveal that the PXR ligand binding domain (LBD) uses a novel sequence insert to form a homodimer unique to the nuclear receptor superfamily. Terminal β-strands from each monomeric LBD interact in an ideal antiparallel fashion to bury potentially exposed surface β-strands, generating a ten-stranded intermolecular β-sheet. Conserved tryptophan and tyrosine residues lock across the dimer interface and provide the first tryptophan-zipper (Trp-Zip) interaction observed in a native protein. We show using analytical ultracentrifugation that the PXR LBD forms a homodimer in solution. We further find that removal of the interlocking aromatic residues eliminates dimer formation but does not affect PXR's ability to interact with DNA, RXRα, or ligands. Disruption of the homodimer significantly reduces receptor activity in transient transfection experiments, however, and effectively eliminates the receptor's recruitment of the transcriptional coactivator SRC-1 both *in vitro* and *in vivo*. Taken together, these results suggest that the unique Trp-Zip-mediated PXR homodimer plays a role in the function of this nuclear xenobiotic receptor.

Introduction

The human pregnane X receptor PXR plays a important role in controlling the expression of genes central to drug and endobiotic metabolism, including those encoding cytochrome P450s (CYPs), UDP-glucuronosyl-transferases, glutathione-S-transferases, and drug efflux pumps (Gardner-Stephen, D., et al. 2004; Geick, A., et al. 2001; Gerbal-Chaloin, S., et al. 2002; Kliewer, S.A. 2003; Xie, W., et al. 2001a). PXR is considered to be a master regulator of the expression of CYP 3A4 isoform, which metabolizes more than 50% of human drugs (Maurel, P. 1996). PXR is expressed largely in the liver and intestines and responds to a wide variety of structurally distinct endobiotic and xenobiotic compounds, including pregnenolone, progesterone, lithocholic acid, paclitaxel, rifampicin, and the St. John's wort constituent hyperforin (Bertilsson, G., et al. 1998; Kliewer, S.A., et al. 1998; Lehmann, J.M., et al. 1998; Moore, L.B., et al. 2000; Wentworth, J.M., et al. 2000). The activation of this xenobiotic sensor has also been linked to clinically-relevant drug interactions. For example, in patients taking the unregulated herbal antidepressant St. John's wort, which contains the potent PXR agonist hyperforin (Moore, L.B., et al. 2000; Wentworth, J.M., et al. 2000), the upregulation of drug metabolism genes has been observed to generate significant decreases in the serum levels of therapeutics including oral contraceptives, anti-viral compounds, and immunosuppressant (Ernst, E. 1999; Fugh-Berman, A. 2000; Piscitelli, S.C., et al. 2000; Ruschitzka, F., et al. 2000).

PXR is a member of the nuclear receptor (NR) superfamily of ligand-activated transcription factors, which includes receptors for estrogen, progesterone, retinoid and thyroid hormones as well as retinoids, cholesterol metabolites and vitamins. Many

nuclear receptors bind to dual DNA response elements of various arrangements as either homodimers or as heterodimers with the retinoid X receptor-alpha (RXRα) (Aranda, A., et al. 2001; Giguere, V. 1999). In the absence of activating ligand, NRs have been shown to associate with transcriptional corepressors, which down-regulate gene expression by a variety of mechanisms including histone deacetylation (Aranda, A., et al. 2001; Rosenfeld, M.G., et al. 2001). In response to an activating ligand, however, NRs interact with transcriptional coactivators that up-regulate target gene expression in part by histone acetylation and by facilitating the recruitment of the basal transcriptional machinery (Aranda, A., et al. 2001; Rosenfeld, M.G., et al. 2001). PXR functions as a heterodimer with RXRα and has been shown to bind to a variety of dual DNA response elements arranged as direct and everted repeats. Upon ligand activation, PXR recruits several of the p160-class of transcriptional coactivators, including the steroid receptor coactivator-1 (SRC-1) (Bertilsson, G., et al. 1998; Blumberg, B., et al. 1998; Kliewer, S.A., et al. 1998; Lehmann, J.M., et al. 1998). For its potent control of CYP3A4 expression, PXR has been shown to employ two DNA response elements, one proximal (bases -172 to -149) and one distal (bases -7836 to -7607) relative to the start site of transcription. Both are required for maximal induction of gene expression in response to ligands (Goodwin, B., et al. 1999). PXR has also been shown to regulate the expression of MDR1 and CYP isoform 2B6 by using a combination of proximal and distal DNA response elements (Geick, A., et al. 2001; Wang, H.B., et al. 2003).

The PXRs of known sequence contain a ~50-amino acid insert unique to members of the nuclear receptor superfamily. This region is located between helices 1 and 3 within the canonical NR LBD fold, and adds a novel helix 2 and two β-strands adjacent to

PXR's ligand binding cavity. Numerous crystal structures of the human PXR LBD have also revealed that the novel β-turn-β motif of this insert extends the two- to three-stranded antiparallel β-sheet common to NRs to a five-stranded β-sheet in PXR (Chrencik, J.E., et al. 2005; Watkins, R.E., et al. 2001; Watkins, R.E., et al. 2003a; Watkins, R.E., et al. 2003b). It is the terminal β-strands in each of these β-sheets that associate in an antiparallel fashion to generate the PXR homodimer, which produces a ten-strand intermolecular antiparallel β-sheet (**Figure 1.2A**). No other nuclear receptor has been observed to homodimerize in this fashion. In this work, structural, biophysical and functional features of this PXR homodimer are examined. Using sedimentation equilibrium experiments, the PXR LBD is shown to form a homodimer in solution with a K_d of 4.5 μM. Key residues at the dimer interface are also mutated and shown to disrupt formation of the PXR dimer, which significantly reduces transcriptional activity and coactivator recruitment without impacting other necessary receptor actions like RXRα, DNA and ligand binding. Taken together, the data presented suggest that the Trp-Zip-mediated PXR homodimer interface plays a potential role in receptor function.

Experimental Procedures

PXR Expression and Purification

Wild-type human PXR LBD (residues 130-434) was coexpressed with a fragment of SRC-1 (residues 623-710) in *E. coli* BL21 (DE3) and purified using nickel-affinity chromatography as previously described (Watkins, R.E., et al. 2001). The

Trp223Ala/Tyr225Ala PXR LBD double-mutant was generated using the QuikChange mutagenesis kit (Stratagene), and expressed under the same conditions as wild-type PXR, but formed inclusion bodies in *E. coli*. The inclusion body pellet was washed twice with buffer containing 0.5% Triton X-100, 20 mM Tris-Cl pH 7.5, 250 mM NaCl, 50 mM imidazole, and 5% glycerol. Following the Triton X-100 wash, the pellet was resuspended in 6 M guanidinium hydrochloride pH 7.5 with the addition of 10 mM β-mercaptoethanol (BME), and stirred at 4 °C for 30 min. The denatured protein was ultra-centrifuged at 28.8K rpm for 30 min, diluted 1:3 with buffer (20 mM Tris-Cl pH 7.5, 250 mM NaCl, 50 mM imidazole, 10 mM BME and 5% glycerol) and then refolded by dialysis against this buffer with four changes. The refolded mutant protein was then purified under the same conditions as wild-type PXR LBD. In preparation for analytical ultracentrifugation, protein samples were concentrated to ~2.0 mg / ml and dialyzed (1:1000 (v/v) protein to dialysate) overnight with two buffer changes. The dialysis buffer (20mM Tris-Cl pH 7.5, 250mM NaCl, 2.5 mM EDTA, 5mM BME and 5% glycerol) was used to dilute protein to relevant concentrations. The cholesterol drug SR12813 (Sigma) was added at a 4-fold molar excess.

Analytical Ultracentrifugation

Sedimentation equilibrium experiments were performed using a Beckman XL-A analytical ultracentrifuge equipped with scanning absorption optics. Equilibrium measurements were obtained at three different rotor speeds (9,000, 13,000 and 16,000 rpm) and three concentrations (8.6, 17.3 and 21.7 μM) for wild-type PXR LBD and Trp223Ala/Tyr225Ala PXR LBD in triplicate. Baseline absorbance offsets were

established by increasing the rotor speed to 45,000 rpm for 6 hrs. Sedimentation equilibrium data was analyzed using the Beckman XL-A/XL-I data Analysis Software Version 4.0 which uses a nonlinear curve fitting procedure to determine the weight-average monomer molecular weight M and the association constant K_a according to the following equation: $c_r = c_{mon,r_0} e^{\left[\frac{\omega^2}{2RT} M\left(1-\bar{\nu}\rho\right)\left(r^2-r_0{}^2\right)\right]} + K_a\left(c_{mon,r_0}\right)^2 e^{\left[\frac{\omega^2}{2RT} 2M\left(1-\bar{\nu}\rho\right)\left(r^2-r_0{}^2\right)\right]} + E$

where c_r is the concentration at radial position r, c_{mon,r_0} is the concentration of the monomer at the reference radius r_0, ω is the angular velocity in radians per second, R is the universal gas constant (8.314 x 10^7 erg·mol^{-1}·K^{-1}), T is the temperature in Kelvin, M is the monomer molecular weight, $\bar{\nu}$ is the partial specific volume, ρ is the density of the solvent, and K_a is the association constant, and E is the baseline offset. The association constant, K_a was converted to the dissociation constant K_d by the following equation:

$$K_d = \frac{2}{K_a b \varepsilon}$$

where b is the path length (1.2 cm) and ε is the molar extinction coefficient (28,390 M^{-1} cm^{-1} for PXR LBD) determined using the program Protean ™.

Circular Dichroism Spectropolarimetry

To confirm that the Trp223Ala/Tyr225Ala double-mutant form of the PXR LBD was properly folded, circular dichroism spectropolarimetry (CD) was performed using an Applied Photophysics PiStar-180 CD spectropolarimeter. The ellipticity from 210-300 nm was measured for wild-type PXR LBD and for the Trp223Ala/Tyr225Ala PXR LBD double-mutant. Both proteins were at 0.2 mg ml^{-1} in 100 mM phosphate buffer, pH 7.8,

100 mM NaCl and 5% glycerol. To examine thermal melting temperatures, the temperature was ramped from 20 to 98 ˚C while monitoring the ellipticity at 222 nm. Plots of fraction denatured versus temperature were produced by defining the upper and lower temperature baselines as 0 and 100%, respectively. Melting temperatures (T_m's) were defined as the point at which 50% of the sample denatured. Trials were performed in triplicate, and T_m's for individual runs were averaged and standard errors calculated.

Transient Transfection Assays

Mutations in full-length PXR were generated with the Stratagene QuikChange site directed mutagenesis kit according to the manufacturer's instructions. Transfections were performed as described previously (Goodwin, B., et al. 1999; Watkins, R.E., et al. 2001). Briefly, CV-1 cells were plated in 96-well plates in phenol red-free Dulbecco's modified Eagle's medium containing high glucose and supplemented with 10% charcoal/dextran treated fetal bovine serum (HyClone, Logan, UT). Transfection mixes contained 5 ng of receptor expression vector, 20 ng of reporter plasmid, 12 ng of β-actin SPAP as internal control, and 43 ng of carrier plasmid. Plasmids for wild-type and mutant forms of human PXR and for the XREM-CYP3A4-LUC reporter, containing the enhancer and promoter of the CYP3A4 gene driving Luciferase expression, were as previously described (Goodwin, B., et al. 1999). Transfections were performed with LipofectAMINE (Life Technologies, Inc., Grand Island, NY) essentially according to the manufacturer's instructions. Drug dilutions of rifampicin (Sigma, St. Louis, MO) and SR12813 (synthesized in-house) were prepared in phenol red-free Dulbecco's modified Eagle's

medium/F-12 medium with 15 mM HEPES supplemented with 10% charcoal-stripped, delipidated calf serum (Sigma, St. Louis, MO) which had previously been heat-inactivated at 62°C for 35 minutes. Serial drug dilutions were performed in triplicate to generate 11-point concentration response curves. Cells were incubated for 24 hours in the presence of drugs, after which the medium was sampled and assayed for alkaline phosphatase activity. Luciferase reporter activity was measured using the LucLite assay system (Packard Instrument Co., Meriden, CT) and normalized to alkaline phosphatase activity. EC_{50} values were determined by standard methods.

Immunocytochemistry

CV-1 cells were maintained in Dulbecco's modified Eagle's medium (DMEM) plus 10% charcoal-stripped calf serum (Hyclone, Logan, UT). The day before transfection, cells were plated at 2 x 10^5 cells per well of a 6 well plate (Becton Dickinson, Franklin Lakes, NJ) on ethanol-washed glass cover slips (Fisher Scientific, Pittsburgh, PA). Transfection was carried out using Effectene (Qiagen, Valencia, CA) according to the manufacturer's specifications, with plasmids expressing wild-type PXR, Trp223Ala/Tyr225Ala PXR, or carrier DNA. Transfection complexes were suspended in phenol red-free DMEM/F12 plus 10% charcoal-stripped, delipidated calf serum (Sigma, St. Louis, MO), and left in contact with the cells overnight. The medium was then replaced, drugs [10 μM rifampicin (Sigma, St. Louis, MO) or 2 μM SR12813 (synthesized in house)] or 0.1% DMSO (Sigma, St. Louis, MO) were added, and the incubation was continued for a further 6 hours. For immunofluorescent staining of exogenous proteins, cultures were placed on ice for 5 minutes, rinsed 3 times with cold

PBS, then the cover slips were immersed in ice-cold acetone for 5 minutes and air-dried. Nonspecific antibody binding was blocked by incubating for 10 minutes in PBS containing 10% normal donkey serum (Jackson Immunoresearch Labs, West Grove, PA). Goat anti-PXR (Santa Cruz Biotechnology, Santa Cruz, CA) was applied in blocking buffer for 1 hour at a dilution of 1:100. The secondary antibody, donkey anti-goat IgG labeled with ALEXA 488 (Molecular Probes, Eugene, OR), was also applied for one hour in blocking buffer, but at a dilution of 1:1,000. Cultures stained without primary antibody were also obtained. Cover slips were mounted in 90% glycerol (Sigma, St. Louis, MO), 10% PBS, 4% n-propyl gallate (Sigma, St. Louis, MO) and 0.2 μM Hoechst 33258 (Molecular Probes, Eugene, OR). Fluorescent images were obtained on a Zeiss Axiovert 100 TV inverted microscope with a 100x objective under oil immersion, using Zeiss Axiovision software (Carl Zeiss, Inc., Thornwood, NY).

Gel Mobility Shift Assays

Gel mobility shift assays were performed as described before (Honkakoski, P., et al. 1998). Full-length human wild-type PXR, double-mutant (Trp223Ala/Tyr225Ala) PXR, and RXRα proteins were synthesized using the TNT quick-coupled in vitro transcription/translation system (Promega). Probes NR3 and ER6 from CYP2B6 and CYP3A4, respectively, were labeled with [γ-^{32}P]dATP and purified by Microspin G-25 columns (Amersham Biosciences). Typically, 10 μL of binding reactions contained 10 mM HEPES (pH 7.6), 0.5 mM dithiothreitol, 15% glycerol, 0.05% Nonidet P-40, 50 mM NaCl, 2 μg of poly(dI-dC), with 0.1, 0.5, or 1 μL of *in vitro* translated nuclear receptor protein, and 4 X 10^4 cpm of labeled probe. After incubation at room temperature for 10

min, reaction mixtures were resolved on 5% acrylamide gels in 1 X Tris-acetic acid, EDTA buffer at 180 V for 1.5 h. Afterward, gels were dried, and autoradiography was performed overnight at -70 ˚C.

Competition Ligand Binding Assay

Polylysine YiO imaging beads (Amersham, GE Healthcare) were coated with histidine-tagged WT PXR LBD or Trp223Ala/Tyr225Ala PXR LBD, by mixing for 60 minutes at room temperature, in Tris buffer pH 8.0. Non-specific binding sites were blocked with a ten-fold excess of BSA for an additional 60 minutes at room temperature. The bead/receptor mix was washed and reconstituted in fresh assay buffer (50 mM Tris pH 8.0 containing 10% glycerol, 200mM KCl, 50uM CHAPS, 0.1 mg/mL BSA and 2mM DTT). Biotin (0.1 mM) was added to the suspension and allowed to mix for a further 60 minutes. The blocked receptor bead-mix was centrifuged at 1000 x g for 10 minutes at 4°C. The supernatant was discarded and the receptor-bead pellet was re-suspended in the appropriate volume of assay buffer. [N-methyl-^{3}H]-GW0438X (synthesized at GSK and custom labeled at Amersham Biosciences, UK) was added to this suspension to achieve a final concentration of 10 nM. The receptor/imaging bead/radioligand mix was added directly to test compounds in 384-well plates in a one step addition. Test compounds were prepared from powder stocks by dissolving in DMSO and then serially diluted for displacement curves. Displacement of 10 nM [N-methyl-^{3}H]-GW0438 was measured in a Viewlux 1430 ultraHTS microplate imager (Perkin Elmer Wallac Inc). Non-specific binding was determined in the presence of 10 μM GW0438. A similar competitive ligand binding assay method is described elsewhere (Nichols, J.S., et al. 1998). Data analysis

was achieved using a 3 parameter fit, assuming a slope of 1. The data were calculated as pIC_{50}'s, but because the ligand concentration was well below the K_d for the receptor, this value was not different from the pK_i. The pK_i is the –log of K_i, the inhibitor concentration at which 50% inhibition is observed. K_i is calculated from the IC_{50} using the Cheng-Prusoff equation:

$$K_i = IC_{50} / 1+([L]/K_d)$$

where L = concentration of free radioligand used in the assay and K_d = dissociation constant of the radioligand for the receptor .

Pull-Down Assays

Pull-down studies were performed using a Profound Pull-Down kit (Promega) at 4 °C according to the manufacturer's instructions. For the PXR-RXRα interaction, the RXRα-LBD (residues 225-462) was cloned into the pMALCH10T vector, expressed in *E.coli* BL21pLysS cells and purified by nickel affinity chromatography as described elsewhere (Ortlund, E.A., et al. 2005). Purified RXRα-LBD was biotinylated using an EZ-Link Sulfo-NHS-LC-Biotinylation kit (Promega) according to the manufacturer's instructions. Biotinylated RXRα-LBD at 0.2 mg / mL was immobilized on streptavidin-agarose beads. The beads were washed with TBS buffer (25 mM Tris-Cl pH 7.0, 150mM NaCl), then blocked with biotin solution. The beads were equilibrated with binding buffer (50mM Tris-Cl pH 7.8, 250mM NaCl, 2.5 mM EDTA, and 5% glycerol) and wild-type (WT) PXR LBD or Trp223Ala/Tyr225Ala PXR LBD at 0.2 mg / mL was added to the beads and incubated for 12 hrs. Following prey capture, the beads were washed with binding buffer, eluted with elution buffer at pH 2.8, and examined by SDS-PAGE. For

the PXR-SRC-1 peptide interaction, biotinylated SRC-1 or random peptides at 0.2 mg / mL were immobilized on streptavidin-agarose beads. The beads were washed with TBS buffer (25 mM Tris-Cl pH 7.0, 150mM NaCl), then blocked with biotin solution. The beads were equilibrated with binding buffer (50mM Tris-Cl pH 7.8, 250mM NaCl, 10% glycerol, 0.5% Triton X-100) and WT PXR LBD or Trp223Ala/Tyr225Ala PXR LBD at 0.2mg / mL was added to the beads and incubated for 12 hrs. Following prey capture, the beads were washed with binding buffer, eluted with buffer at pH 2.8, and examined by SDS-PAGE.

Mammalian Two-Hybrid Studies

HepG2 cells were cultured in minimal essential medium (MEM) (Invitrogen) containing 10% fetal bovine serum albumin supplemented with 0.1 mM non-essential amino acids and 1 mM sodium pyruvate. 1000 ng of VP16_PXR (full-length WT PXR or Trp223Ala/Tyr225Ala PXR), 1000 ng of pM_SRC-1 NRID (nuclear receptor interaction domain I; SRC-1 residues 621-765), 900 ng 5xGal4Luc3 reporter plasmid (Chang, C., et al. 1999) and 100 ng pCMVB-gal (for normalization) were used for transfections performed in triplicate. Transfections were achieved with Lipofectin according to the manufacturer's instructions (Invitrogen). Equal levels of PXR and RXRα protein expression in transfected HepG2 cells was confirmed by Western analysis (data not shown). Cells were treated with 1 μM SR12813 sixteen hrs after transfection. Twenty-four hours after ligand treatment, cells were lysed and assayed for luciferase and β-galactosidase activity (Norris, J., et al. 1995).

Results

The PXR LBD Forms a Unique Homodimer

The human PXR ligand binding domain (PXR LBD) forms either a crystallographic or non-crystallographic homodimer in all structures determined to date (Chrencik, J.E., et al. 2005; Watkins, R.E., et al. 2001; Watkins, R.E., et al. 2003a; Watkins, R.E., et al. 2003b). The homodimer interface is formed in large part by the β1′ strands from each monomer, which interact in an ideal anti-parallel fashion to generate a ten-stranded intermolecular β-sheet (**Figures 1.2A and 3.1**) (Watkins, R.E., et al. 2003a). The β1 and β1′ strands of the PXR LBD are part of the ~50 amino acid insert novel to the PXRs relative to other members of the nuclear superfamily. In addition to six main-chain to main-chain intermolecular hydrogen bonds, interdigitating tryptophan (Trp223) and tyrosine (Tyr225) residues from each monomer lock across the dimer interface (**Figure 3.1**). It has been shown that tryptophan and tyrosine residues tend to cluster at protein-protein interaction "hot spots" (Bogan, A.A., et al. 1998; DeLano, W.L. 2002). Pro175 from the loop that follows α1 helps to bury these aromatic side chains, and forms a hydrogen bond between its main-chain carbonyl oxygen and the indol nitrogen on Trp223. The residues involved in this dimer interface are largely conserved in the PXRs of known sequence, including those from human, rhesus monkey, pig, dog, rabbit, mouse and rat. The only exception is dog PXR, which contains a glutamine in place of Trp223; however, glutamine in this position could still hydrogen bond with Pro175 and interdigitate with Tyr225. The formation of the PXR homodimer buries 1,610 $Å^2$ of

solvent accessible surface area, which is sufficient to suggest physiological relevance (Lo Conte, L., et al. 1999).

The PXR LBD Forms a Homodimer in Solution

Sedimentation equilibrium experiments were performed with wild-type PXR LBD to determine whether the homodimer observed in crystal structures is also formed in solution. Experimental data were collected at three speeds (9,000, 13,000 and 16,000 rpm) and three protein concentrations (8.6, 17.3 and 21.7 μM) using a Beckman XL-A analytical ultracentrifuge. When data were fit to a single species model, the molecular weight determined was 67.2 kDa (for n = 9 data sets), which is nearly 2 times the molecular weight of the monomer PXR LBD (36.2 kDa; **Table 3.1**). The subsequent application of a monomer-dimer equilibrium model produced more random residuals and provided the optimal fit for the experimental data, and generated a dissociation constant of 4.5 ± 0.8 μM (**Figure 3.2A**). Experiments repeated in the presence of the PXR agonist SR12813 yielded a similar K_d value of 3.9 ± 1.2 μM using the same monomer-dimer equilibrium model.

We next examined the impact that replacing the interlocking aromatic residues at the dimer interface with alanines would have on receptor LBD dimerization. Thus, a Trp223Ala/Tyr225Ala PXR LBD double-mutant was tested by analytical ultracentrifugation using the same speeds and protein concentrations. These data fit well to a single species model and indicated a measured molecular weight of 36.3 kDa, nearly identical to the calculated molecular weight for the PXR LBD of 36.2 kDa (**Figure 3.2B**). Possibly due to its inability to form a stabilizing dimer, the Trp223Ala/Tyr225Ala double-

mutant form of the PXR LBD formed inclusion bodies during protein expression in *E. coli* cells and had to be refolded using guanidinium hydrochloride to conduct these ultracentrifugation studies. To confirm that this refolded double-mutant form of the PXR LBD was properly folded, we performed circular dichroism (CD) spectropolarimetry experiments. The CD spectrum from 210-300 nm for the Trp223Ala/Tyr225Ala PXR LBD double-mutant was identical to the spectrum of the wild-type PXR LBD (data not shown), indicating that both proteins have the same secondary structural features. We also measured the melting temperatures (T_m) of the wild-type and double-mutant forms of the PXR LBD using CD spectropolarimetry monitored at 222 nm. The T_m's of wild-type PXR LBD and the Trp223Ala/Tyr225Ala PXR LBD double-mutant were 43.0 ± 0.8 and 39.8 ± 0.5, respectively (data not shown). These data indicate that the overall fold and stability of the double-mutant and wild-type forms of the PXR LBD are similar. Indeed, as shown below, the same refolded PXR double-mutant LBD was able to bind to RXRα LBD *in vitro*, which further supports the conclusion that it retains a wild-type structure overall. Taken together, these results establish that mutation of the interdigitating aromatic residues at the PXR dimer interface eliminates dimer formation in solution.

We also conducted sedimentation equilibrium experiments in the presence of a peptide of the sequence NH_3-GSVWNYKP-CO_2, which mimics the dimer interface in PXR. Data analysis indicated that PXR dimerization was partially inhibited by the presence of this peptide. The molecular weight of the PXR LBD measured in the presence of 10-fold molar excess peptide was 70.0 kDa, whereas the molecular weight determined in the presence of 20-fold molar excess peptide (172, 346, or 434 μM) was

50.3 kDa (**Table 3.1**). Thus, the PXR LBD homodimer interaction can be disrupted in solution using relatively high concentrations of an eight amino acid peptide corresponding in sequence to the dimer interface.

Dimer Interface Residues and Transcription

To examine the impact of dimer interface mutations on PXR function, Trp223Ala and Tyr225Ala alterations were introduced into full-length PXR and the activation of a luciferase reporter gene under control of the CYP3A4 promoter was examined in CV-1 cells. As expected, robust up-regulation in these transient transfection experiments was observed for wild-type PXR in the presence of the agonists SR12813 and rifampicin (**Figures 3.3A,B**). However, all mutant forms of the receptor were found to be significantly reduced in their ability to respond to ligands, and exhibited no basal (ligand-independent) transcriptional activation. While the single-site mutant Trp223Ala was found to be more responsive to SR12813 and rifampicin than the Tyr225Ala single mutant, the Trp223Ala/Tyr225Ala double-mutant exhibited little response to SR12813 and essentially no response to rifampicin (**Figures 3.3A,B**). These results indicate that mutations that eliminate PXR homodimer formation significantly reduce the ability of the receptor to upregulate gene expression in ligand-dependent and -independent fashions.

To confirm the proper sub-cellular trafficking of the Trp223Ala/Tyr225Ala double-mutant form of PXR, immunocytochemistry techniques were employed in CV-1 cells, the same cell type used for transfection assays. Wild-type full-length PXR translocated to the nucleus of CV-1 cells both in the absence of agonist and in the presence of either rifampicin or SR12813 (**Figure 3.4A**). Similarly, the

Trp223Ala/Tyr225Ala double-mutant PXR was also found to translocate to the nucleus in the absence of ligand and in the presence of either rifampicin or SR12813 (**Figure 3.4A**). These results confirm that the dramatic changes in transcriptional activity observed for the mutant forms of PXR in transient transfection assays are not caused by improper subcellular localization relative to wild-type PXR.

Monomeric PXR Binds Ligands, DNA and RXRα

We next examined whether the Trp223Ala/Tyr225Ala double-mutant form of PXR, which is incapable of homodimerizing and activating transcription, was able to perform basic molecular functions critical to nuclear receptor action. First, the ability of the double-mutant PXR LBD to interact with ligands was examined in a radioligand competition assay. Both wild-type and double-mutant PXRs bound equally well to the agonists SR12813, rifampicin, estradiol and 5β-pregnane-3,20-dione (**Table 3.2**). Second, gel mobility shift assays were employed to investigate DNA binding. Heterodimeric complexes of full-length RXRα with either full-length wild-type or double-mutant PXRs bound strongly to NR3 and ER6 DNA elements (Bertilsson, G., et al. 1998; Blumberg, B., et al. 1998; Lehmann, J.M., et al. 1998; Wang, H.B., et al. 2003) (**Figure 3.4B**). Third, the ability of the double-mutant PXR LBD to interact with the LBD of its physiological heterodimer partner RXRα was examined using *in vitro* pull-down assays (**Figure 3.4C**). Both wild-type and double-mutant PXR LBDs were found to form complexes with biotinylated RXRα LBDs. Taken together, these results demonstrate that the Trp223Ala/Tyr225Ala double-mutant PXR retains many of its key

molecular functions: its ability to associate with ligands, with its functional heterodimer partner RXRα, and with DNA.

Monomeric PXR Cannot Recruit Coactivator

Because mutant forms of PXR were transcriptionally compromised both alone and in the presence of agonists, the recruitment of the transcriptional coactivator SRC-1 by the double-mutant PXR was examined using two approaches. First, in mammalian two-hybrid studies, the ability of wild-type and Trp223Ala/Tyr225Ala double-mutant full-length PXRs to interact with the nuclear receptor interaction domain (NRID) of SRC-1 in HepG2 cells was tested. It was found that wild-type PXR efficiently complexed with SRC-1, an interaction that was enhanced by the presence of agonist SR12813; however, the Trp223Ala/Tyr225Ala double-mutant PXR failed to interact with SRC-1 either alone or with SR12813 (**Figure 3.5A**). Second, the same interaction was examined *in vitro* using pull-down assays with a biotin-labeled SRC-1 peptide. Similar to the *in vivo* experiments, only wild-type PXR LBD was observed to complex with the SRC-1 peptide, and this interaction was significantly improved by the presence of SR12813. In contrast, double-mutant PXR LBD was incapable of interacting with the same peptide, even in the presence of SR12813 (**Figure 3.5B**). Thus, the inability of Trp223Ala/Tyr225Ala double-mutant PXR to activate transcription appears to be the result of a defect in binding to p160-type coactivators like SRC-1. These results suggest that the unique PXR homodimer formed is involved in coactivator recruitment by the receptor.

Discussion

In all crystal structures of the ligand binding domain of human PXR examined to date, the protein forms a homodimer involving amino acids unique to PXR. The dimerization interface is essentially created by the association of the β1' strands of each monomer in an ideal antiparallel fashion, which generates a ten-stranded antiparallel inter-molecular β-sheet (**Figure 1.2A**). The β1 and β1' strands of PXR are on a ~50-residue insert that is unique in sequence and structure in the nuclear receptor superfamily. In this report, we show that the LBD of human PXR forms a homodimer in solution by sedimentation equilibrium studies, and that a double-mutant form of PXR, in which key aromatic residues at the dimer interface are eliminated, is an obligate monomer (**Table 3.1**; **Figure 3.2**). The mutations at the interface (Trp223Ala and Tyr225Ala) also severely impact the response of full-length human PXR to the agonists SR12813 and rifampicin in transient transfections (**Figure 3.3**). These mutations do not prevent full-length PXR from entering the nucleus, or from binding to DNA, ligands or RXRα (**Figure 3.4; Table 3.2**). Significantly, however, they do prevent PXR from associating with the transcriptional coactivator SRC-1 in both mammalian two-hybrid studies *in vivo* and in pull-down experiments *in vitro* (**Figure 3.5**). Indeed, the loss of basal activity by the Trp223Ala and Tyr225Ala variant forms of the receptor likely reflects the inability of the unliganded mutant PXR-RXRα heterodimers to recruit sufficient coactivator to promote a low level of gene expression. Similar "long-range" effects have recently been observed in the monomeric nuclear receptor human liver receptor homologue-1, in which disruption of the position of a non-DNA binding helix in the DNA binding domain of this

receptor significantly impacts coactivator recruitment by the distantly-located ligand binding domain (Solomon, I.H., et al. 2005). In summary, the accumulated data presented here suggest that the PXR homodimer may play a role in the proper physiological function of this nuclear xenobiotic receptor.

The interlocking tryptophan and tyrosine residues that form the PXR dimer interface represent the first tryptophan zipper (TrpZip) observed in a native protein. TrpZips have been examined extensively in the design of stable peptide sequences that form predictable secondary structures (Cochran, A.G., et al. 2001; Russell, S.J., et al. 2000), and it was found that Trp-Trp pairs placed in designed β-hairpins formed the most stable structures of all combinations of amino acids examined (Cochran, A.G., et al. 2001). We superimposed the homodimer interface of human PXR with the nuclear magnetic resonance (NMR) structure of TrpZip4, a designed β-hairpin structure containing tryptophan zippers. The two tryptophans and two tyrosines in PXR line up well with the four tryptophans in TrpZip4; in addition, the main-chain regions of this native protein dimer and this designed β-hairpin also superimpose well (**Figure 3.6A**) (Cochran, A.G., et al. 2001). A search of the Protein Data Bank (http://www.rcsb.org/pdb/) yielded only one other possible naturally occurring TrpZip in a β-sheet dimer interface, the E2 DNA binding domain of papillomavirus-1. Trp360 from each monomer of the E2 DNA binding domain is in van der Waals contact and contributes a major stabilizing effect (Hegde, R.S., et al. 1992). However, the tryptophans in this structure are orthogonal and face to face but do not interdigitate like the aromatic residues observed in PXR (Hegde, R.S., et al. 1992).

Richardson and Richardson have shown that it is rare for monomeric proteins to expose terminal β-strands of a β-sheet (Richardson, J.S., et al. 2002). Exposed β-strands have the potential to form dangerous interactions with other β-strands, leading to intra- or intercellular aggregates like amyloid fibers. Proteins employ a variety of techniques to cap the terminal strands of a β-sheet, including covering loops, β-bulges, and the central placement of charged residues (Richardson, J.S., et al. 2002). Nuclear receptors, which typically contain a two- to three-stranded antiparallel β-sheet, use several of these methods to cap their terminal β-strands. The PPARs, for example, use a short terminal β-strand, a proline that introduces a kink just prior to the β-strand, and a capping α-helix (Nolte, R.T., et al. 1998). Similarly, CAR, which is structurally and functionally related to PXR, caps its terminal β-strand with a short α-helix (**Figure 3.6B**) (Shan, L., et al. 2004; Suino, K., et al. 2004; Xu, R.X., et al. 2004). RXRα, LXR and VDR all employ loops or helices that cap their terminal β-strands, and VDR further places two charged residues in the center of the terminal strand to disrupt potential non-specific contacts with other β-structures (Gampe, R.T., Jr., et al. 2000b; Rochel, N., et al. 2000; Williams, S., et al. 2003). The observations that PXR leaves the terminal strand in its five-stranded antiparallel β-sheet uncapped, and places residues able to form a TrpZip-like structure on this exposed strand, support the conclusion that the PXRs evolved to form a homodimer . We note, however, that the region of the PXR LBD between residues 178 and 192 has not been visualized structurally to date (**Figure 1.2B**). It is possible that this stretch of amino acids caps the terminal β1' strand but is displaced when the protein forms a homodimer.

PXR forms a heterodimer with RXRα to control the transcription of target genes. We examined whether the PXR homodimer would interfere with the formation of the

PXR-RXRα heterodimer. Using the crystal structure of the PPARγ-RXRα ligand binding domain heterodimer, we replaced the PPARγ LBD with the PXR LBD to generate a model of the PXR-RXRα LBD heterodimeric complex that maintained most of the key hydrophobic and electrostatic contacts at the interface (Gampe, R.T., Jr., et al. 2000a). We also noted that the surfaces used for PXR-RXRα heterodimerization and PXR homodimerization do not overlap; thus, a structurally-compelling model for a PXR-RXRα heterotetramer can be generated (**Figure 3.6C**). It is of interest that no PXR-RXRα heterotetramer was observed in gel mobility shift assays (**Figure 3.4B**), although this is perhaps due to the moderate strength of the dissociation constant (μM) for the PXR homodimer interface. There are several potential ways that a PXR-RXRα heterotetramer could be involved in receptor function. First, a heterotetramer could form between the two PXR-RXRα heterodimers bound to both the proximal and distal DNA elements in the regulatory regions of genes. Recall that two PXR-RXRα binding elements exist in the CYP3A4 promoter, at bases -172 to -149 (proximal) and -7836 to -7607 (distal), and that both elements are required for maximal transcriptional activation (Goodwin, B., et al. 1999). In this model, both PXR-RXRα heterodimers would be bound to DNA, and the DNA would be expected to form a long-range loop to generate the heterotetramer. Second, only one PXR-RXRα heterodimer could bind to a DNA element and the second heterodimer may simply associate with the first (but not with DNA) to form the heterotetramer. In this case, the role of a PXR-RXRα heterotetramer may be to enhance the initial recruitment (and local concentration) of transcriptional coactivators. Third, the heterotetramer may be a crucial trafficking form of the complex required to position the proteins appropriately within the nucleus and/or adjacent to euchromatin.

The structural basis of the impact that the homodimer interface has on coactivator binding may be through the indirect stabilization of αAF and the AF-2 surface. Ordering of the β1-β1' region by dimerization would be expected to stabilize the pseudohelix α2 (which starts at residue 198) that bridges the space between the β-sheet and α-helices 10 and AF in PXR (**Figure 1.2A**). Note that β-strands 1 and 1', as well as α-helix 2, are all on the novel sequence insert unique to PXR and, as we have shown, the contacts they make appear to be involved in receptor function. These observations raise the possibility that disruption of the PXR homodimer interface by small molecule modulators could provide a mechanism to control specifically the regulation of drug metabolism gene expression by PXR during the therapeutic treatment of disease.

Table 3.1. Sedimentation Equilibrium Results for PXR LBDs

$M_{w,calc}$ for PXR LBD = 36,200 Da

	$M_{w,app}$ (Da)	K_d (x 10^{-6} M)
WTPXR*	67,200 ± 3500	4.5 ± 0.8
WTPXR + SR12813	71,100 ± 2100	3.9 ± 1.2
WTPXR + 10-fold peptide	70,050 ± 1397	5.3 ± 0.9
WTPXR + 20-fold peptide	50,317 ± 3022	42.8 ± 13.9
Trp223Ala/Tyr225Ala PXR	36,300 ± 981	N.A.

*WTPXR: wild-type PXR.

N.A.: not applicable.

Table 3.2. Ligand Binding to PXR LBDs

	Wild-Type PXR	**W223A/Y225A PXR**
	pKi	*pKi*
SR12813	5.7	5.6
Rifampicin	5.3	5.6
Estradiol	5.8	5.7
5β-pregnane-3,20-dione	5.0	5.0

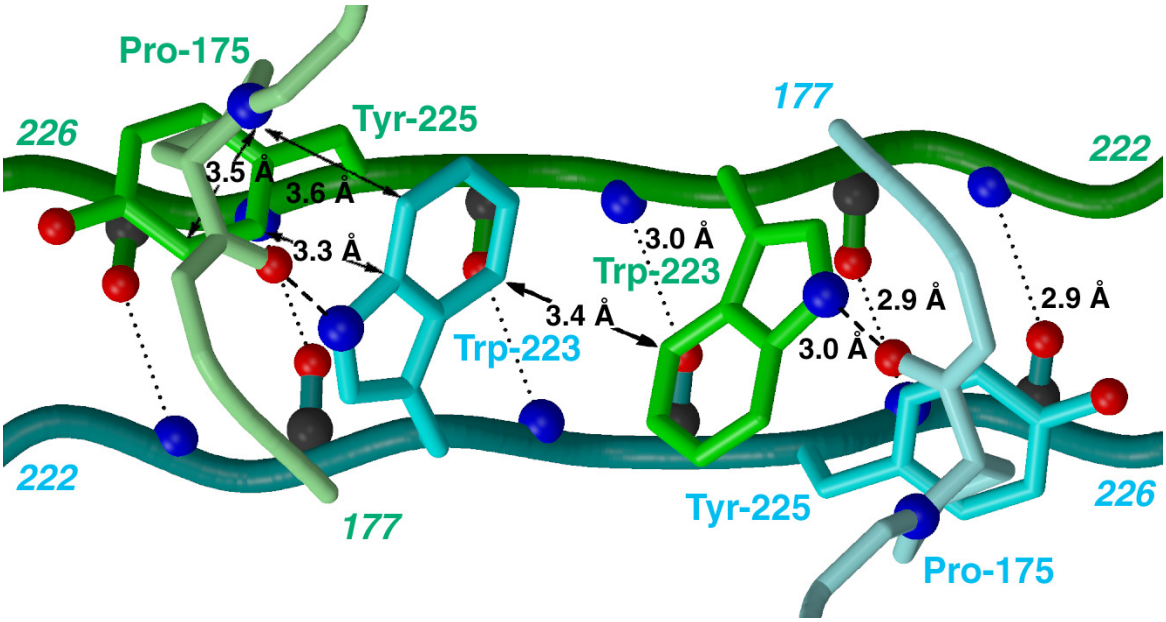

Figure 3.1. PXR LBD homodimer interface. Detailed view of the PXR LBD homodimer interface, rotated 180° about the vertical axis relative to Figure 1A. Novel β1′-strands from each monomer are shown in green and cyan. Inter-locking tryptophan and tyrosine residues from each monomer are rendered in green and cyan, respectively. Hydrogen bonding interactions are indicated (dashed or dotted lines), as are Van der Waals contacts (solid arrows).

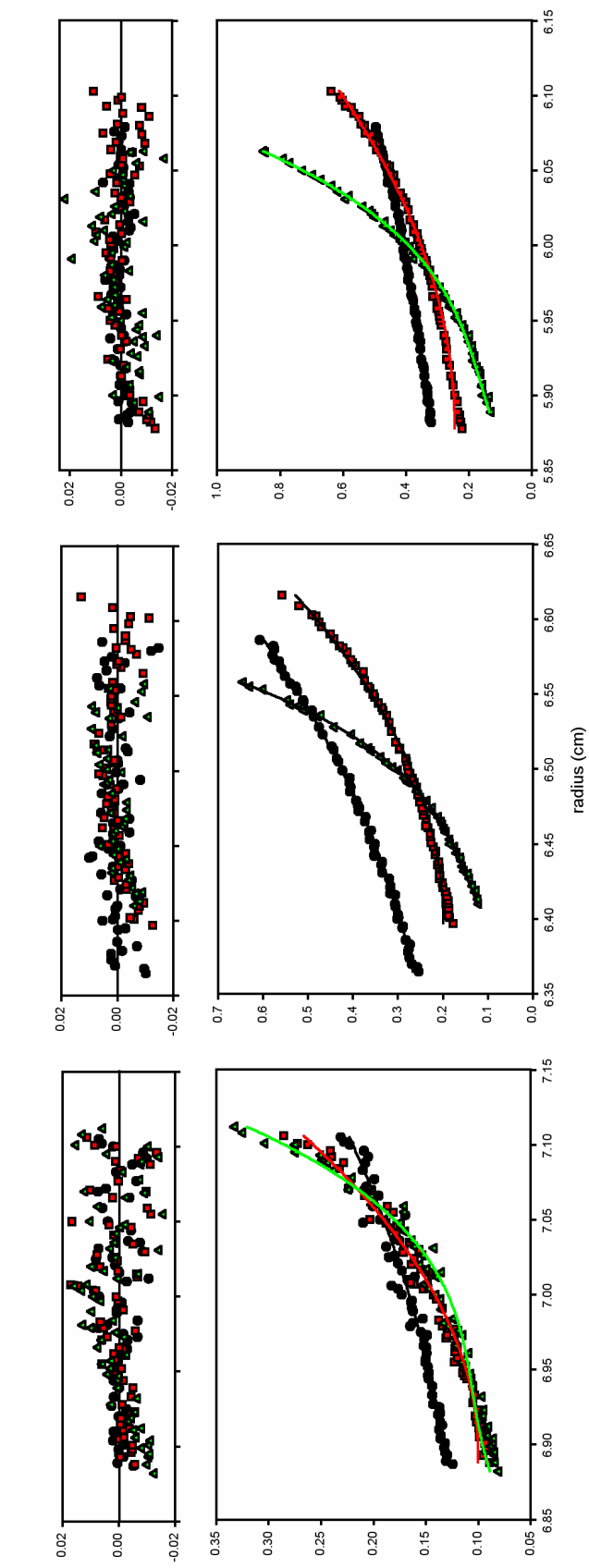

Figure 3.2A. Sedimentation equilibrium data for wild-type human PXR LBD. Each graph indicates a single concentration (left: 8.6 μM, center: 17.3 μM, right: 21.7 μM) collected at 9,000 rpm (circles), 13,000 rpm (squares) and 16,000 rpm (triangles). The data in the figure was fit to a monomer-dimer equilibrium model (solid lines) with the residuals for each fit shown in the upper panels.

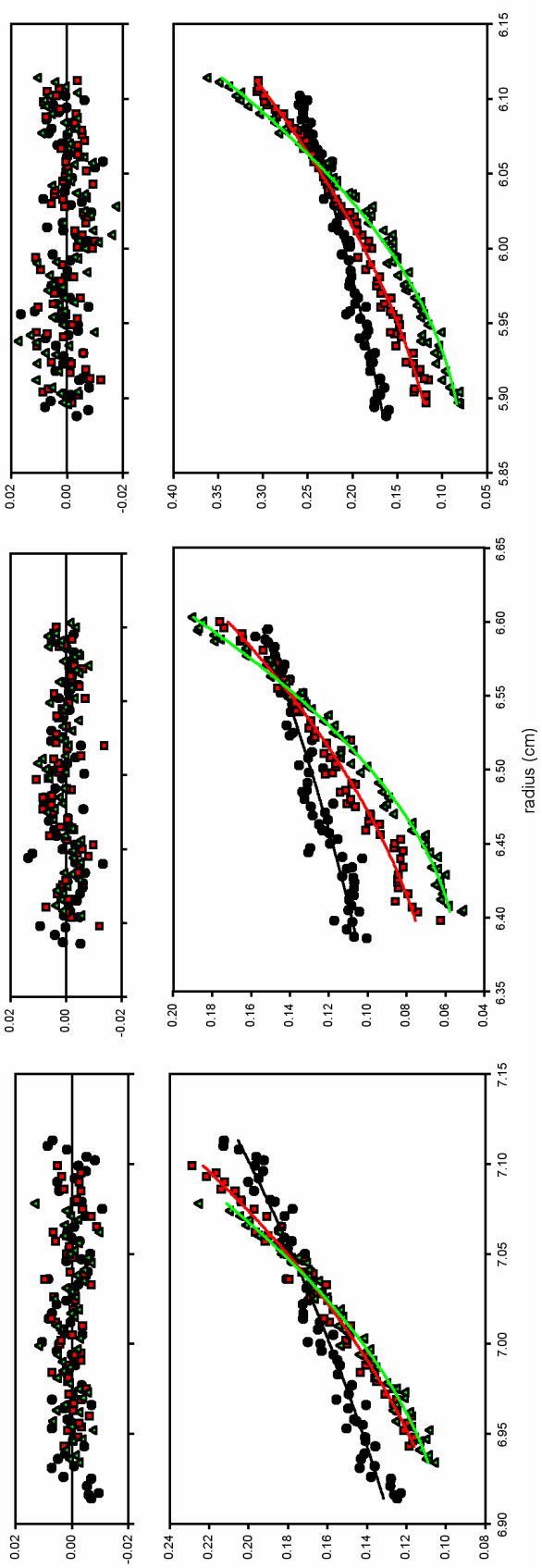

Figure 3.2B. Sedimentation equilibrium data for mutant human PXR LBD (Trp223Ala/Tyr225Ala). Each graph indicates a single concentration (left: 8.6 μM, center: 17.3 μM, right: 21.7 μM) collected at 9,000 rpm (circles), 13,000 rpm (squares) and 16,000 rpm (triangles). Sedimentation equilibrium data obtained for Trp223Ala/Tyr225Ala mutant PXR. The data in the figure were fit to a singles species model (solid lines) with the residuals for each fit shown above.

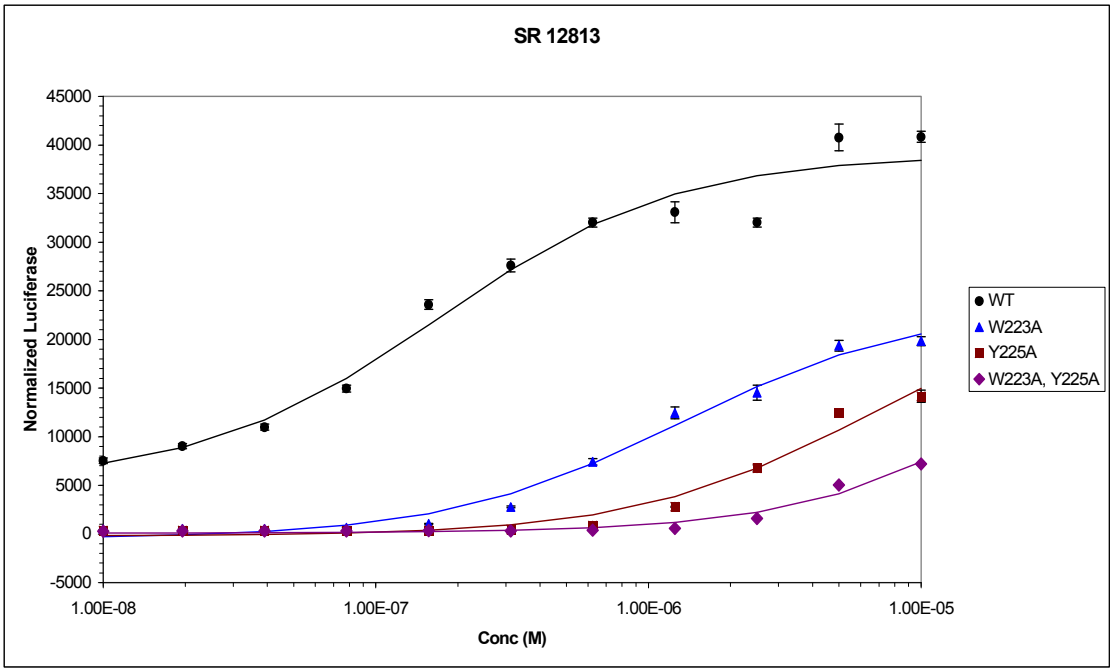

Figure 3.3A. Transcriptional activity of wild-type and mutant PXR in the presence of SR12813. Transient transfections in CV-1 cells using a luciferase reporter construct and wild-type or mutant forms of full-length human PXR. Responses in the presence of increasing concentrations of SR12813 is shown.

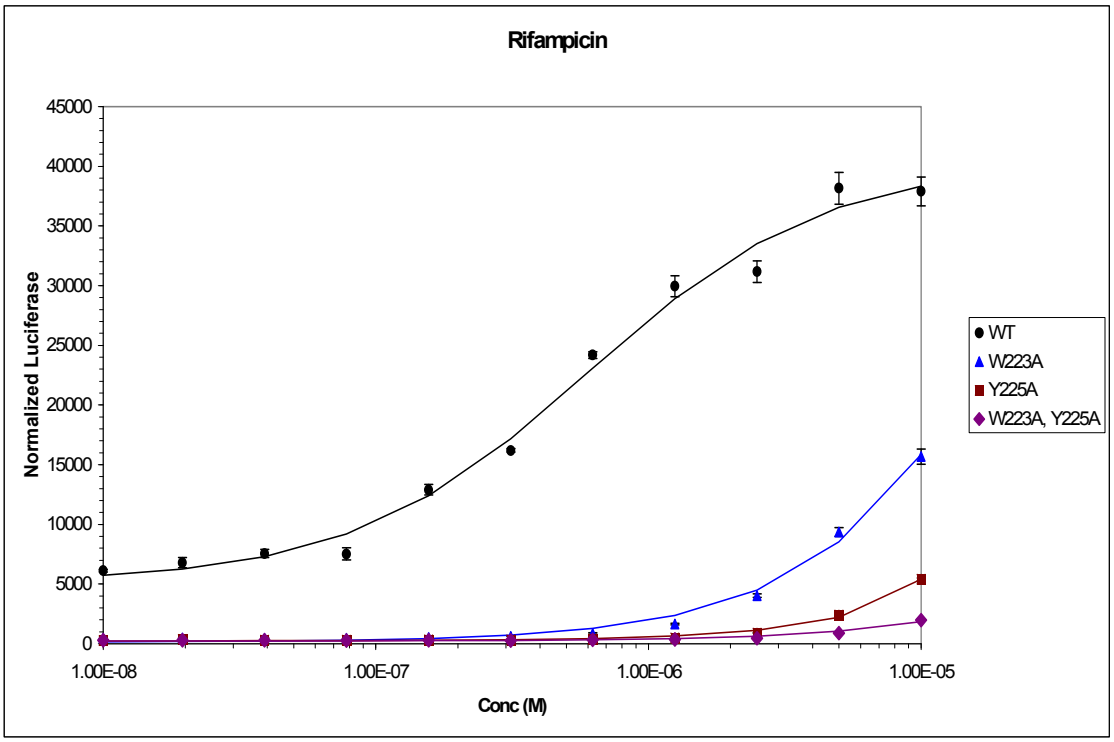

Figure 3.3B. Transcriptional activity of wild-type and mutant PXR in the presence of rifampicin. Transient transfections in CV-1 cells using a luciferase reporter construct and wild-type or mutant forms of full-length human PXR. Responses in the presence of increasing concentrations of rifampicin is shown.

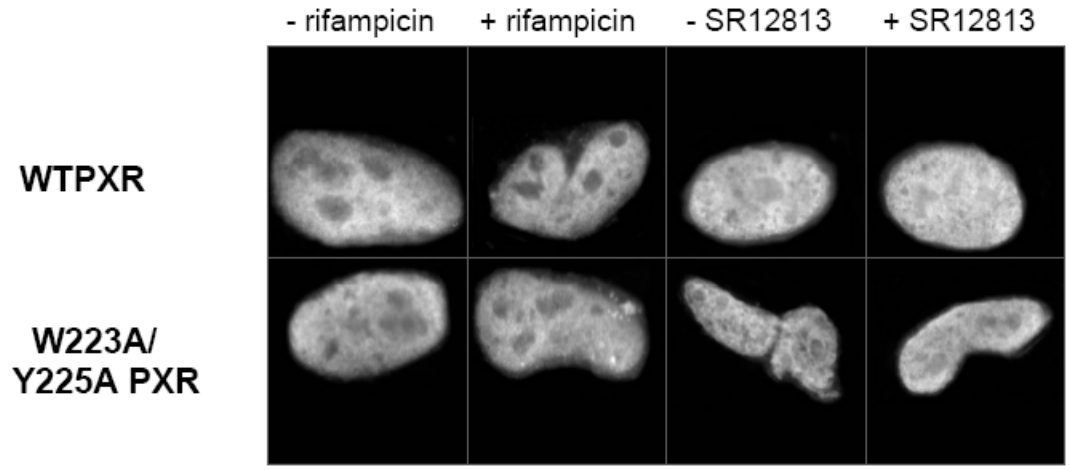

Figure 3.4A. Cellular localization of full-length mutant and wild-type PXR. Full-length wild-type PXR (WTPXR) and Trp223Ala/Tyr225Ala double-mutant PXR are competent for nuclear translocation in CV-1 cells. Fluorescence due to specific staining of exogenous WTPXR or Trp223Ala/Tyr225Ala PXR in transfected CV-1 cells was concentrated in nuclei, as confirmed by colocalization with the nuclear stain Hoechst 33258 (not shown). Neither untransfected cells nor transfected cells treated with secondary antibody only were stained (not shown). The general distribution of PXR and Trp223Ala/Tyr225Ala PXR within the nuclei was not observed to differ in the presence of either rifampicin or SR12813.

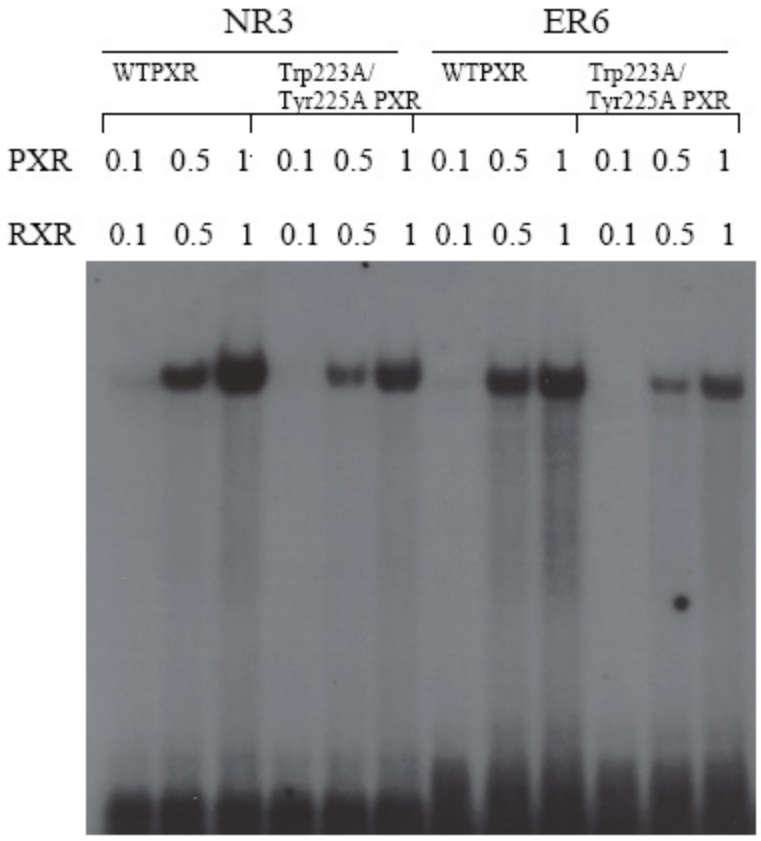

Figure 3.4B. Mutant PXR binds NR3 and ER6 DNA elements. Full-length PXR/RXRα heterodimers containing wild-type or double mutant (Trp233Ala/Tyr225Ala) PXR bind to CYP2B6 and CYP3A4 responsive elements. *In vitro* translated wild-type or Trp223Ala/Tyr225Ala PXR (0.1, 0.5 or 1 μL) were combined with equal amounts of RXRα protein and incubated with NR3 (caTGGACTttccTGACCCca) or ER6 (ataTGGACTcaaaggAGGTCAgtg) elements from CYP2B6 and CYP3A4, respectively. Oligonucleotides were labeled with [γ-^{32}P]dATP, and mobility shift assays were performed as described in "Experimental Procedures".

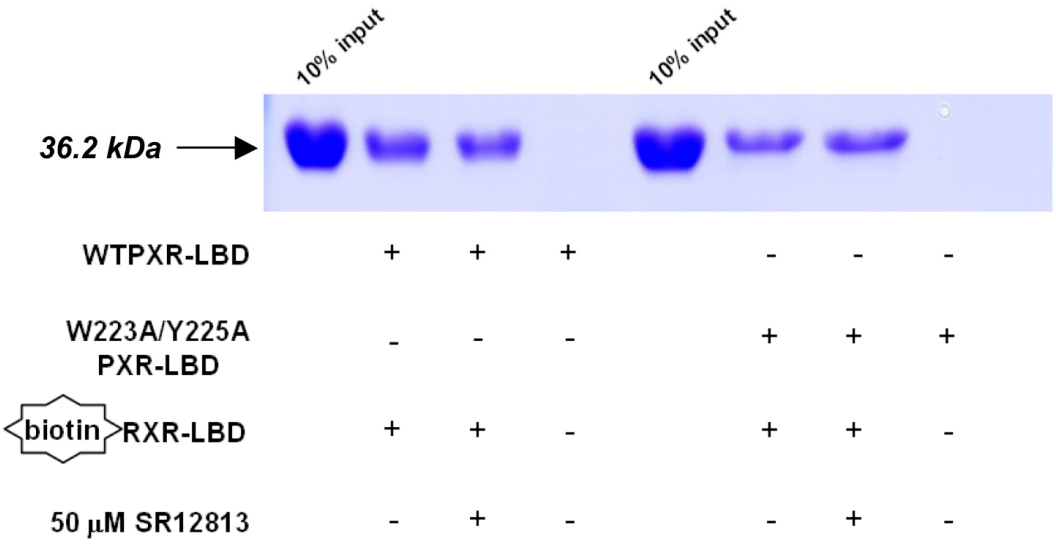

Figure 3.4C. Mutant PXR LBD can bind to RXRα LBD in vitro. Trp223Ala/Tyr225Ala double-mutant PXR LBD is competent to bind to the LBD of RXRα. Wild-type or double-mutant PXR LBD's were incubated with biotin-labeled RXRα LBD in the absence and presence of the PXR agonist SR12813 at 50 μM. RXR was then immobilized on streptavidin beads, and the beads extensively washed. Bound proteins were eluted and examined by SDS-PAGE, and the bands for the 36.2 kDa PXR LBD are shown.

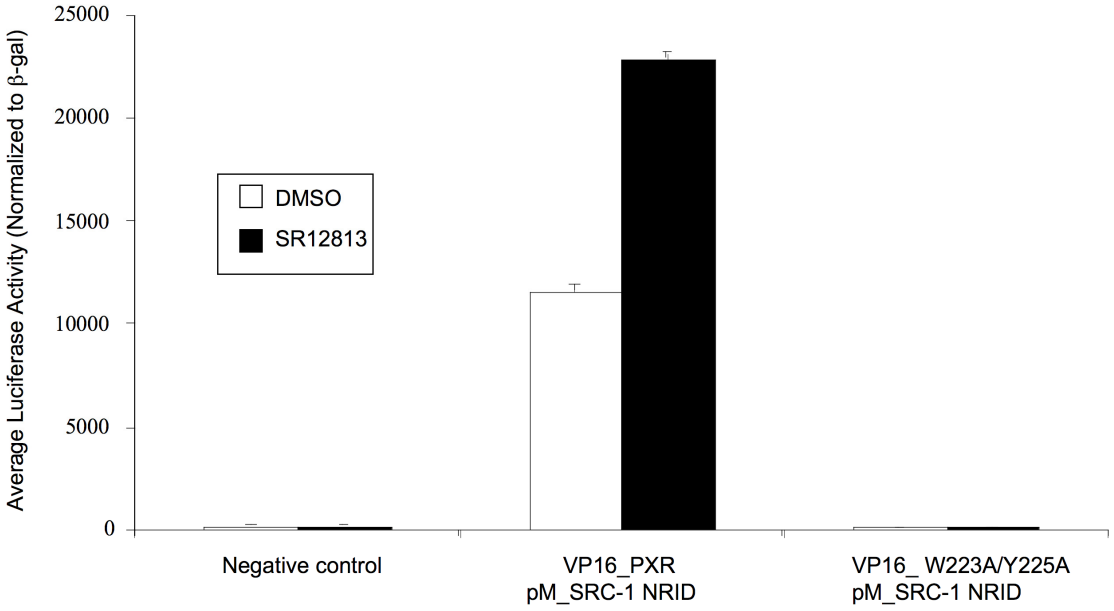

Figure 3.5A. Mutant PXR does not interact with SRC-1 in mammalian two-hybrid assay. Mammalian two-hybrid examination of the interaction between full-length PXR and the nuclear receptor interaction domain (NRID) of the transcriptional coactivator SRC-1. Wild-type and Trp223Ala/Tyr225Ala double-mutant PXR were examined alone and in the presence of the PXR agonist SR12813.

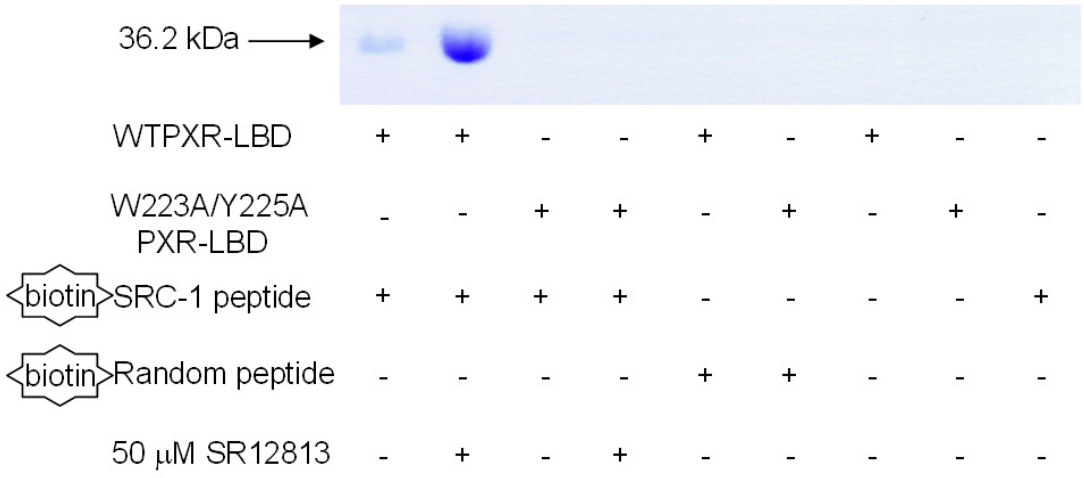

Figure 3.5B. Mutant PXR LBD does not interact with SRC-1 peptide pull-down assay. *In vitro* examination of the interaction between PXR LBDs and an SRC-1 peptide. Only wild-type PXR LBD interacted with a biotinylated SRC-1 peptide, while a Trp223Ala/Tyr225Ala double-mutant PXR LBD was not observed to bind to the same peptide.

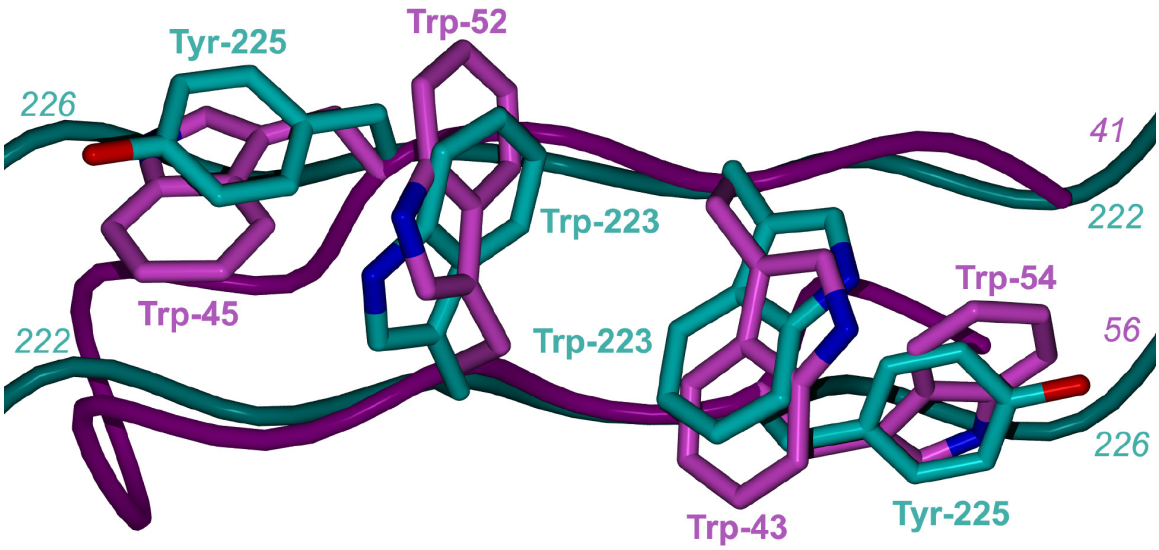

Figure 3.6A. Superposition of PXR LBD homodimer interface on TrpZip4. Superposition of the PXR LBD homodimer interface on TrpZip4 (Cochran, A.G., et al. 2001). PXR residues 222-226 are shown in cyan. Residues 41-56 of Trpzip4 are rendered in magenta.

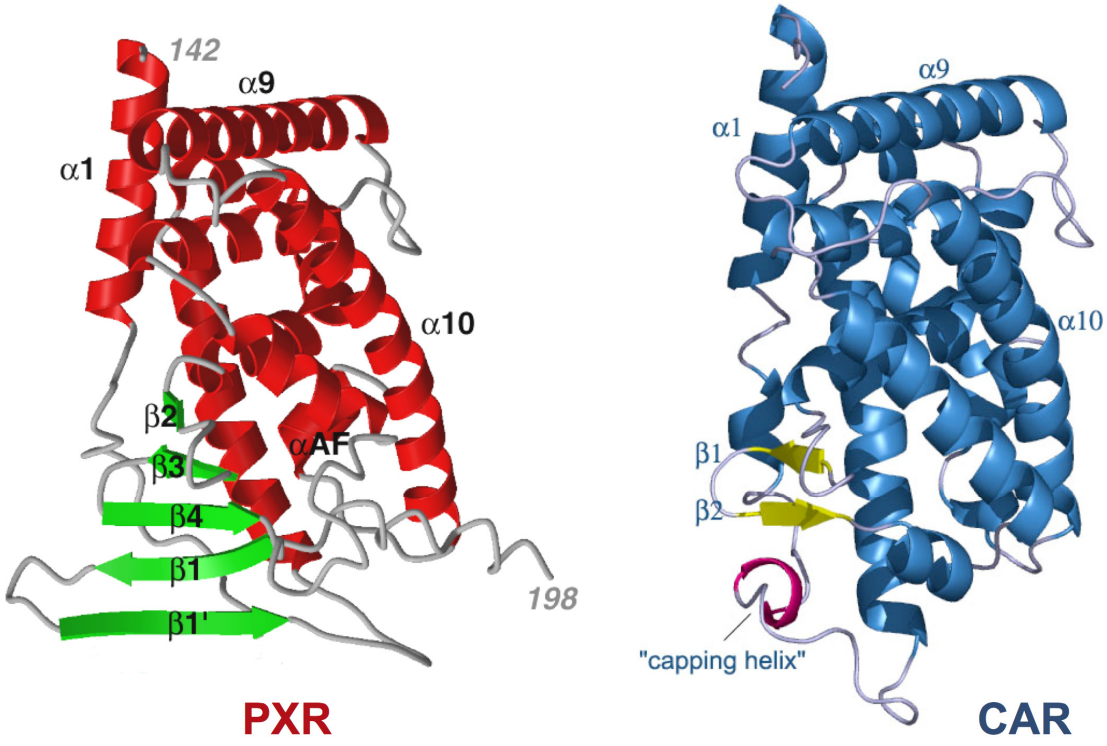

Figure 3.6B. Comparison of PXR and CAR LBD structures. A side-by-side representation of the LBDs of PXR and CAR (Shan, L., et al. 2004; Suino, K., et al. 2004; Xu, R.X., et al. 2004). The extended β-sheet region of PXR is rendered in green. The β-sheet region of CAR is depicted in yellow. Unlike PXR, CAR contains a capping α-helix (shown in magenta) that protects its edge β-strand from non-specific interactions.

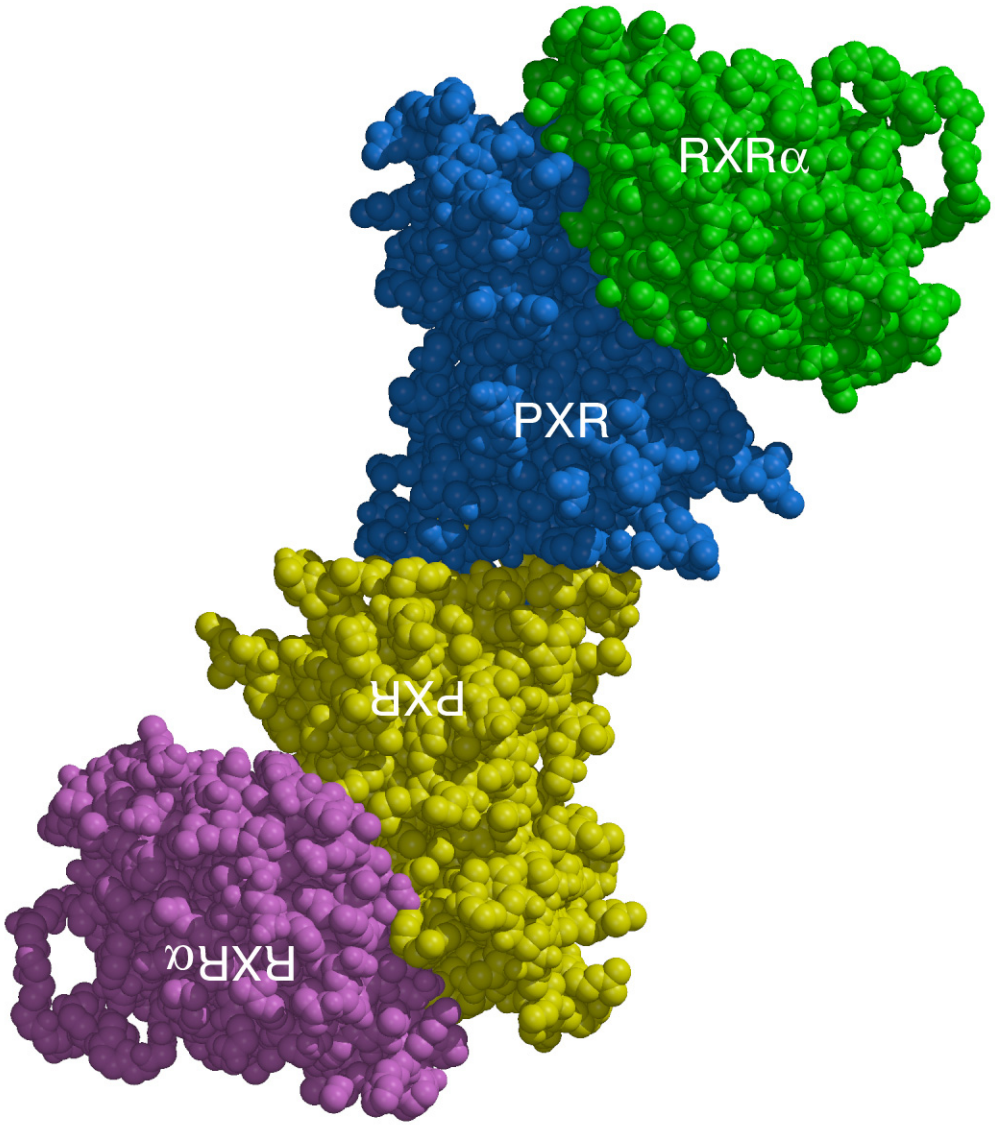

Figure 3.6C. Model of the PXR/RXRα heterotetramer. A model for the PXR/RXRα heterotetramer complex of ligand binding domains. The PXR-RXRα heterotetramer was generated using the structure of PPARγ-RXRα complex as a template (Gampe, R.T., Jr., et al. 2000a). The PXR LBD homodimer is shown in blue and yellow with the RXRα-LBDs in green and magenta. The PXR LBDs in this figure are viewed in the same orientation shown in **Figure 1.2A**.

Chapter 4

Biophysical Characterization of PXR LBD and Mutants

Abstract

The nuclear pregnane X receptor (PXR) regulates expression of many genes essential in mammalian drug metabolism including cytochrome P450-3A4 (CYP3A4), which metabolizes more than 50% of all prescription drugs. PXR is a ligand-activated transcription factor that responds to a wide variety of structurally distinct compounds. Biophysical characterization of wild-type PXR LBD and two specific mutants that confer changes in basal transcriptional activity was carried out. The mutants are based on salt bridges on the surface of PXR's LBD that appear to gate the entrance to the ligand binding pocket. Individual mutations of "charge-gate" residues to alanine significantly impact the basal transcriptional activity of PXR, and therefore could shed light on the regulation of PXR. These mutations could impact basal transcriptional activity of the receptor by introducing detailed structural changes that are reflected in gross alterations in protein stability and changes in the ability to recruit transcriptional coregulators. The thermal stabilities of wild-type and mutant forms of PXR LBD were determined using circular dichroism spectropolarimetry (CD).

Introduction

The nuclear pregnane X receptor (PXR) regulates expression of many genes essential in mammalian drug metabolism including members from the 2B and 3A subfamilies of cytochrome P450s (CYP2B and CYP3A) and the xenobiotic efflux pump MDR1 (human multidrug resistance 1 protein) (Goodwin, B., et al. 2002) The 3A4 isoform is the predominant CYP expressed in the human adult liver and small intestine; this isoform is known to metabolize greater than 50% of prescription drugs and is thought to be the key player in drug-drug interactions (Guengerich, F.P. 1999; Li, A.P., et al. 1995; Maurel, P. 1996; Michalets, E.L. 1998). PXR is a ligand-activated transcription factor that responds to a wide variety of structurally distinct compounds. Ligand-activated transcription by other nuclear receptors is mediated by coactivator and corepressor proteins (collectively called coregulators). The interactions of PXR with coactivators are relatively well-characterized, and a crystal structure of a fragment of SRC-1 (steroid receptor coactivator-1) bound to the PXR ligand binding domain (LBD) has been determined (Watkins, R.E., et al. 2003a).

The PXR LBD structure is shown in **Figure 1.2B**; it contains ten alpha helices and a five-stranded beta sheet (in comparison to the typical nuclear receptor's three-stranded beta sheet). (Watkins, R.E., et al. 2001; Watkins, R.E., et al. 2003a; Watkins, R.E., et al. 2003b) The ligand-binding pocket is very large (1100-1500$Å^3$) and predominantly hydrophobic with the eight polar residues evenly distributed throughout the twenty hydrophobic residues that line the pocket. (Watkins, R.E., et al. 2001) The coactivator fragment (yellow in **Figure 1.2B**) binds in a groove formed with residues

from αAF (activation function), α3, and α4; the coactivator binds adjacent to the AF2 helix that is responsible for ligand-dependent transcriptional activation (labeled αAF in **Figure 1.2B**).

In the crystal structures of the human PXR ligand binding domain (LBD) two salt bridges (R410-E321 and R413-D205) on the surface of PXR appear to gate the entrance to the ligand binding pocket (**Figure 4.1**). (Watkins, R.E., et al. 2001) Interestingly, individual mutations of these "charge-gate" residues to alanine significantly impact the basal transcriptional activity of PXR as determined by a luciferase reporter gene assay in CV-1 cells transfected with human PXR and the xenobiotic-responsive enhancer module from CYP3A4, then treated with SR12813 or rifampicin (**Figure 4.2**). (Watkins, R.E., et al. 2001) The largest effects were observed in the R410A mutant, which increased the basal activity of PXR, and the D205A mutant, which eliminated basal activity. (Watkins, R.E., et al. 2001) Addition of ligand was able to restore all activity for the D205A mutant; and, although R410A responded to ligand, the difference between R410A and wild type activity at the highest concentration of ligand was much smaller than the difference observed in the absence of ligand and at low concentrations. These mutations could impact basal transcriptional activity of the receptor by introducing detailed structural changes that are reflected in gross alterations in protein stability and changes in the ability to recruit transcriptional coactivators and corepressors. Thermal stability of wild-type PXR LBD and the R410A and D205A mutant LBDs was determined using circular dichroism spectropolarimetry. Results of this study demonstrate that the changes due to charge gate mutations do confer an overall change in the thermal stability of the protein. To determine whether the mutations changed the structure of the PXR LBD,

crystallization trials were conducted; however, neither the R410A nor the D205A protein produced crystals.

Materials and Methods

Protein Expression and Purification

Pure wild-type and mutant PXR LBDs were expressed and purified using modifications of the published protocols (Watkins, R.E., et al. 2001). Briefly, human PXR LBD (residues 130-434) was His-tagged and coexpressed with a fragment of SRC-1 in BL-21 Gold cells (Stratagene). Cells were lysed by sonication, and the clarified cell lysate was purified using ProBond nickel-chelating resin (Invitrogen). For CD studies, the fractions appearing pure based on SDS PAGE were combined and dialyzed into a low salt, phosphate buffer (20 mM sodium phosphate pH 7.8, 100 mM NaCl, 2.5 mM EDTA, 10 mM β-mercaptoethanol, 5% glycerol) which is necessary to minimize noise in the spectrum and maintain a moderate absorbance level. After dialysis, the protein was concentrated to 0.5 mg/mL. Using this method, 3 mg of pure wild-type PXR, 10 mg of PXR R410A, and 5 mg of D205A were obtained per 8 L culture. For crystallization trials, the Ni-column fractions were analyzed using a Bradford assay only, and all fractions containing protein were loaded to an SP sepharose column as they eluted from the Ni-column. Protein eluted from the SP column was diluted to prevent precipitation caused by high salt concentrations. The fractions containing PXR were concentrated to 7 mg/mL for crystallographic studies. Using the additional column decreases the yield of all forms of

PXR to approximately 1 mg per 8 L culture, but removes low concentration impurities (visible by SDS PAGE only with silver staining) that seem to impede crystallization.

Thermal Denaturation.

Thermal stabilities of wild-type, D205A, and R410A PXR LBD in the presence and absence of ligands and a fragment of the coactivator SRC-1 were determined using circular dichroism spectropolarimetry (CD). Biophysical characterization of wild-type PXR and mutants of PXR was initiated by Paula-Davis Searles at University of North Carolina at Chapel Hill. The circular dichroism signal at 222 nm (indicative of alpha helix) was monitored as the temperature was changed by 1ºC/min from 4ºC to 85ºC. Samples were prepared and incubated on ice for at least 15 minutes after 10x ligand or 10x SRC-1 was added. Data was collected on an AVIV circular dichroism spectrometer Model 62DS at the Macromolecular Interactions Facility at University of North Carolina at Chapel Hill. The 25 amino acid fragment of coactivator SRC-1 (676-CPSSHSSLTERHKI**LHRLL**QEGSPS-700, where the LxxLL motif is in bold) >98% pure was purchased from SynPep. Rifampicin was purchased from Sigma Aldrich, and SR12813 was a gift from GlaxoSmithKline.

Once collected, the data was analyzed in Sigma Plot using a two-state fit for denaturation according to the reaction scheme

$$N \rightleftharpoons D$$

The equations combined for the regression have been previously described.(Allen, D.L., et al. 1998; Cohen, D.S., et al. 1994) (**Equations 1 and 2.**)

$$A_{\lambda,T} = \frac{\lambda_{N,T} + K_{D,T}(\lambda_{D,T})}{1 + K_{D,T}}$$ **Equation 1.**

$$K_{D,T} = -\exp\left\{\frac{\Delta H_m\left[1 - \left(\frac{T}{T_m}\right)\right] - \Delta C_p\left[(T_m - T) + T\ln\left(\frac{T}{T_m}\right)\right]}{RT}\right\}$$ **Equation 2.**

Where $A_{\lambda,T}$ is the polarization of the light at wavelength λ and temperature T (in Kelvin), $\lambda_{N,T}$ is the polarization due to the native (N) baseline at temperature T, $K_{D,T}$ is the apparent equilibrium constant for denaturation at temperature T, $\lambda_{D,T}$ is the absorbance due to the denatured (D) baseline at temperature T, ΔH_m is the van't Hoff enthalpy of denaturation, T_m is the temperature at which half of the protein molecules are denatured, ΔC_p is the heat capacity of D minus N, and R is the gas constant.

Results and Discussion

The results obtained thus far for wild-type, D205A, and R410A PXR LBD in the presence and absence of ligands or coactivator fragment are presented in **Table 4.1**. Indeed, a correlation is evident between thermal stability and basal transcriptional activity; the mutant without basal activity shows a decreased thermal stability (from 43.1 ± 0.1°C for wild-type to 37.7 ± 0.4°C for D205A), while the mutant with increased basal activity shows an increased thermal stability (from 43.1±0.1°C for wild-type to 46.5±0.8°C for R410A). In addition, both ligand and coactivator binding confer stability to all forms of PXR. Ligand induced a greater increase in D205A T_m than in wild-type T_m and less increase in R410A T_m than in wild-type T_m, while SRC-1 binding conferred

greater increases in T_m to both mutants than it did to wild-type. This pattern of stability change conferred by SRC-1 for R410A could contribute to its ability to act above the maximal level established by wild-type in the luciferase reporter gene assays.

An unusual structural feature of the PXR LBD is the novel α2 helix present when coactivator peptide is observed bound (**Figure 1.2B**).(Watkins, R.E., et al. 2003a) This helix is not present in any other nuclear receptors or PXR LBD in the absence of coactivator peptide. The residue that shows that greatest change in position is Leu209, which is shifted significantly (7.7 Å) between the PXR LBD structure with SR12813 and the PXR LBD/SR12813/SRC-1 structure suggests that α2 is linked to coactivator binding. **Figure 4.3** shows Asp205 and Leu 209 side chains rendered as sticks; Asp205 is on the same face of the helix, one turn away, as Leu209. The transcriptional activity data from the charge-gate mutants may suggest that the positioning of α2 is critical to transcriptional activation because loss of Asp205, which holds α2 in its position, abolishes basal activity. This would also explain why individual loss of Glu321 or Arg413 has less of an effect on activity; as **Figure 4.1** shows, Glu321 is not involved in positioning α2 at all and loss of Arg413 could be mitigated by weak interactions between Asp205 and the remaining Arg410. Therefore, it is possible that mutating Asp205 to alanine favors a conformation that facilitates corepressor binding. Addition of agonist is able to fully restore transcriptional activity of D205A, suggesting the induced change is completely overcome by ligand contacts. The effect of the R410A mutation is more difficult to understand. Arg410 does make a water-mediated contact to the ligand (SR12813) in structures, but it is not clear that changing the residue to alanine could effect this interaction in a way to contribute to its high basal activity. Because the ligand

makes van der Waals contacts with the αAF-2 helix, the R410A activity could also be explained by causing a favorable change in the AF2 region for binding of coactivator. It is also possible that removing Arg410 allows a better interaction of Asp205 and Arg413, and thereby stabilizes α2. These questions cannot be answered until crystal structures for the mutants are determined.

Crystallization trials were performed with the PXR R410A mutant using both sparse matrix and focused screens (using previously determined crystallization conditions from Syrxx screen and the literature (Watkins, R.E., et al. 2001; Watkins, R.E., et al. 2003a; Watkins, R.E., et al. 2003b)). Unfortunately, many wells of the sparse matrix screens contained denatured precipitate. The focused screens produced denatured precipitate, phase separation, and birefringent spherulites. Some small crystal plates of R410A grew in the screens around Syrxx conditions (100 mM HEPES, PEG 6000, LiCl, pH 6.8-6.9 and 7.2-7.3). However, the crystal quality was poor and optimization was unsuccessful. To date, crystallization conditions for R410A and D205A remain elusive.

Although additional data on E321A and R413A would augment this study, the results presented here demonstrate that the mutants that change basal transcriptional activity have reflective changes in protein stability *in vitro*. Because the position of the residues and their link to the αAF helix suggest that these changes in thermal stability reflect structural changes that could also alter the receptor's ability to bind coregulator, the ability of different coactivators to potentiate transcription of wild-type and mutant PXRs should be compared. *In vivo* effects of stability changes should be investigated by examining degradation and the effects of proteosomal inhibitors. The mutants examined in this proposal are worthy of investigation for gene therapy as they could significantly

alleviate severe cases drug-drug interactions by allowing medical practitioners to attenuate PXR's response to specific xenobiotics.

	no ligand	SR12813	rifampicin	SRC-1	SR12813 +SRC-1	rif + SRC-1	Basal Activity
hPXR (wt)	43.1 ± 0.1 (3)	48.1 ± 0.7 (4)	46.5 ± 0.5 (4)	47.8 ± 0.6 (3)	50.2 ± 0.1 (3)	52.6 ± 0.3 (3)	++
hPXR-D205A	37.7 ± 0.4 (3)	46.6 ± 0.3 (6)	45.8 ± 0.2 (8)	44.7 ± 0.1 (7)	48.8 ± 0.2 (5)	47.9 ± 0.1 (8)	None
hPXR-R410A	46.5 ± 0.7 (4)	48.9 ± 0.1 (3)	47.0 ± 1.6 (4)	52.0 ± 2.1 (5)	55.1 (1)	53.6 ± 5.0 (4)	++++
hPXR-R413A	n.d.	n.d.	n.d.	n.d.	n.d.	n.d.	+
hPXR-E321A	n.d.	n.d.	n.d.	n.d.	n.d.	n.d.	+

Table 4.1. Melting temperatures of wild-type and mutant PXR LBD. Melting temperatures (in °C) of wild-type and mutant forms of the PXR LBD determined by CD. (Numbers in parenthesis indicate number of replicates, n.d. indicates values not yet determined.)

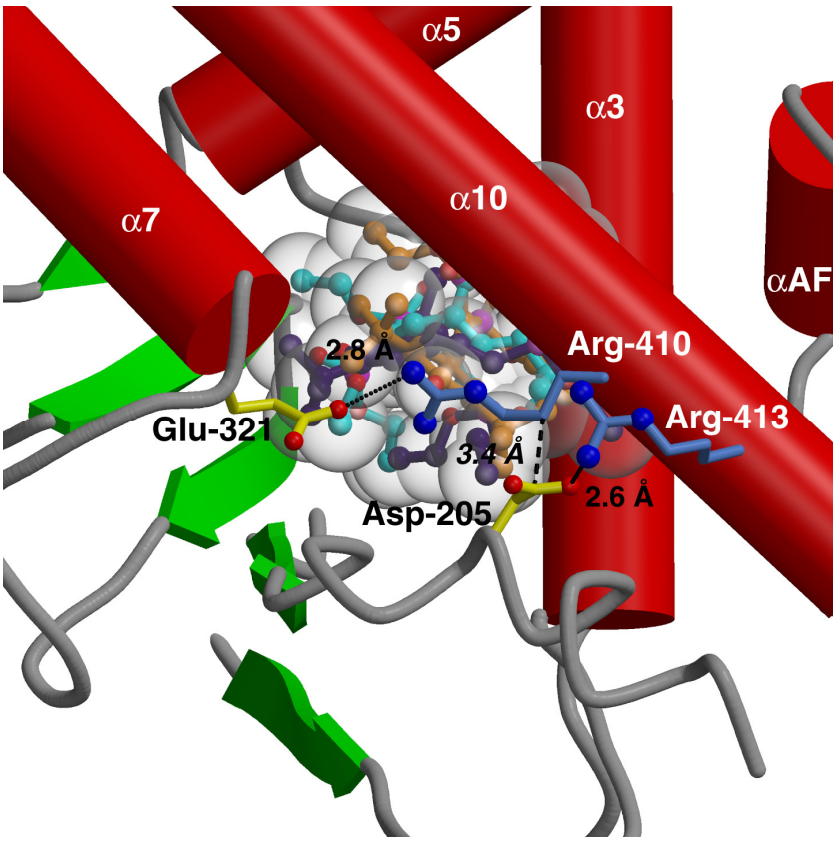

Figure 4.1. Charge-gate residues of PXR ligand binding pocket. [Figure from R.E. Watkins et al. (2001) *Science* **292**:2329-33. Reprinted with permission from AAAS.] Close-up view of the R410-E321 and R413-D205 salt bridges gating the ligand binding pocket of PXR LBD. (The ligand SR12813 is shown in three different orientations in the ligand binding pocket.)

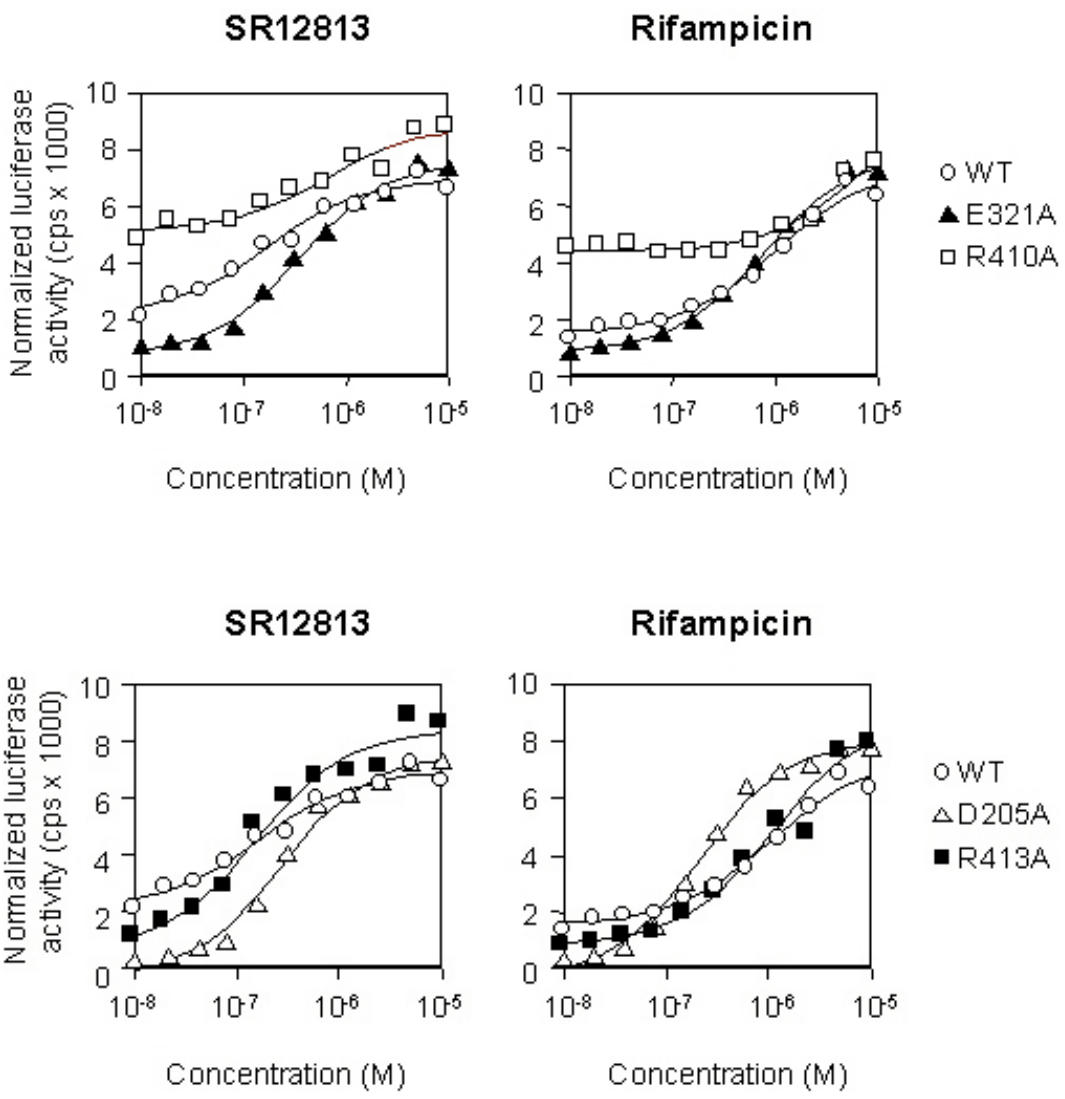

Figure 4.2. Transcriptional activity of wild type and mutant PXR LBD. [From R.E. Watkins et al. (2001) *Science* **292**:2329-33. Reprinted with permission from AAAS.] Results of the luciferase reporter gene assay for wild-type and mutant PXR, performed in CV-1 cells with increasing concentrations of ligand.

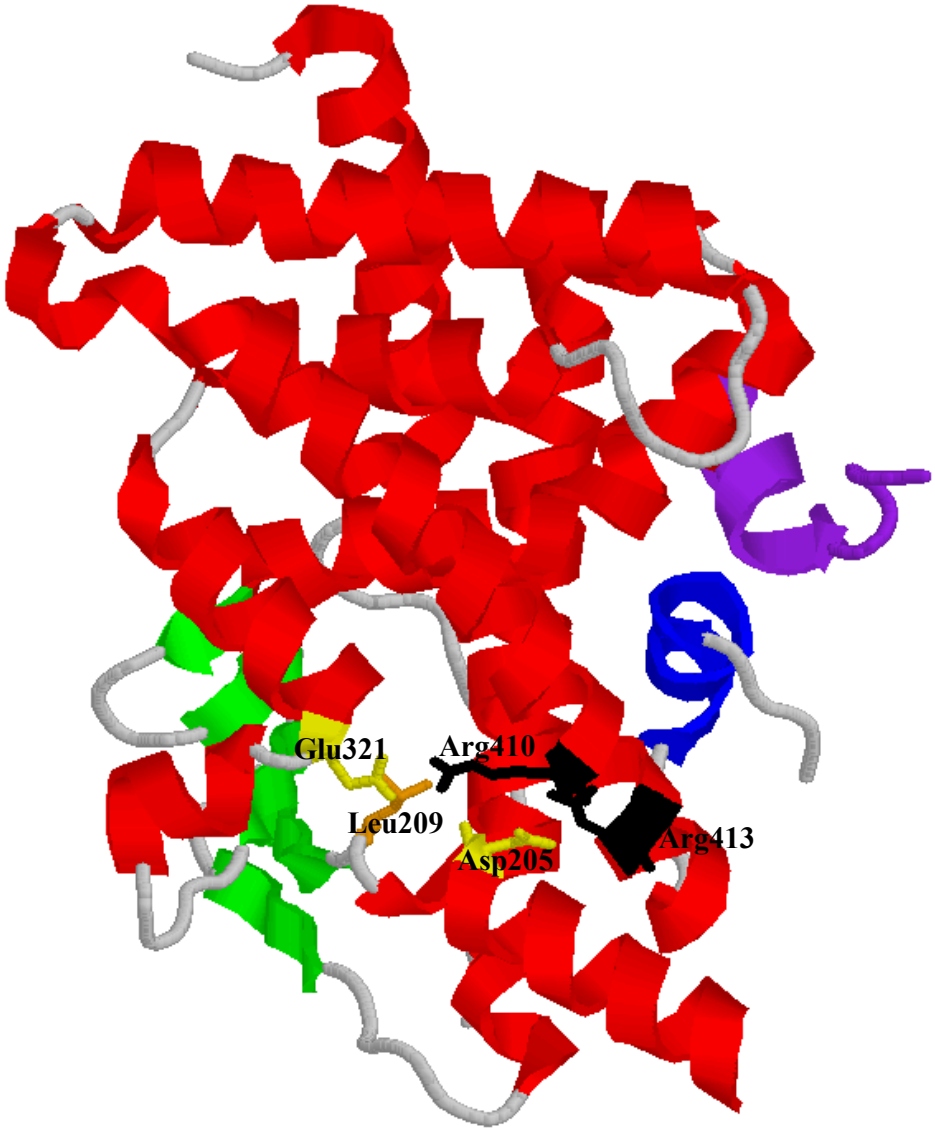

Figure 4.3. Location of leu209 in relation to charge-gate residues. Structure of human PXR LBD with SRC-1 peptide (purple) and SR12813 bound (not shown). Generated from 1NRL.(Watkins, R.E., et al. 2003a) The αAF is shown in blue. The arginines side chains that participate in the charge gate are shown in black, while the acidic residue side chains are shown in yellow. Leu209 (orange) moves the most when compared to the structure where activator is not bound and is Leu209 is on the same side of the helix as Asp205.

References

Allen, D.L. and Pielak, G.J. (1998). "Baseline length and automated fitting of denaturation data." *Protein Science* **7**: 1262-1263.

Aranda, A. and Pascual, A. (2001). "Nuclear hormone receptors and gene expression." *Physiol Rev* **81**: 1269-304.

Bachs, L., Pares, A., Elena, M., Piera, C. and Rodes, J. (1992). "Effects of long-term rifampicin administration in primary biliary cirrhosis." *Gastroenterology* **102**: 2077-2080.

Bertilsson, G., Heidrich, J., Svensson, K., Asman, M., Jendeberg, L., Sydow-Backman, M., Ohlsson, R., Postlind, H., Blomquist, P. and Berkenstam, A. (1998). "Identification of a human nuclear receptor defines a new signaling pathway for CYP3A induction." *Proceedings of the National Academy of Sciences of the United States of America* **95**: 12208-12213.

Bhalla, S., Ozalp, C., Fang, S.S., Xiang, L.J. and Kemper, K. (2004). "Ligand-activated pregnane X receptor interferes with HNF-4 signaling by targeting a common coactivator PGC-1 alpha - Functional implications in hepatic cholesterol and glucose metabolism." *Journal of Biological Chemistry* **279**: 45139-45147.

Blom, N., Gammeltoft, S. and Brunak, S. (1999). "Sequence and structure-based prediction of eukaryotic protein phosphorylation sites." *Journal of Molecular Biology* **294**: 1351-1362.

Blumberg, B., Sabbagh, W., Juguilon, H., Bolado, J., van Meter, C.M., Ono, E.S. and Evans, R.M. (1998). "SXR, a novel steroid and xenobiotic-sensing nuclear receptor." *Genes & Development* **12**: 3195-3205.

Bogan, A.A. and Thorn, K.S. (1998). "Anatomy of hot spots in protein interfaces." *J Mol Biol* **280**: 1-9.

Chang, C., Norris, J.D., Gron, H., Paige, L.A., Hamilton, P.T., Kenan, D.J., Fowlkes, D. and McDonnell, D.P. (1999). "Dissection of the LXXLL nuclear receptor-coactivator interaction motif using combinatorial peptide libraries: discovery of peptide antagonists of estrogen receptors alpha and beta." *Mol Cell Biol* **19**: 8226-39.

Chrencik, J.E., Orans, J., Moore, L.B., Xue, Y., Peng, L., Collins, J.L., Wisely, G.B., Lambert, M.H., Kliewer, S.A. and Redinbo, M.R. (2005). "Structural Disorder in the

Complex of Human PXR and the Macrolide Antibiotic Rifampicin." *Mol Endocrinol* me.2004-0346.

Cochran, A.G., Skelton, N.J. and Starovasnik, M.A. (2001). "Tryptophan zippers: stable, monomeric beta -hairpins." *Proc Natl Acad Sci U S A* **98**: 5578-83.

Cohen, D.S. and Pielak, G.J. (1994). "Stability of yeast iso-1-ferricytochrome c as a function of pH and temperature." *Protein Science* **3**: 1253-1260.

DeLano, W.L. (2002). "Unraveling hot spots in binding interfaces: progress and challenges." *Curr Opin Struct Biol* **12**: 14-20.

Ding, X.S. and Staudinger, J.L. (2005). "Induction of drug metabolism by forskolin: The role of the pregnane X receptor and the protein kinase A signal transduction pathway." *Journal of Pharmacology and Experimental Therapeutics* **312**: 849-856.

Dotzlaw, H., Leygue, E., Watson, P. and Murphy, L.C. (1999). "The human orphan receptor PXR messenger RNA is expressed in both normal and neoplastic breast tissue." *Clinical Cancer Research* **5**: 2103-2107.

Duffy, S., Tsao, K.L. and Waugh, D.S. (1998). "Site-specific, enzymatic biotinylation of recombinant proteins in Spodoptera frugiperda cells using biotin acceptor peptides." *Anal Biochem* **262**: 122-8.

Dunn, R.T., Gleason, B.A., Hartley, D.P. and Klaassen, C.D. (1999). "Postnatal ontogeny and hormonal regulation of sulfotransferase SULT1B1 in male and female rats." *Journal of Pharmacology and Experimental Therapeutics* **290**: 319-324.

Dussault, I., Lin, M., Hollister, K., Wang, E.H., Synold, T.W. and Forman, B.M. (2001). "Peptide mimetic HIV protease inhibitors are ligands for the orphan receptor SXR." *Journal of Biological Chemistry* **276**: 33309-33312.

Dussault, I., Yoo, H.D., Lin, M., Wang, E., Fan, M., Batta, A.K., Salen, G., Erickson, S.K. and Forman, B.M. (2003). "Identification of an endogenous ligand that activates pregnane X receptor-mediated sterol clearance." *Proceedings of the National Academy of Sciences of the United States of America* **100**: 833-838.

Ernst, E. (1999). "Second thoughts about safety of St John's wort." *Lancet* **354**: 2014-2016.

Falkner, K.C., Pinaire, J.A., Xiao, G.H., Geoghegan, T.E. and Prough, R.A. (2001). "Regulation of the rat glutathione S-transferase A2 gene by glucocorticoids: Involvement of both the glucocorticoid and pregnane X receptors." *Molecular Pharmacology* **60**: 611-619.

Fugh-Berman, A. (2000). "Herb-drug interactions." *Lancet* **355**: 134-138.

Gaillard, S., Grasfeder, L.L., Haeffele, C.L., Lobenhofer, E.K., Chu, T.M., Wolfinger, R., Kazmin, D., Koves, T.R., Muoio, D.M., Chang, C.Y., McDonnell, D.P., Dwyer, M.A., Safi, R., Kovacic, A., Murata, Y., Simpson, E.R. and Clyne, C.D. (2006). "Receptor-selective coactivators as tools to define the biology of specific receptor-coactivator pairs Definition of the molecular basis for estrogen receptor-related receptor-alpha-cofactor interactions
Coactivation of liver receptor homologue-1 by peroxisome proliferator-activated receptor gamma coactivator-1alpha on aromatase promoter II and its inhibition by activated retinoid X receptor suggest a novel target for breast-specific antiestrogen therapy." *Mol Cell* **24**: 797-803.

Gaillard, S., Dwyer, M.A. and McDonnell, D.P. (2007). "Definition of the molecular basis for estrogen receptor-related receptor-alpha-cofactor interactions." *Mol Endocrinol* **21**: 62-76.

Gampe, R.T., Jr., Montana, V.G., Lambert, M.H., Miller, A.B., Bledsoe, R.K., Milburn, M.V., Kliewer, S.A., Willson, T.M. and Xu, H.E. (2000a). "Asymmetry in the PPARgamma/RXRalpha crystal structure reveals the molecular basis of heterodimerization among nuclear receptors." *Mol Cell* **5**: 545-55.

Gampe, R.T., Jr., Montana, V.G., Lambert, M.H., Wisely, G.B., Milburn, M.V. and Xu, H.E. (2000b). "Structural basis for autorepression of retinoid X receptor by tetramer formation and the AF-2 helix." *Genes Dev* **14**: 2229-41.

Gardner-Stephen, D., Heydel, J.M., Goyal, A., Lu, Y., Xie, W., Lindblom, T., Mackenzie, P. and Radominska-Pandya, A. (2004). "Human PXR variants and their differential effects on the regulation of human UDP-glucuronosyltransferase gene expression." *Drug Metabolism and Disposition* **32**: 340-347.

Geick, A., Eichelbaum, M. and Burk, O. (2001). "Nuclear receptor response elements mediate induction of intestinal MDR1 by rifampin." *Journal of Biological Chemistry* **276**: 14581-14587.

Gerbal-Chaloin, S., Daujat, M., Pascussi, J.M., Pichard-Garcia, L., Vilarem, M.J. and Maurel, P. (2002). "Transcriptional regulation of CYP2C9 gene. Role of glucocorticoid receptor and constitutive androstane receptor." *J Biol Chem* **277**: 209-17.

Giguere, V. (1999). "Orphan nuclear receptors: from gene to function." *Endocr Rev* **20**: 689-725.

Goodwin, B., Hodgson, E. and Liddle, C. (1999). "The orphan human pregnane X receptor mediates the transcriptional activation of CYP3A4 by rifampicin through a distal enhancer module." *Mol Pharmacol* **56**: 1329-39.

Goodwin, B., Redinbo, M.R. and Kliewer, S.A. (2002). "Regulation of CYP3A gene transcription by the pregnane X receptor." *Annual Review of Pharmacology and Toxicology* **42**: 1-+.

Goodwin, B., Gauthier, K.C., Umetani, M., Watson, M.A., Lochansky, M.I., Collins, J.L., Leitersdorf, E., Mangelsdorf, D.J., Kliewer, S.A. and Repa, J.J. (2003). "Identification of bile acid precursors as endogenous ligands for the nuclear xenobiotic pregnane X receptor." *Proceedings of the National Academy of Sciences of the United States of America* **100**: 223-228.

Guengerich, F.P. (1999). "Cytochrome P-450 3A4: regulation and role in drug metabolism." *Annu. Rev. Pharmacol. Toxicol.* **39**: 1-17.

Hall, J.M., McDonnell, D.P. and Korach, K.S. (2002). "Allosteric regulation of estrogen receptor structure, function, and coactivator recruitment by different estrogen response elements." *Molecular Endocrinology* **16**: 469-486.

Hariparsad, N., Nallani, S.C., Sane, R.S., Buckley, D.J., Buckley, A.R. and Desai, P.B. (2004). "Induction of CYP3A4 by Efavirenz in Primary Human Hepatocytes: Comparison With Rifampin and Phenobarbital." *J Clin Pharmacol* **44**: 1273-1281.

Hegde, R.S., Grossman, S.R., Laimins, L.A. and Sigler, P.B. (1992). "Crystal structure at 1.7 A of the bovine papillomavirus-1 E2 DNA-binding domain bound to its DNA target." *Nature* **359**: 505-12.

Honkakoski, P., Moore, R., Washburn, K.A. and Negishi, M. (1998). "Activation by diverse xenochemicals of the 51-base pair phenobarbital-responsive enhancer module in the CYP2B10 gene." *Mol Pharmacol* **53**: 597-601.

Huang, H.J., Norris, J.D. and McDonnell, D.P. (2002). "Identification of a negative regulatory surface within estrogen receptor alpha provides evidence in support of a role for compressors in regulating cellular responses to agonists and antagonists." *Molecular Endocrinology* **16**: 1778-1792.

Hustert, E., Zibat, A., Presecan-Siedel, E., Eiselt, R., Mueller, R., Fuss, C., Brehm, I., Brinkmann, U., Eichelbaum, M., Wojnowski, L. and Burk, O. (2001). "Natural protein variants of pregnane X receptor with altered transactivation activity toward CYP3A4." *Drug Metabolism and Disposition* **29**: 1454-1459.

Itoh, M., Nakajima, M., Higashi, E., Yoshida, R., Nagata, K., Yamazoe, Y. and Yokoi, T. (2006). "Induction of human CYP2A6 is mediated by the pregnane X receptor with peroxisome proliferator-activated receptor-gamma coactivator 1alpha." *J Pharmacol Exp Ther* **319**: 693-702.

Johnson, D.R., Li, C.W., Chen, L.Y., Ghosh, J.C. and Chen, J.D. (2006). "Regulation and binding of pregnane X receptor by nuclear receptor corepressor silencing mediator of retinoid and thyroid hormone receptors (SMRT)." *Mol Pharmacol* **69**: 99-108.

Jones, S.A., Moore, L.B., Shenk, J.L., Wisely, G.B., Hamilton, G.A., McKee, D.D., Tomkinson, N.C.O., LeCluyse, E.L., Lambert, M.H., Willson, T.M., Kliewer, S.A. and Moore, J.T. (2000). "The pregnane x receptor: A promiscuous xenobiotic receptor that has diverged during evolution." *Molecular Endocrinology* **14**: 27-39.

Kast, H.R., Goodwin, B., Tarr, P.T., Jones, S.A., Anisfeld, A.M., Stoltz, C.M., Tontonoz, P., Kliewer, S., Willson, T.M. and Edwards, P.A. (2002). "Regulation of multidrug resistance-associated protein 2 (ABCC2) by nuclear receptors pregnane X receptor, farnesoid X-activated receptor, and constitutive androstane receptor." *Journal of Biological Chemistry* **277**: 2908-2915.

Kawana, K., Ikuta, T., Kobayashi, Y., Gotoh, O., Takeda, K. and Kawajiri, K. (2003). "Molecular mechanism of nuclear translocation of an orphan nuclear receptor, SXR." *Molecular Pharmacology* **63**: 524-531.

Kliewer, S.A., Moore, J.T., Wade, L., Staudinger, J.L., Watson, M.A., Jones, S.A., McKee, D.D., Oliver, B.B., Willson, T.M., Zetterstrom, R.H., Perlmann, T. and Lehmann, J.M. (1998). "An orphan nuclear receptor activated by pregnanes defines a novel steroid signaling pathway." *Cell* **92**: 73-82.

Kliewer, S.A. (2003). "The nuclear pregnane X receptor regulates xenobiotic detoxification." *Journal of Nutrition* **133**: 2444S-2447S.

Koyano, S., Kurose, K., Ozawa, S., Saeki, M., Nakajima, Y., Hasegawa, R., Komamura, K., Ueno, K., Kamakura, S., Nakajima, T., Saito, H., Kimura, H., Goto, Y., Saitoh, O., Katoh, M., Ohnuma, T., Kawai, M., Sugai, K., Ohtsuki, T., Suzuki, C., Minami, N., Saito, Y. and Sawada, J.I. (2002). "Eleven Novel Single Nucleotide Polymorphisms in the NR1I2 (PXR) Gene, Four of which Induce Non-synonymous Amino Acid Alterations." *Drug Metabolism and Pharmacokinetics* **17**: 561-565.

Koyano, S., Kurose, K., Saito, Y., Ozawa, S., Hasegawa, R., Komamura, K., Ueno, K., Kamakura, S., Kitakaze, M., Nakajima, T., Matsumoto, K., Akasawa, A., Saito, H. and Sawada, J.I. (2004). "Functional characterization of four naturally occurring variants of human pregnane X receptor (PXR): One variant causes dramatic loss of both DNA binding activity and the transactivation of the CYP3A4 promoter/enhancer region." *Drug Metabolism and Disposition* **32**: 149-154.

Krasowski, M.D., Yasuda, K., Hagey, L.R. and Schuetz, E.G. (2005). "Evolution of the pregnane X receptor: adaptation to cross-species differences in biliary bile salts." *Mol Endocrinol* me.2004-0427.

Lamba, V., Yasuda, K., Lamba, J.K., Assem, M., Davila, J., Strom, S. and Schuetz, E.G. (2004). "PXR (NR1I2): splice variants in human tissues, including brain, and identification of neurosteroids and nicotine as PXR activators." *Toxicology and Applied Pharmacology* **199**: 251-265.

Landes, N., Pfluger, P., Kluth, D., Birringer, M., Ruhl, R., Bol, G.F., Glatt, H. and Brigelius-Flohe, R. (2003). "Vitamin E activates gene expression via the pregnane X receptor." *Biochemical Pharmacology* **65**: 269-273.

Lehmann, J.M., McKee, D.D., Watson, M.A., Willson, T.M., Moore, J.T. and Kliewer, S.A. (1998). "The human orphan nuclear receptor PXR is activated by compounds that regulate CYP3A4 gene expression and cause drug interactions." *Journal of Clinical Investigation* **102**: 1016-1023.

Li, A.P., Kaminski, D.L. and Rasmussen, A. (1995). "Substrates of human hepatic cytochrome P450 3A4." *Toxicology* **104**: 1-8.

Li, T., Chen, W. and Chiang, J.Y. (2007). "PXR induces CYP27A1 and regulates cholesterol metabolism in the intestine." *J Lipid Res* **48**: 373-84.

Li, T.G. and Chiang, J.Y.L. (2005). "Mechanism of rifampicin and pregnane X receptor inhibition of human cholesterol 7 alpha-hydroxylase gene transcription." *American Journal of Physiology-Gastrointestinal and Liver Physiology* **288**: G74-G84.

Lipinski, C.A., Lombardo, F., Dominy, B.W. and Feeney, P.J. (2001). "Experimental and computational approaches to estimate solubility and permeability in drug discovery and development settings." *Advanced Drug Delivery Reviews* **46**: 3-26.

Lo Conte, L., Chothia, C. and Janin, J. (1999). "The atomic structure of protein-protein recognition sites." *J Mol Biol* **285**: 2177-98.

Maglich, J.M., Stoltz, C.M., Goodwin, B., Hawkins-Brown, D., Moore, J.T. and Kliewer, S.A. (2002). "Nuclear pregnane X receptor and constitutive androstane receptor regulate overlapping but distinct sets of genes involved in xenobiotic detoxification." *Molecular Pharmacology* **62**: 638-646.

Mangelsdorf, D.J. and Evans, R.M. (1995). "The Rxr Heterodimers and Orphan Receptors." *Cell* **83**: 841-850.

Masuyama, H., Hiramatsu, Y., Kunitomi, M., Kudo, T. and MacDonald, P.N. (2000). "Endocrine disrupting chemicals, phthalic acid and nonylphenol, activate Pregnane X receptor-mediated transcription." *Molecular Endocrinology* **14**: 421-428.

Masuyama, H., Hiramatsu, Y., Mizutani, Y., Inoshita, H. and Kudo, T. (2001). "The expression of pregnane X receptor and its target gene, cytochrome P450 3A1, in perinatal mouse." *Molecular and Cellular Endocrinology* **172**: 47-56.

Masuyama, H., Inoshita, H., Hiramatsu, Y. and Kudo, T. (2002). "Ligands have various potential effects on the degradation of pregnane X receptor by proteasome." *Endocrinology* **143**: 55-61.

Masuyama, H., Hiramatsu, Y., Kodama, J.I. and Kudo, T. (2003). "Expression and potential roles of pregnane X receptor in endometrial cancer." *Journal of Clinical Endocrinology and Metabolism* **88**: 4446-4454.

Masuyama, H., Suwaki, N., Tateishi, Y., Nakatsukasa, H., Segawa, T. and Hiramatsu, Y. (2005). "The Pregnane X Receptor Regulates Gene Expression in a Ligand- and Promoter-selective Fashion." *Mol Endocrinol* me.2004-0434.

Maurel, P. (1996). "The CYP3A family" in *Cytochromes P450: Metabolic and Toxicological Aspects*. Ioannides, C., Ed. Boca Raton, FL, CRC Press, Inc. 241-270.

McDonnell, D.P. (1999). "The molecular pharmacology of SERMs." *Trends Endocrinol. Metab.* **10**: 301-311.

Michalets, E.L. (1998). "Update: clinically significant cytochrome P-450 drug interactions." *Pharmacotherapy* **18**: 84-112.

Moore, D.D. (2005). "CAR: Three new models for a problem child." *Cell Metabolism* **1**: 6-8.

Moore, L.B., Goodwin, B., Jones, S.A., Wisely, G.B., Serabjit-Singh, C.J., Willson, T.M., Collins, J.L. and Kliewer, S.A. (2000). "St. John's wort induces hepatic drug metabolism through activation of the pregnane X receptor." *PNAS* **97**: 7500-7502.

Nichols, J.S., Parks, D.J., Consler, T.G. and Blanchard, S.G. (1998). "Development of a scintillation proximity assay for peroxisome proliferator-activated receptor gamma ligand binding domain." *Anal Biochem* **257**: 112-9.

Nolte, R.T., Wisely, G.B., Westin, S., Cobb, J.E., Lambert, M.H., Kurokawa, R., Rosenfeld, M.G., Willson, T.M., Glass, C.K. and Milburn, M.V. (1998). "Ligand binding and co-activator assembly of the peroxisome proliferator-activated receptor-gamma." *Nature* **395**: 137-43.

Norris, J., Fan, D., Aleman, C., Marks, J.R., Futreal, P.A., Wiseman, R.W., Iglehart, J.D., Deininger, P.L. and McDonnell, D.P. (1995). "Identification of a new subclass of Alu DNA repeats which can function as estrogen receptor-dependent transcriptional enhancers." *J Biol Chem* **270**: 22777-82.

Ortlund, E.A., Lee, Y., Solomon, I.H., Hager, J.M., Safi, R., Choi, Y., Guan, Z., Tripathy, A., Raetz, C.R., McDonnell, D.P., Moore, D.D. and Redinbo, M.R. (2005). "Modulation of human nuclear receptor LRH-1 activity by phospholipids and SHP." *Nat Struct Mol Biol* **12**: 357-63.

Ozturk, Y., Aydin, S., Baser, K.H.C., Kirimer, N. and Kurtarozturk, N. (1992). "Hepatoprotective Activity of Hypericum-Perforatum L Alcoholic Extract in Rodents." *Phytother. Res.* **6**: 44-46.

Piscitelli, S.C., Burstein, A.H., Chaitt, D., Alfaro, R.M. and Falloon, J. (2000). "Indinavir concentrations and St John's wort." *Lancet* **355**: 547-548.

Renaud, J.P., Rochel, N., Ruff, M., Vivat, V., Chambon, P., Gronemeyer, H. and Moras, D. (1995). "Crystal structure of the RAR-gamma ligand-binding domain bound to all-trans retinoic acid." *Nature* **378**: 681-9.

Richardson, J.S. and Richardson, D.C. (2002). "Natural beta-sheet proteins use negative design to avoid edge-to-edge aggregation." *Proc Natl Acad Sci U S A* **99**: 2754-9.

Rochel, N., Wurtz, J.M., Mitschler, A., Klaholz, B. and Moras, D. (2000). "The crystal structure of the nuclear receptor for vitamin D bound to its natural ligand." *Mol Cell* **5**: 173-9.

Rochette-Egly, C. (2003). "Nuclear receptors: integration of multiple signalling pathways through phosphorylation." *Cellular Signalling* **15**: 355-366.

Rosenfeld, J.M., Vargas, R., Xie, W. and Evans, R.M. (2003). "Genetic profiling defines the xenobiotic gene network controlled by the nuclear receptor pregnane X receptor." *Molecular Endocrinology* **17**: 1268-1282.

Rosenfeld, M.G. and Glass, C.K. (2001). "Coregulator codes of transcriptional regulation by nuclear receptors." *J Biol Chem* **276**: 36865-8.

Runge-Morris, M., Wu, W. and Kocharek, T.A. (1999). "Regulation of rat hepatic hydroxysteroid sulfotransferase (SULT2-40/41) gene expression by glucocorticoids: Evidence for a dual mechanism of transcriptional control." *Molecular Pharmacology* **56**: 1198-1206.

Ruschitzka, F., Meier, P.J., Turina, M., Luscher, T.F. and Noll, G. (2000). "Acute heart transplant rejection due to Saint John's wort." *Lancet* **355**: 548-549.

Russell, S.J. and Cochran, A.G. (2000). "Designing Stable β-Hairpins: Energetic Contributions from Cross-Strand Residues." *J. Am. Chem. Soc.* **122**: 12600-12601.

Shan, L., Vincent, J., Brunzelle, J.S., Dussault, I., Lin, M., Ianculescu, I., Sherman, M.A., Forman, B.M. and Fernandez, E.J. (2004). "Structure of the murine constitutive androstane receptor complexed to androstenol: A molecular basis for inverse agonism." *Molecular Cell* **16**: 907-917.

Solomon, I.H., Hager, J.M., Safi, R., McDonnell, D.P., Redinbo, M.R. and Ortlund, E.A. (2005). "Crystal structure of the human LRH-1 DBD-DNA complex reveals Ftz-F1 domain positioning is required for receptor activity." *J Mol Biol* **354**: 1091-102.

Song, X.L., Xie, M.X., Zhang, H., Li, Y.X., Sachdeva, K. and Yan, B.F. (2004). "The pregnane X receptor binds to response elements in a genomic context-dependent manner, and PXR activator rifampicin selectively alters the binding among target genes." *Drug Metabolism and Disposition* **32**: 35-42.

Sonoda, J., Chong, L.W., Downes, M., Barish, G.D., Coulter, S., Liddle, C., Lee, C.-H. and Evans, R.M. (2005). "Pregnane X receptor prevents hepatorenal toxicity from cholesterol metabolites." *PNAS* **102**: 2198-2203.

Squires, E.J., Sueyoshi, T. and Negishi, M. (2004). "Cytoplasmic localization of pregnane X receptor and ligand-dependent nuclear translocation in mouse liver." *Journal of Biological Chemistry* **279**: 49307-49314.

Staudinger, J.L., Goodwin, B., Jones, S.A., Hawkins-Brown, D., MacKenzie, K.I., Latour, A., Liu, Y.P., Klaassen, C.D., Brown, K.K., Reinhard, J., Willson, T.N., Koller, B.H. and Kliewer, S.A. (2001). "The nuclear receptor PXR is a lithocholic acid sensor that protects against liver toxicity." *Proceedings of the National Academy of Sciences of the United States of America* **98**: 3369-3374.

Sueyoshi, T. and Negishi, M. (2001). "Phenobarbital response elements of cytochrome P450 genes and nuclear receptors." *Annual Review of Pharmacology and Toxicology* **41**: 123-143.

Sugatani, J., Nishitani, S., Yamakawa, K., Yoshinari, K., Sueyoshi, T., Negishi, M. and Miwa, M. (2005). "Transcriptional regulation of human UGT1A1 gene expression: activated glucocorticoid receptor enhances constitutive androstane receptor/pregnane X receptor-mediated UDP-glucuronosyltransferase 1A1 regulation with glucocorticoid receptor-interacting protein 1." *Mol Pharmacol* **67**: 845-55.

Suino, K., Peng, L., Reynolds, R., Li, Y., Cha, J.Y., Repa, J.J., Kliewer, S.A. and Xu, H.E. (2004). "The nuclear xenobiotic receptor CAR: Structural determinants of constitutive activation and heterodimerization." *Molecular Cell* **16**: 893-905.

Synold, T.W., Dussault, I. and Forman, B.M. (2001). "The orphan nuclear receptor SXR coordinately regulates drug metabolism and efflux." *Nature Medicine* **7**: 584-590.

Tabb, M.M., Sun, A.X., Zhou, C.C., Grun, F., Errandi, J., Romero, K., Pham, H., Inoue, S., Mallick, S., Lin, M., Forman, B.M. and Blumberg, B. (2003). "Vitamin K-2 regulation of bone homeostasis is mediated by the steroid and xenobiotic receptor SXR." *Journal of Biological Chemistry* **278**: 43919-43927.

Takeshita, A., Koibuchi, N., Oka, J., Taguchi, M., Shishiba, Y. and Ozawa, Y. (2001). "Bisphenol-A, an environmental estrogen, activates the human orphan nuclear receptor, steroid and xenobiotic receptor-mediated transcription." *European Journal of Endocrinology* **145**: 513-517.

Takeshita, A., Taguchi, M., Koibuchi, N. and Ozawa, Y. (2002). "Putative role of the orphan nuclear receptor SXR (steroid and xenobiotic receptor) in the mechanism of CYP3A4 inhibition by xenobiotics." *Journal of Biological Chemistry* **277**: 32453-32458.

Tirona, R.G., Leake, B.F., Podust, L.M. and Kim, R.B. (2004). "Identification of amino acids in rat pregnane X receptor that determine species-specific activation." *Molecular Pharmacology* **65**: 36-44.

Ueda, A., Matsui, K., Yamamoto, Y., Pedersen, L.C., Sueyoshi, T. and Negishi, M. (2004). "Thr 176 regulates the activity of the mouse nuclear receptor CAR and is conserved in the NR1I subfamily-members PXR and VDR." *Biochem J*

Uppal, H., Toma, D., Saini, S.P.S., Ren, S.R., Jones, T.J. and Xie, W. (2005). "Combined loss of orphan receptors PXR and CAR heightens sensitivity to toxic bile acids in mice." *Hepatology* **41**: 168-176.

Wang, H.B., Faucette, S., Sueyoshi, T., Moore, R., Ferguson, S., Negishi, M. and LeCluyse, E.L. (2003). "A novel distal enhancer module regulated by pregnane x receptor/constitutive androstane receptor is essential for the maximal induction of CYP2B6 gene expression." *Journal of Biological Chemistry* **278**: 14146-14152.

Watkins, R.E., Wisely, G.B., Moore, L.B., Collins, J.L., Lambert, M.H., Williams, S.P., Willson, T.M., Kliewer, S.A. and Redinbo, M.R. (2001). "The human nuclear xenobiotic receptor PXR: Structural determinants of directed promiscuity." *Science* **292**: 2329-2333.

Watkins, R.E., Davis-Searles, P.R., Lambert, M.H. and Redinbo, M.R. (2003a). "Coactivator binding promotes the specific interaction between ligand and the pregnane X receptor." *Journal of Molecular Biology* **331**: 815-828.

Watkins, R.E., Maglich, J.M., Moore, L.B., Wisely, G.B., Noble, S.M., Davis-Searles, P.R., Lambert, M.H., Kliewer, S.A. and Redinbo, M.R. (2003b). "2.1 angstrom crystal structure of human PXR in complex with the St. John's wort compound hyperforin." *Biochemistry* **42**: 1430-1438.

Wentworth, J.M., Agostini, M., Love, J., Schwabe, J.W. and Chatterjee, V.K.K. (2000). "St John's wort, a herbal antidepressant, activates the steroid X receptor." *Journal of Endocrinology* **166**: R11-R16.

Williams, S., Bledsoe, R.K., Collins, J.L., Boggs, S., Lambert, M.H., Miller, A.B., Moore, J., McKee, D.D., Moore, L., Nichols, J., Parks, D., Watson, M., Wisely, B. and Willson, T.M. (2003). "X-ray crystal structure of the liver X receptor beta ligand binding domain: regulation by a histidine-tryptophan switch." *J Biol Chem* **278**: 27138-43.

Xie, W. and Evans, R.M. (2001a). "Orphan nuclear receptors: The exotics of xenobiotics." *Journal of Biological Chemistry* **276**: 37739-37742.

Xie, W., Radominska-Pandya, A., Shi, Y.H., Simon, C.M., Nelson, M.C., Ong, E.S., Waxman, D.J. and Evans, R.M. (2001b). "An essential role for nuclear receptors SXR/PXR in detoxification of cholestatic bile acids." *Proceedings of the National Academy of Sciences of the United States of America* **98**: 3375-3380.

Xie, W., Yeuh, M.F., Radominska-Pandya, A., Saini, S.P.S., Negishi, Y., Bottroff, B.S., Cabrera, G.Y., Tukey, R.H. and Evans, R.M. (2003). "Control of steroid, heme, and carcinogen metabolism by nuclear pregnane X receptor and constitutive androstane receptor." *Proceedings of the National Academy of Sciences of the United States of America* **100**: 4150-4155.

Xu, H.E., Stanley, T.B., Montana, V.G., Lambert, M.H., Shearer, B.G., Cobb, J.E., McKee, D.D., Galardi, C.M., Plunket, K.D., Nolte, R.T., Parks, D.J., Moore, J.T., Kliewer, S.A., Willson, T.M. and Stimmel, J.B. (2002). "Structural basis for antagonist-mediated recruitment of nuclear co-repressors by PPARalpha." *Nature* **415**: 813-7.

Xu, R.X., Lambert, M.H., Wisely, B.B., Warren, E.N., Weinert, E.E., Waitt, G.M., Williams, J.D., Collins, J.L., Moore, L.B., Willson, T.M. and Moore, J.T. (2004). "A structural basis for constitutive activity in the human CAR/RXR alpha heterodimer." *Molecular Cell* **16**: 919-928.

Zhang, J., Kuehl, P., Green, E.D., Touchman, J.W., Watkins, P.B., Daly, A., Hall, S.D., Maurel, P., Relling, M., Brimer, C., Yasuda, K., Wrighton, S.A., Hancock, M., Kim, R.B., Strom, S., Thummel, K., Russell, C.G., Hudson, J.R., Schuetz, E.G. and Boguski, M.S.

(2001). "The human pregnane X receptor: genomic structure and identification and functional characterization of natural allelic variants." *Pharmacogenetics* **11**: 555-572.

Zhang, Y., Castellani, L.W., Sinal, C.J., Gonzalez, F.J. and Edwards, P.A. (2004). "Peroxisome proliferator-activated receptor-gamma coactivator 1alpha (PGC-1alpha) regulates triglyceride metabolism by activation of the nuclear receptor FXR." *Genes Dev* **18**: 157-69.

Zhou, C.C., Tabb, M.M., Sadatrafiei, A., Grun, F. and Blumberg, B. (2004). "Tocotrienols activate the steroid and xenobiotic receptor, SXR, and selectively regulate expression of its target genes." *Drug Metabolism and Disposition* **32**: 1075-1082.